Chebyshev with Domain Decomposition in the Two–Dimension Turbulence and in the Typhoon Vortex Dynamics

Prof. Hung-Chi Kuo

9/28/2008

Department of Atmospheric Sciences
National Taiwan University

The ENIAC

Electronic Numerical Integrator and Computer

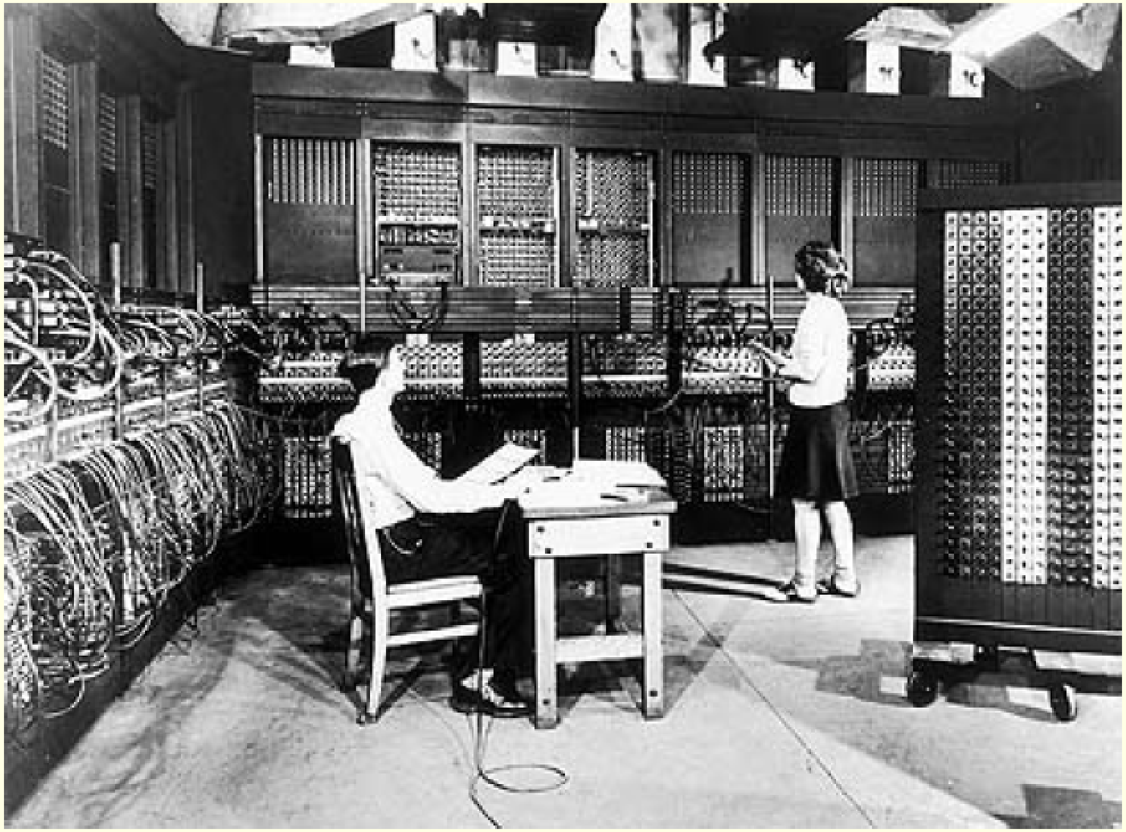

18000 vacuum tubes
70000 resistors
10000 capacitor
6000 switches

140 K Watts power

No high-level language
Assembly language

500 Flops
Function Table 0.001 s

3,700,000,000 times slower than current day large computer

第一部電腦　氣象預報

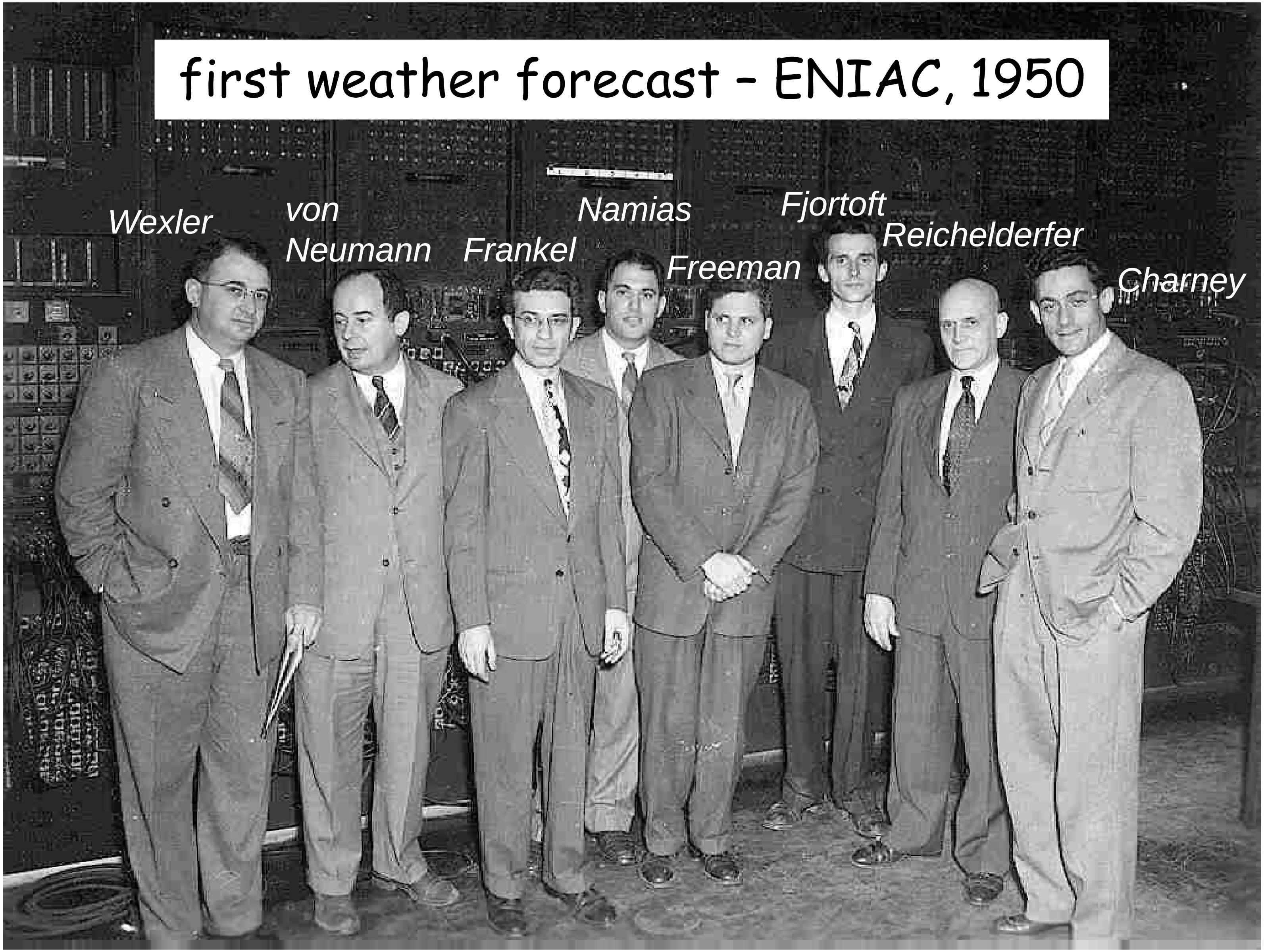

In front of the Eniac, Aberdeen Proving Ground, April 4, 1950, on the occasion of the first numerical weather computations carried out with the aid of a high-speed computer.

ENIAC – late 40s

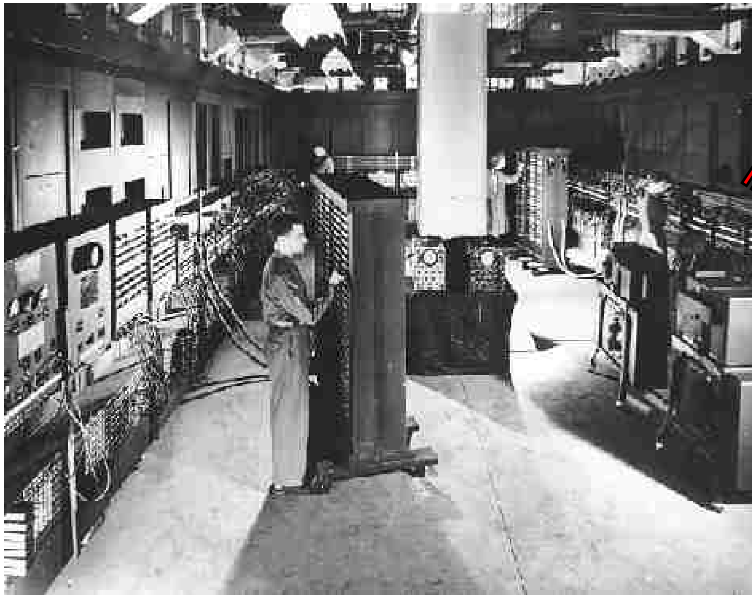

Earth Simulator -- 2002

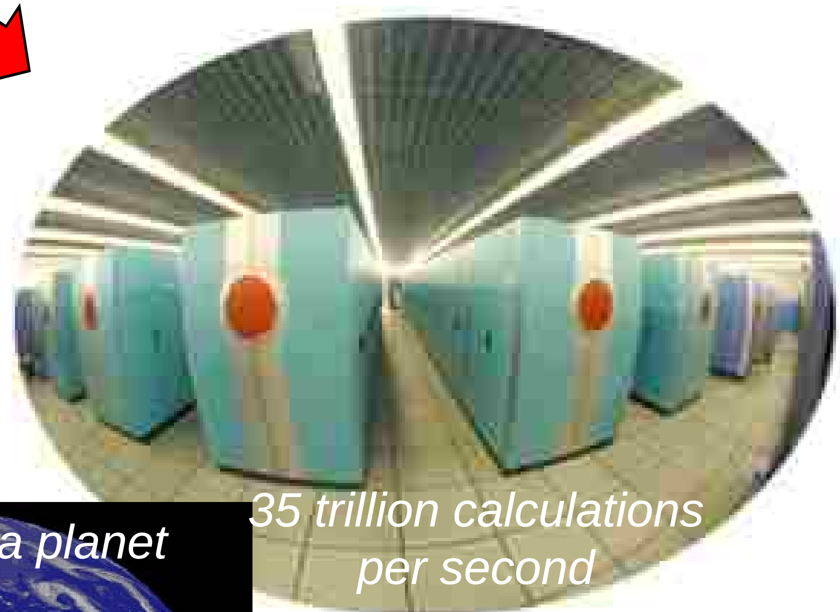

NASDA, JAERI, JAMSTEC

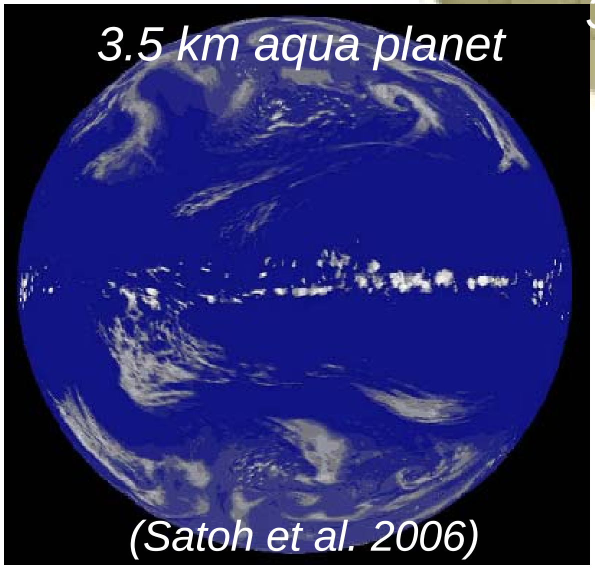

(Satoh et al. 2006)

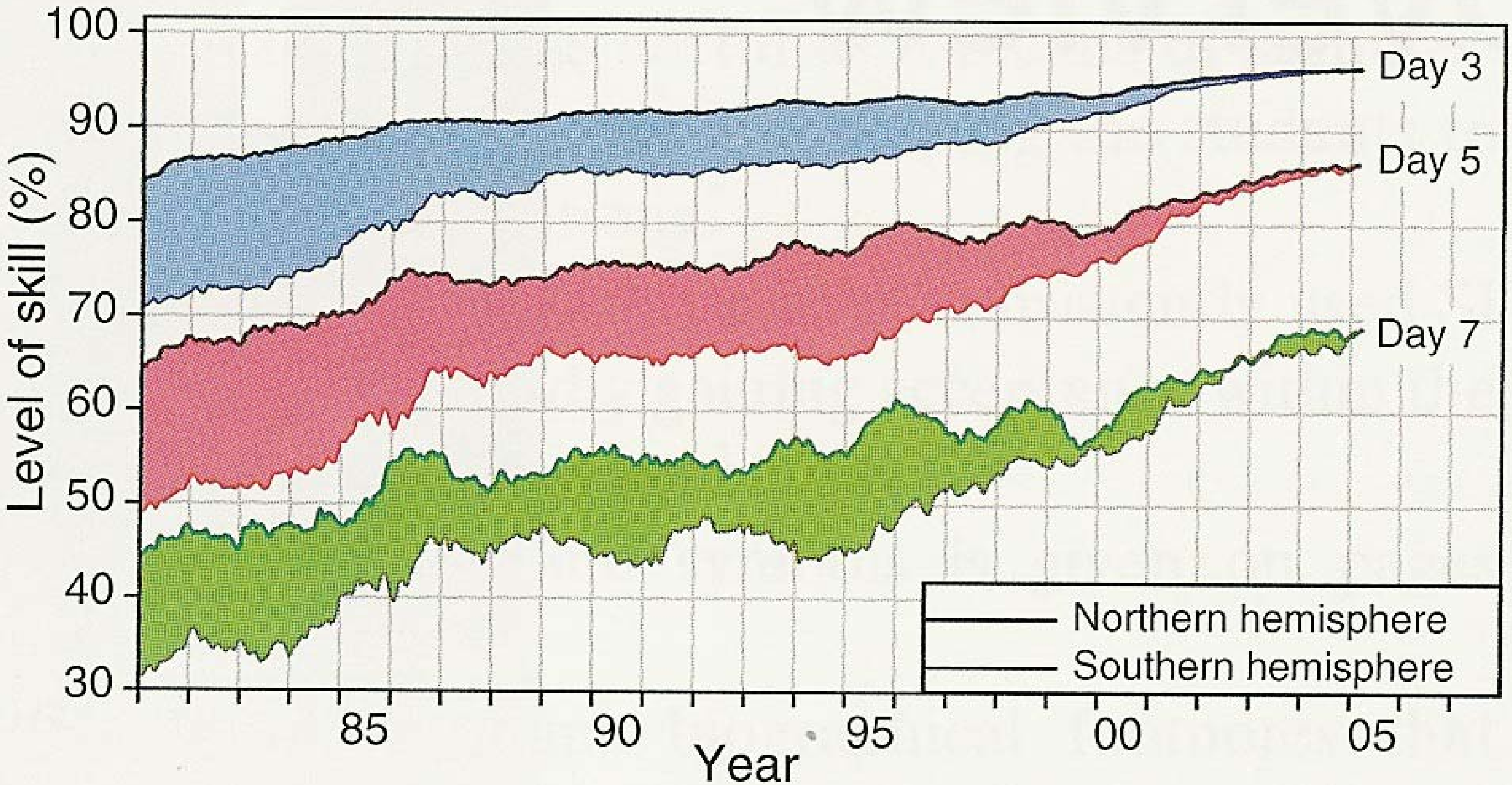

Level of skill (%)
100
90
80
70
60
50
40
30
85
90
95
00
05
Year
Day 3
Day 5
Day 7
Northern hemisphere
Southern hemisphere

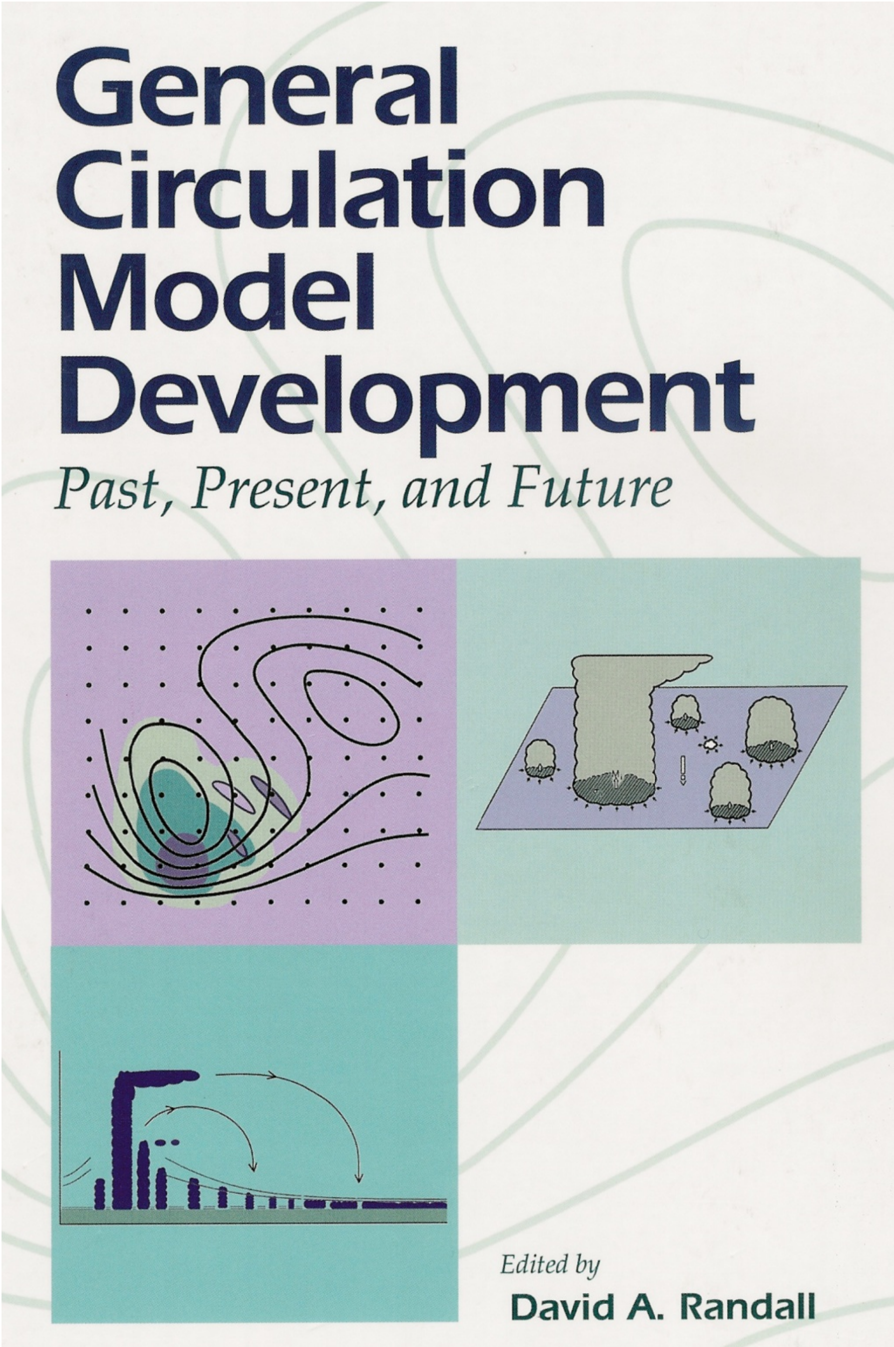

1. Two dimensional Turbulence
   Discretization Method
   Dynamics

2. Cumulus Parameterization

3. Hadley Dynamics
   Dynamics + Cloud
   Boundary Dynamics
   Climate Asymmetry

Atmosphere + Ocean + Land

颱風潛熱與其它能量的比較

賀伯颱風的全台灣平均總雨量

爲400*mm*

400 *mm* = 0.4 *m*

$0.4\ m * 1000\ kg\ m^{-3} * 2.5\times10^{6}\ J\ kg^{-1}$

$= 10^{9}\ J\ m^{2}$

$10^{9}\ J\ m^{2} * 3.5\times10^{10}\ m^{2}$

$= 3.5\times10^{19}\ J \sim 10^{20} J$

$${}^{1}_{0}\mathrm{n} + {}^{235}_{92}\mathrm{U} \rightarrow {}^{142}_{56}\mathrm{Ba} + {}^{91}_{36}\mathrm{Kr} + 3\,{}^{1}_{0}\mathrm{n}$$

$1.68 * m * 10^{13} J/mol$

$\Rightarrow \boxed{1.46\times10^{6}\ kg\ U^{235}\ (6*10^{6}\ \mathrm{mol})}$

能量估計值		備註
賀伯颱風降雨總潛熱能量	10^{20} J	可使台灣整層大氣增溫100度
台灣一年用電量	$5*10^{17}$ J	需數百年用電量才相當
全世界核子彈爆炸釋放能量	$2*10^{19}$ ~$2*10^{20}$ J	與賀伯颱風同等級
核戰後燃燒釋放能量	$2*10^{20}$ J	與賀伯颱風同等級
地球一天接受的太陽能量	$1.5*10^{22}$ J	數百個賀伯颱風
Tunguska隕石撞地球（西元1908年，西伯利亞）	10^{16} J	賀伯颱風的萬分之一
火流星撞地球（恐龍滅絕？）	$4*10^{23}$ J	數千個賀伯颱風

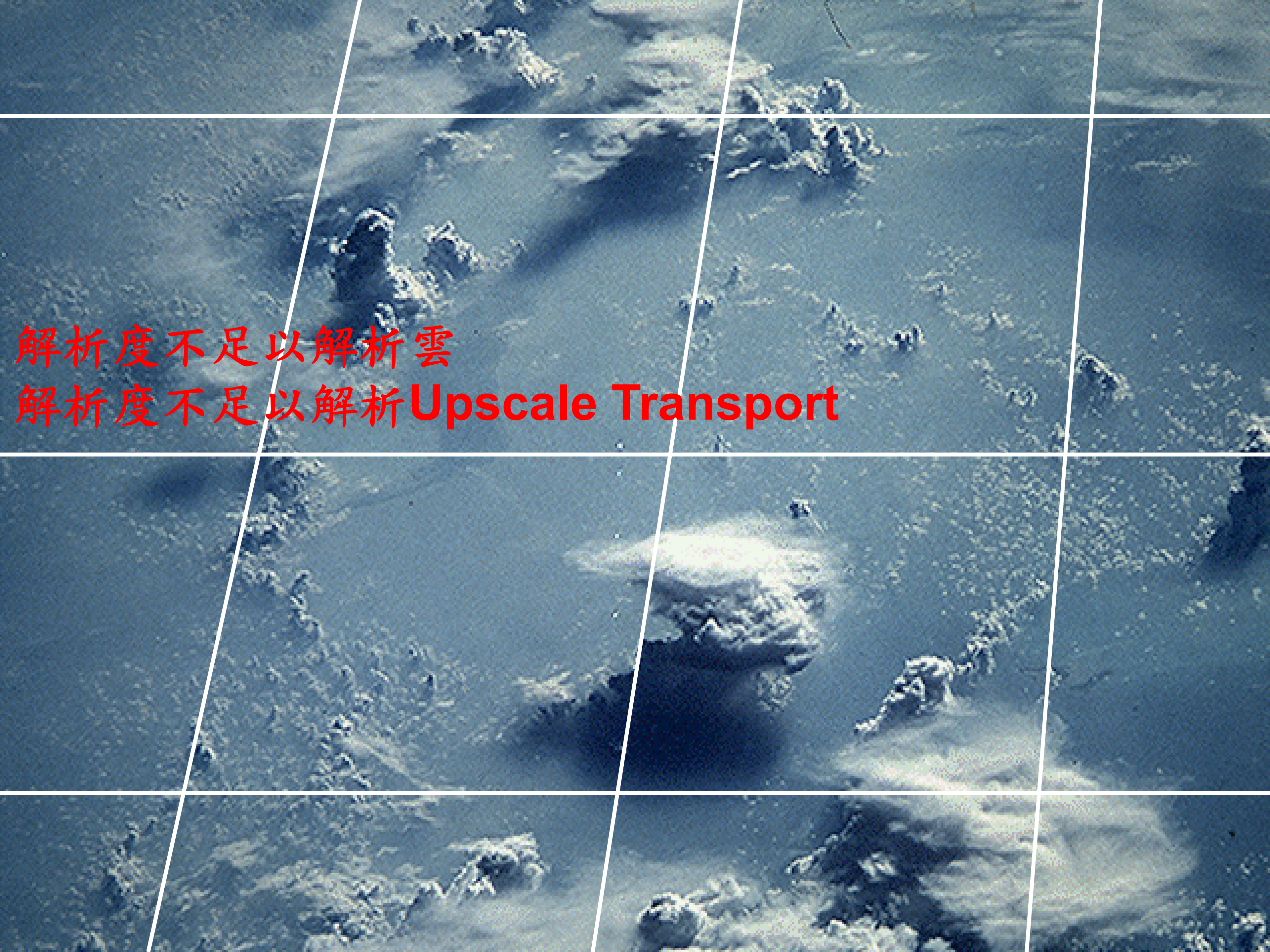
解析度不足以解析雲
解析度不足以解析Upscale Transport

The Downstream Influences of the Extratropical Transition of Tropical Cyclones

Patrick Harr

Naval Postgraduate School

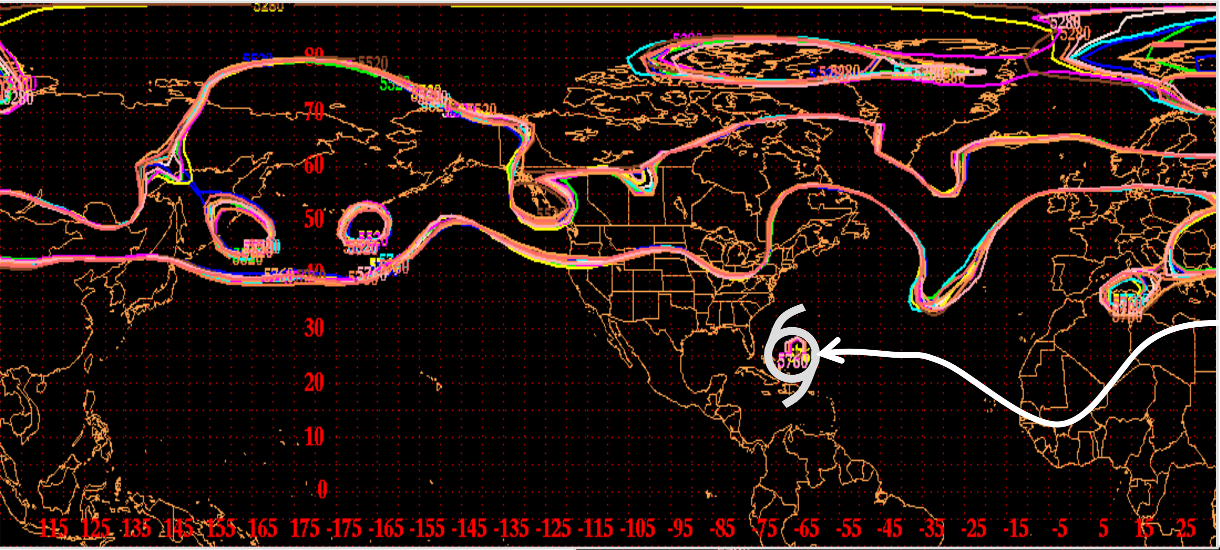

0000 UTC 16 Sep 2003
GFS Ensembles +00

Hurricane Isabel

GFS 500 hPa Ensembles
+108 h
VT 1200 UTC 20 Sep 03

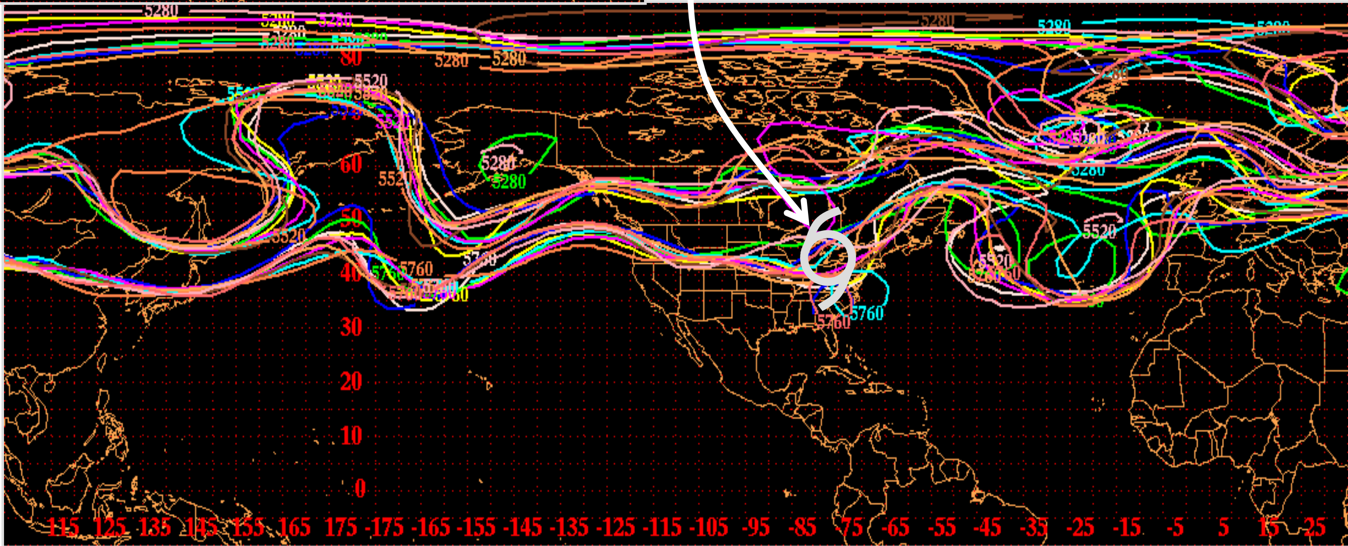

Acknowledgment: Office of Naval Research, Marine Meteorology Program

Von Karman's Statement:

To my mind, there are two great unexplained mysteries in our understanding of the universe. One is the nature of a unified generalized theory to explain both gravitation and electromagnetism. The other is an understanding of the nature of turbulence. After I die, I expect god to clarify general field theory for me. *I have no such hope for turbulence*.

Euler 1755

$$\frac{d}{dt}\int_{v_m} \rho\vec{v}\,dv = -\int_{\partial v_m} p\,d\vec{s}$$

$$\int_{v_m} \rho\frac{d\vec{v}}{dt}\,dv = -\int_{v_m} \nabla p\,dv$$

$$\rho\,\frac{d\vec{v}}{dt} = -\nabla p$$

Lagrange 1781

$$\frac{\partial \vec{u}}{\partial t} + \vec{\zeta} \times \vec{u} = -\frac{1}{\rho}\nabla p - \nabla K - \nabla \Phi$$

Rotation Vortex

Lorentz Force Law

$$\mathbf{F} = q(\mathbf{E} + \mathbf{v} \times \mathbf{B})$$

$$\mathbf{F} = q(-\nabla V + \mathbf{v} \times \mathbf{B})$$

Ertel's Derivation Potential Vorticity

$$\frac{\partial \zeta_i}{\partial t} + u_j \frac{\partial \zeta_i}{\partial x_j} + \zeta_i \frac{\partial u_j}{\partial x_j} = \zeta_j \frac{\partial u_i}{\partial x_j} + B_i$$ **Helmholtz Vorticity Equation (1858)**

$$\frac{\partial \rho}{\partial t} + \frac{\partial \rho u_j}{\partial x_j} = 0$$ **Euler Continuity Equation (1750)**

$$\frac{d}{dt}\left(\frac{\zeta_i}{\rho}\right) = \frac{\zeta_j}{\rho}\frac{\partial u_i}{\partial x_j} + \frac{B_i}{\rho}$$

$$\frac{d}{dt}\psi = \dot{\psi}$$ **(some scalar function ψ)**

$$\frac{d}{dt}\frac{\partial \psi}{\partial x_i} = -\frac{\partial u_j}{\partial x_i}\frac{\partial \psi}{\partial x_j} + \frac{\partial \dot{\psi}}{\partial x_i}$$

$$\frac{\zeta_i}{\rho}\frac{d}{dt}\frac{\partial \psi}{\partial x_i} = -\frac{\zeta_i}{\rho}\frac{\partial u_j}{\partial x_i}\frac{\partial \psi}{\partial x_j} + \frac{\zeta_i}{\rho}\frac{\partial \dot{\psi}}{\partial x_i}$$

+) $$\frac{\partial \psi}{\partial x_i}\frac{d}{dt}\left(\frac{\zeta_i}{\rho}\right) = \frac{\zeta_j}{\rho}\frac{\partial u_i}{\partial x_j}\frac{\partial \psi}{\partial x_i} + \frac{B_i}{\rho}\frac{\partial \psi}{\partial x_i}$$ $$\left(\frac{B_i}{\rho}\frac{\partial \psi}{\partial x_i} = \frac{1}{\rho}N(\rho, P, \psi)\right)$$

$$\boxed{\frac{d}{dt}\left(\frac{\zeta_i}{\rho}\frac{\partial \psi}{\partial x_i}\right) = \frac{\zeta_i}{\rho}\frac{\partial \dot{\psi}}{\partial x_i} + \frac{1}{\rho}N(\rho, P, \psi)}$$

Coriolis Force

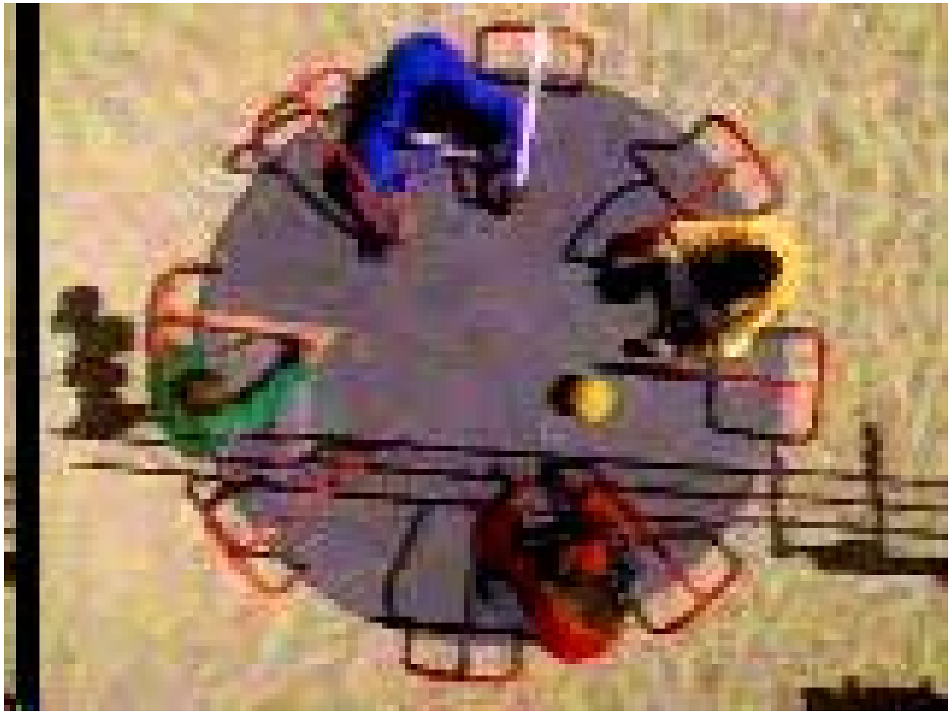

Non-inertial Frame

Two Dimensional Turbulence

3D

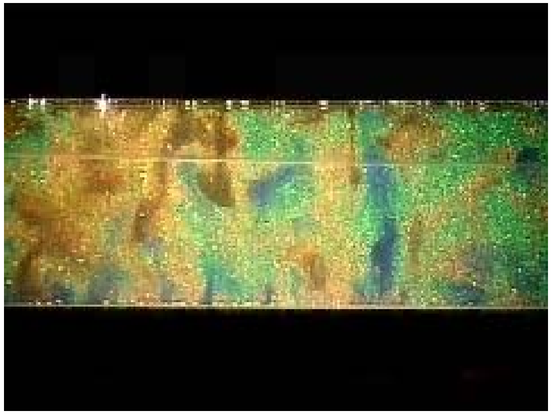

2D (strong rotation)

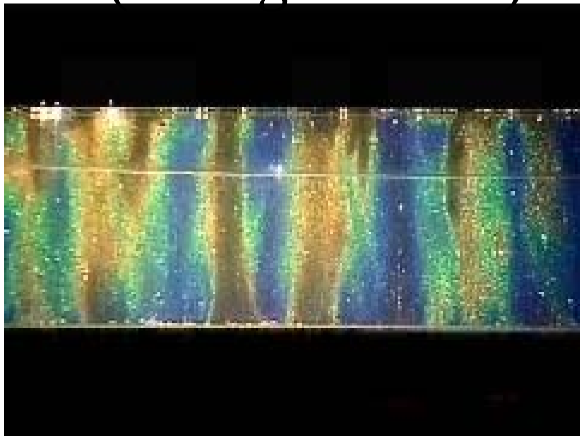

Taylor columns

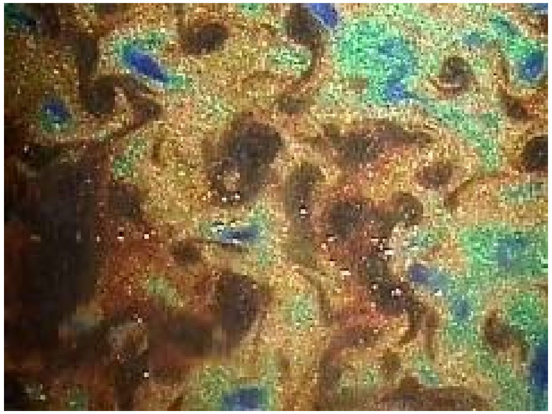

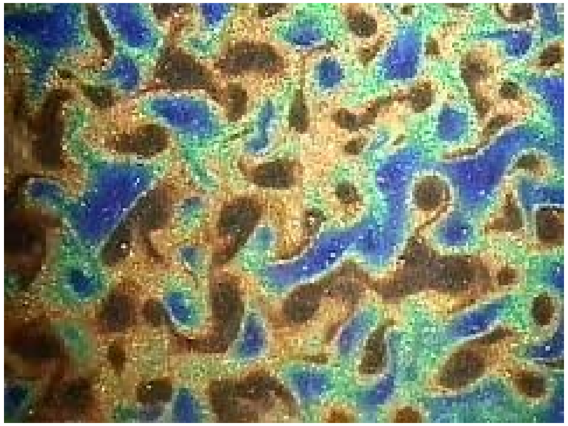

Vortices with sharp edge

Kyoto University

2D Turbulence

Stratification and/or Rotation

Vortex Waves Turbulence

$$\frac{\partial \zeta}{\partial t} + u\frac{\partial \zeta}{\partial x} + v\frac{\partial \zeta}{\partial y} = \nu \nabla^2 \zeta$$

$$u = -\frac{\partial \psi}{\partial y}, \qquad v = \frac{\partial \psi}{\partial x}.$$

$$\boxed{\frac{\partial \zeta}{\partial t} + \frac{\partial(\psi, \zeta)}{\partial(x, y)} = \nu \nabla^2 \zeta}$$

Weiss(1981,1991), Rozoff et al. (2004)

$$\frac{D}{Dt}(\nabla\zeta) = -J(\nabla\psi,\zeta)$$

$$\rightarrow \nabla\zeta(t) \propto \exp(\lambda t) \qquad \lambda = \pm\frac{1}{2}\sqrt{Q} = \pm\frac{1}{2}\sqrt{S_1{}^2 + S_2{}^2 - \zeta^2}$$

$$S_1 = \frac{\partial u}{\partial x} - \frac{\partial v}{\partial y} \quad \text{(stretch deformation)}$$

$$S_2 = \frac{\partial v}{\partial x} + \frac{\partial u}{\partial y} \quad \text{(shear deformation)}$$

$Q > 0$ (strain dominates)

→vorticity gradient will be stretched

$Q < 0$ (vorticity dominates)

→vortex is stable (survival of eyewall meso-vortices)

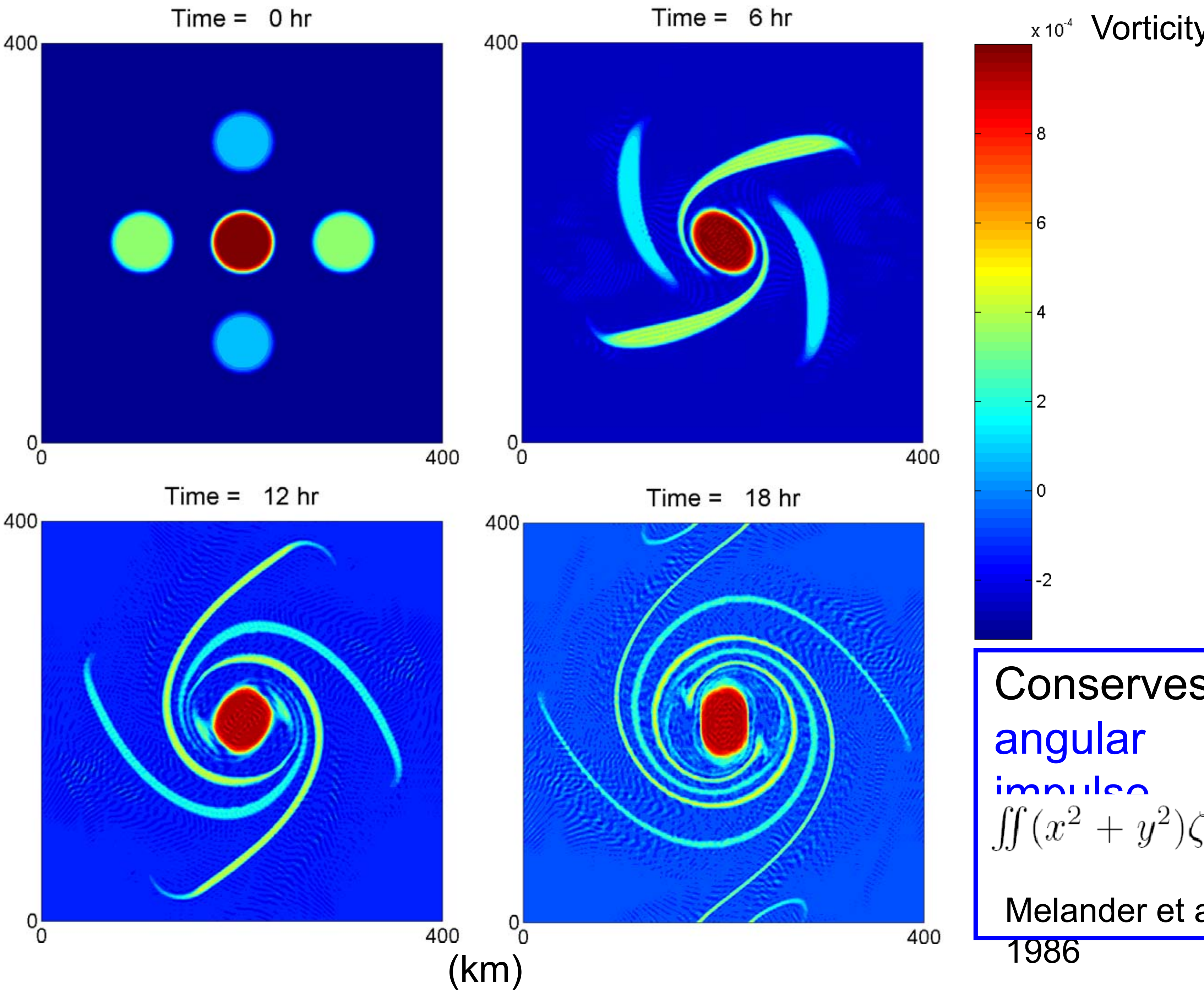

Conserves the angular impulse

$$\iint (x^2 + y^2)\zeta \, dx dy$$

Melander et al. 1986

Non-divergent barotropic model (Nearly Inviscid Fluid)

$$\frac{\partial}{\partial t}\zeta + J(\psi, \zeta) = \upsilon \nabla^2 \zeta \qquad \boxed{\nabla^2 \psi = \zeta}$$

The energy and enstrophy relations

$$\frac{d\mathcal{E}}{dt} = -2\upsilon \mathcal{Z} \qquad \mathcal{E} = \iint \frac{1}{2}\left(u^2 + v^2\right) dx\, dy$$ kinetic energy

$$\mathcal{Z} = \iint \frac{1}{2}\zeta^2\, dx\, dy$$ enstrophy

$$\frac{d\mathcal{Z}}{dt} = -2\upsilon \mathcal{P} \qquad \mathcal{P} = \iint \frac{1}{2}\nabla\zeta \cdot \nabla\zeta\, dx\, dy$$ palinstrophy

Batchelor 1969

$$\frac{d}{dt}\int E(k)dk = 0. \qquad \frac{d}{dt}\left(\int k^2 E(k)dk\right) = \frac{d}{dt}\int Z(k)dk = 0;$$

$$\frac{d}{dt}\left(\int (k-k_1)^2 E(k)dk\right) > 0$$

$$\frac{d}{dt}\left(\int k^2 E(k)dk + k_1^2 \int E(k)dk - 2k_1 \int kE(k)dk\right) > 0$$

$$\frac{d}{dt}\left(\frac{\int kE(k)dk}{\int E(k)dk}\right) < 0,$$

Kinetic energy moves toward large scales

$$\frac{d}{dt}\left(\int (k^2-k_1^2)^2 E(k)dk\right) > 0$$

$$\frac{d}{dt}\left(\int k^2 Z(k)dk + k_1^4 \int E(k)dk - 2k_1^2 \int k^2 E(k)dk\right) > 0$$

$$\frac{d}{dt}\left(\frac{\int k^2 Z(k)dk}{\int Z(k)dk}\right) > 0,$$

Enstrophy moves toward small scales

$E \sim p'^2 / L^2$ (KE) geostrophy

$Z \sim p'^2 / L^4$ (Enstrophy)

KE nearly conserved $L \sim p'$

Enstrophy cascade $L \uparrow$ (L increase Z decrease)

Selective Decay of 2D turbulence

The vortices become, on the average,
larger, stronger, and fewer.

Merger and Axisymmetrization Dynamics

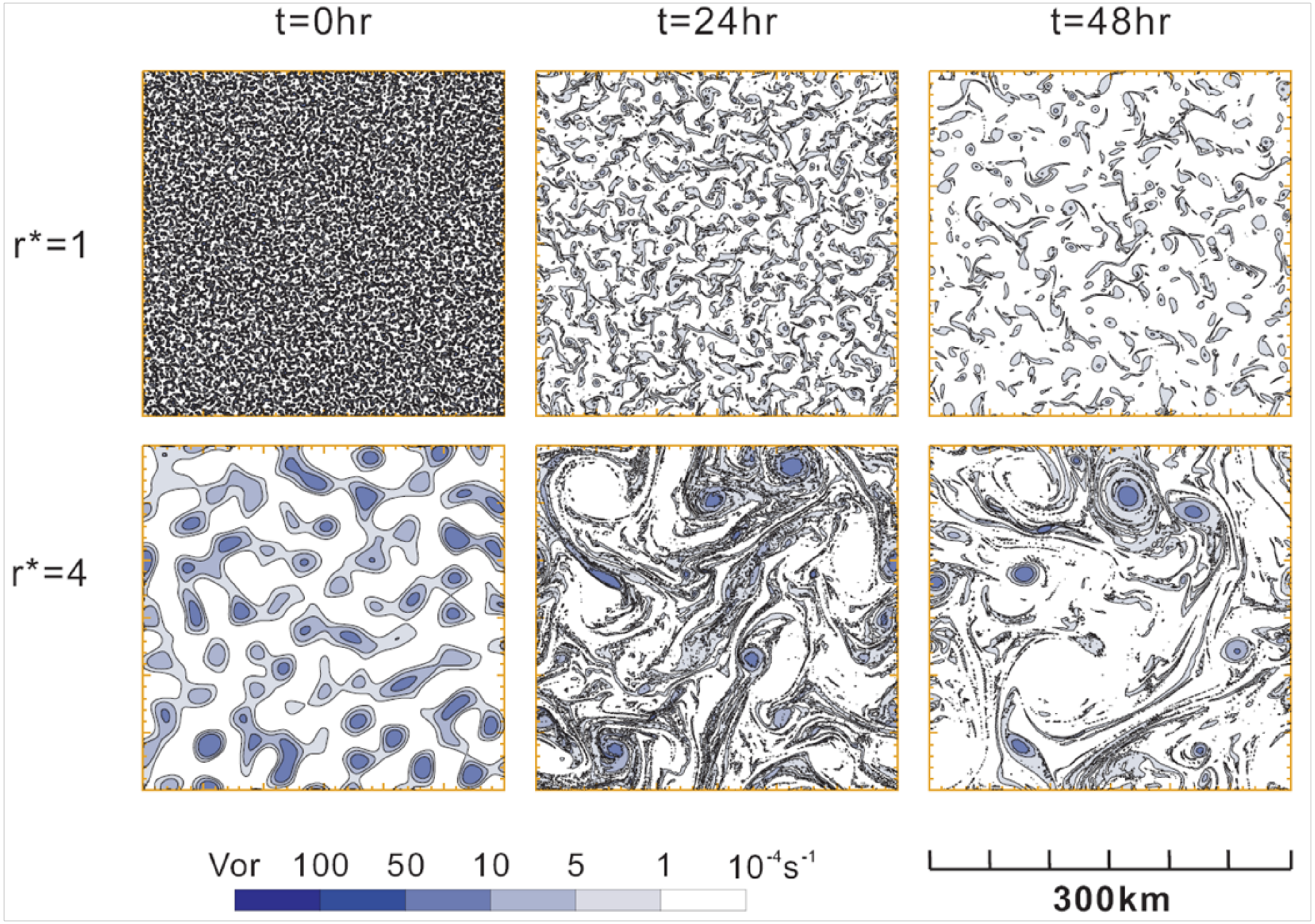

Fewer and stronger vortices !!!

小尺度變大尺度

Coherent structure with filamentations in 2-D turbulence

Huang and Robinson 1998

Forcing added

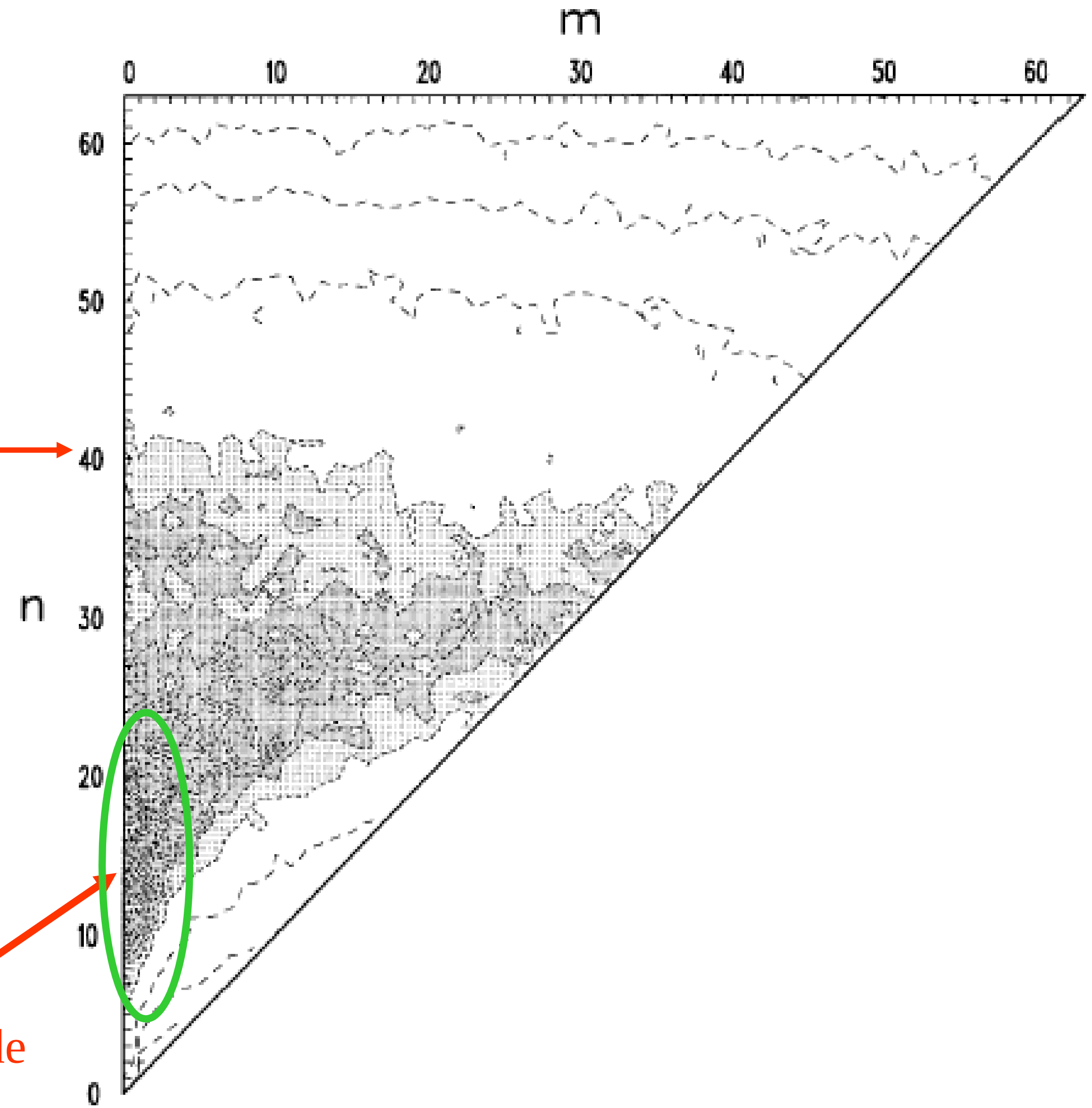

Inverse energy cascade to zonal Harmonics

FIG. 2. Energy spectrum $E(m, n)$ of an ensemble mean at day 80 of 10 decaying turbulence experiments. The magnitude of the spectrum is normalized by the maximum value on the map. Contour levels are 0.0001, 0.001, 0.01, 0.1–0.9 with increment 0.1. Area with $E(m, n) > 0.1$ is lightly shaded, $E(m, n) > 0.2$ heavily shaded.

Huang and Robinson 1998

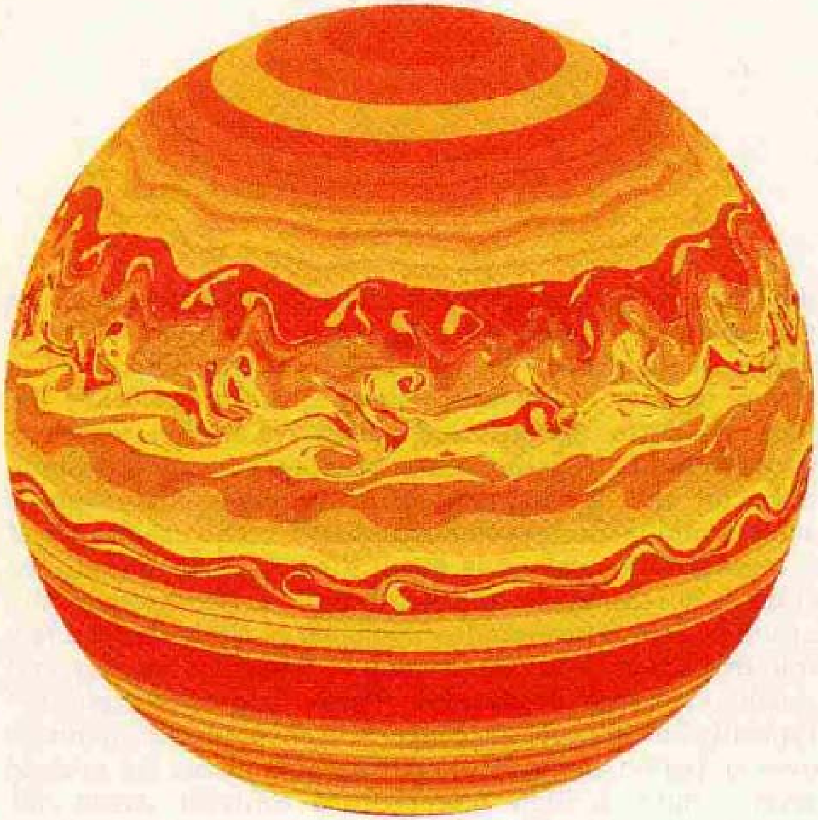

Simulated Jovian atmosphere calculated by contour surgery for a single-layer planetary atmosphere starting with the observed zonal winds of Jupiter.[10] The overall strong potential-vorticity gradient from pole to pole (from positive to negative q) is characteristic of rapid, almost rigid rotation of the atmosphere. Superposed on this global gradient are numerous latitudinal striations indicating zonal gradient reversals, some of which give rise here to nonlinear instabilities. **Figure 4**

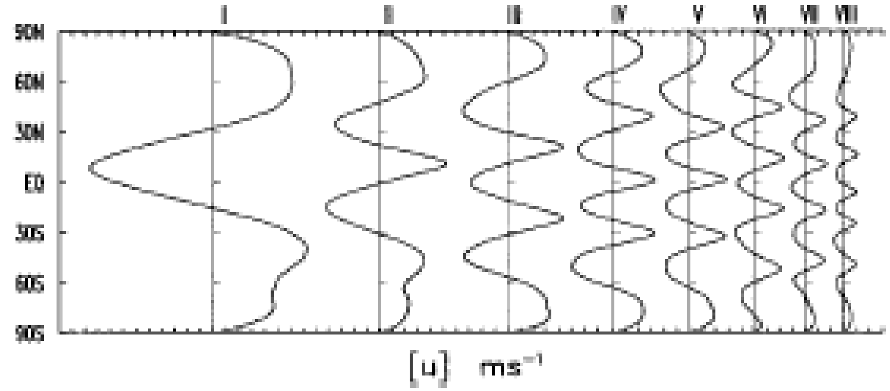

FIG. 4. Time-mean zonal-mean zonal wind profiles for cases I–VIII in Table 1 (the eight open circles in Fig. 3). Each grid on the abscissa represents 1 m s^{-1}.

These alternating Easterly and westerly Jets are similar to observed patterns on Jupiter and Saturn.

Bowmen and Mangus (1993)

Observations of deformation and mixing of the total ozone field in the Antarctic polar vortex

臭氧洞衛星觀測

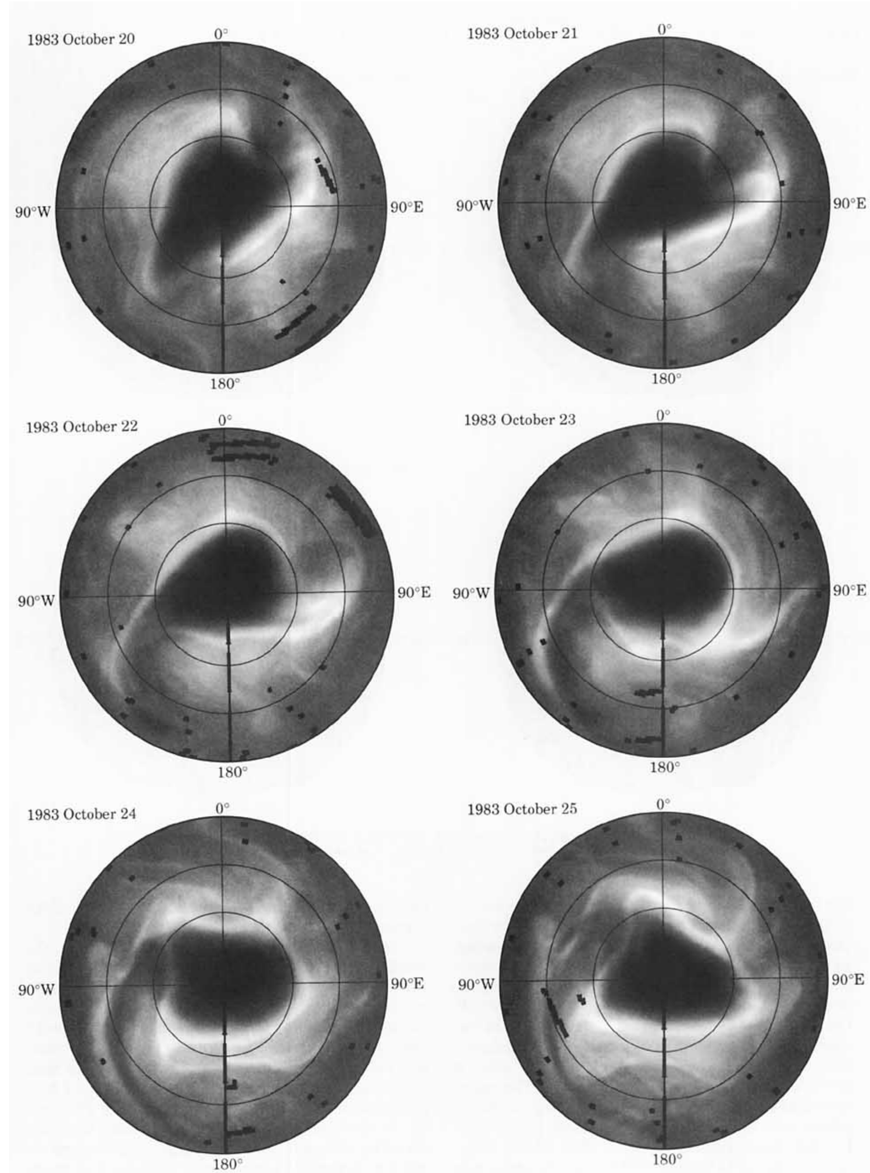

Fig.1: Daily TOMS images of total ozone in the Southern Hemisphere for six consecutive days in October 1983. Latitude circles are drawn at 40°,60°, and 80 °S. The outermost latitude is 20 °S.

Electron density redistribution in experimental plasma physics

single sign charge

+

axial magnetic field

confinement

Axisymmetrization 軸對稱化

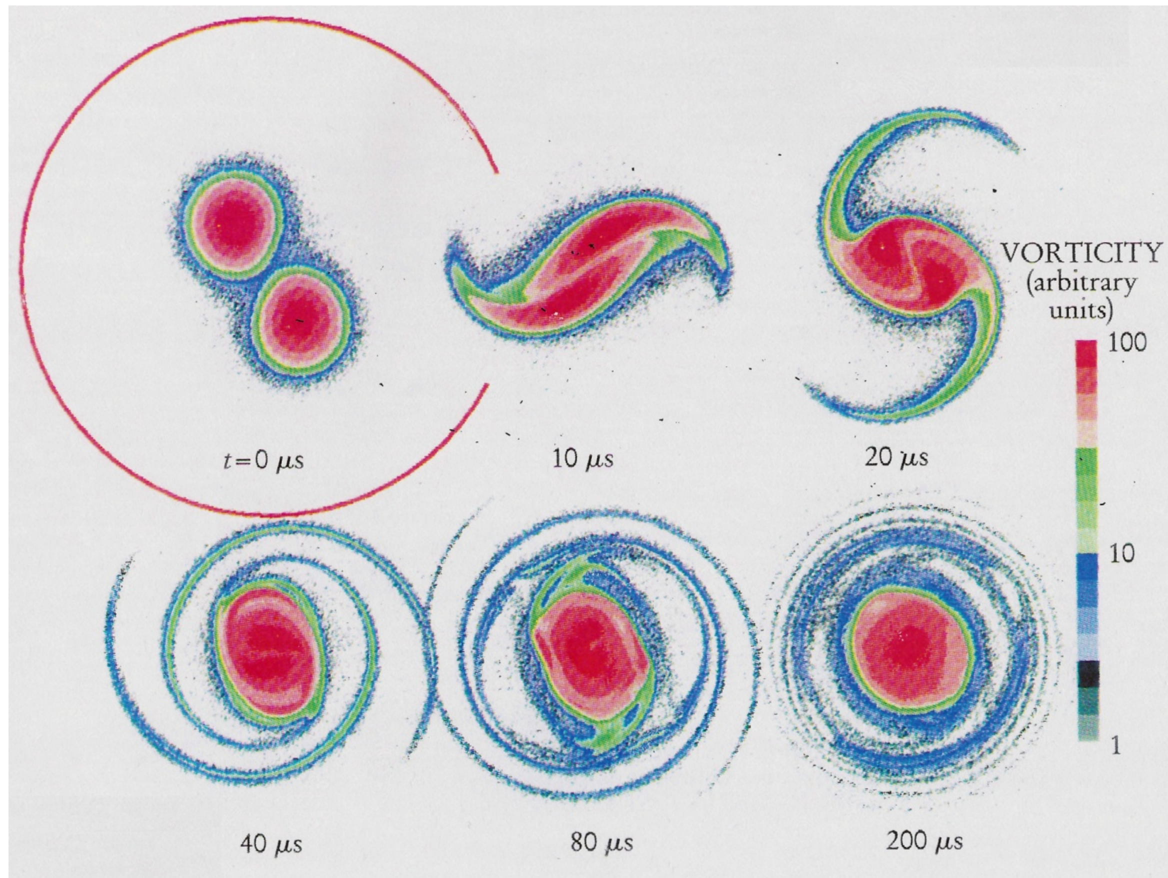

$$\mathbf{E} = -\nabla\psi$$

$$\nabla\cdot\mathbf{E} = -\nabla^2\psi = \frac{\rho}{\epsilon}$$

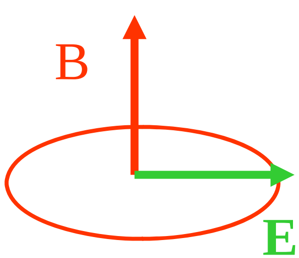

$\vec{\mathrm{E}}\times\vec{\mathrm{B}}$ drift

Coriolis force

Core is protected, thin filaments from edges

Error cut in half since 1990

Edward Fukada

JTWC

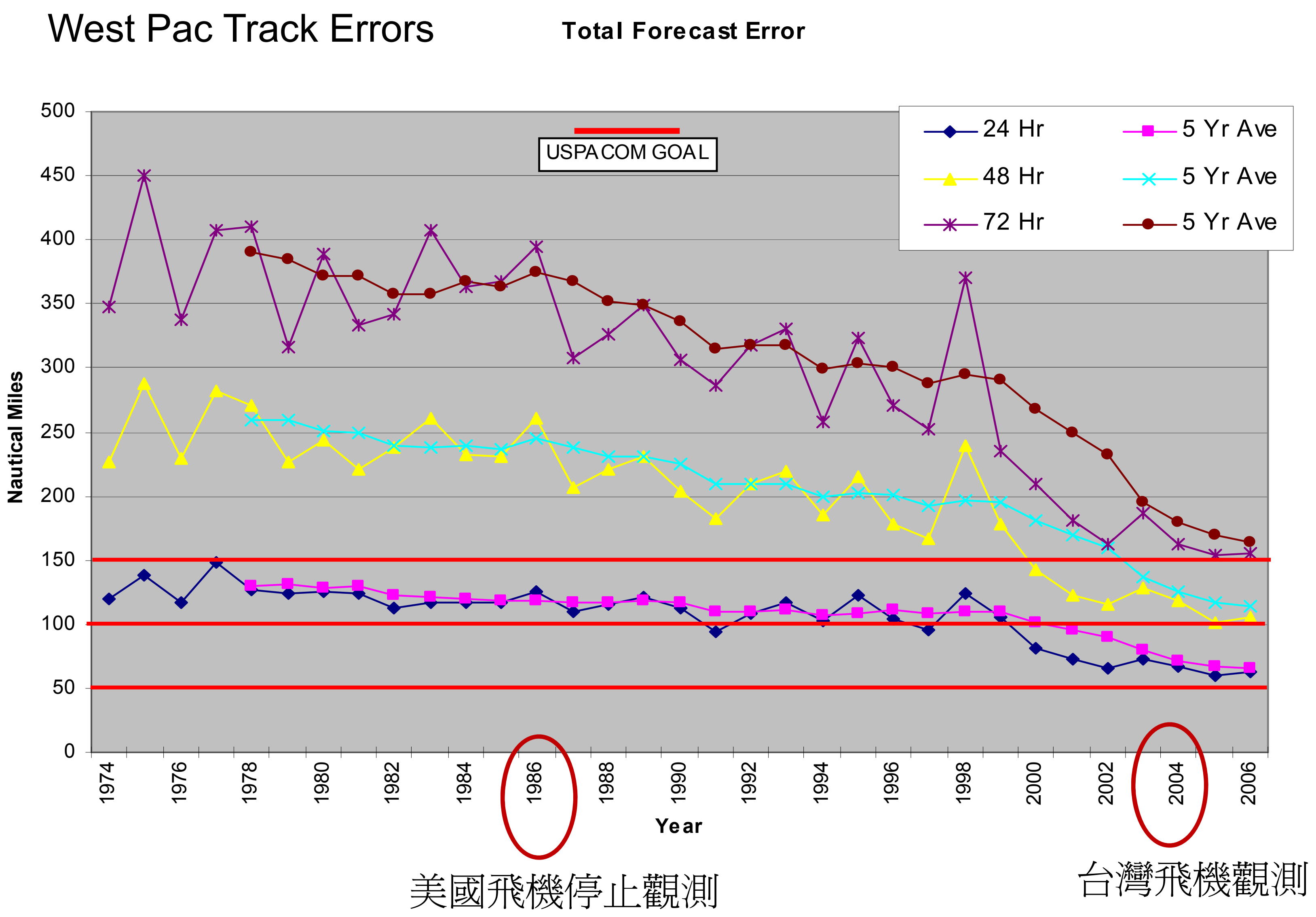

No progress with intensity

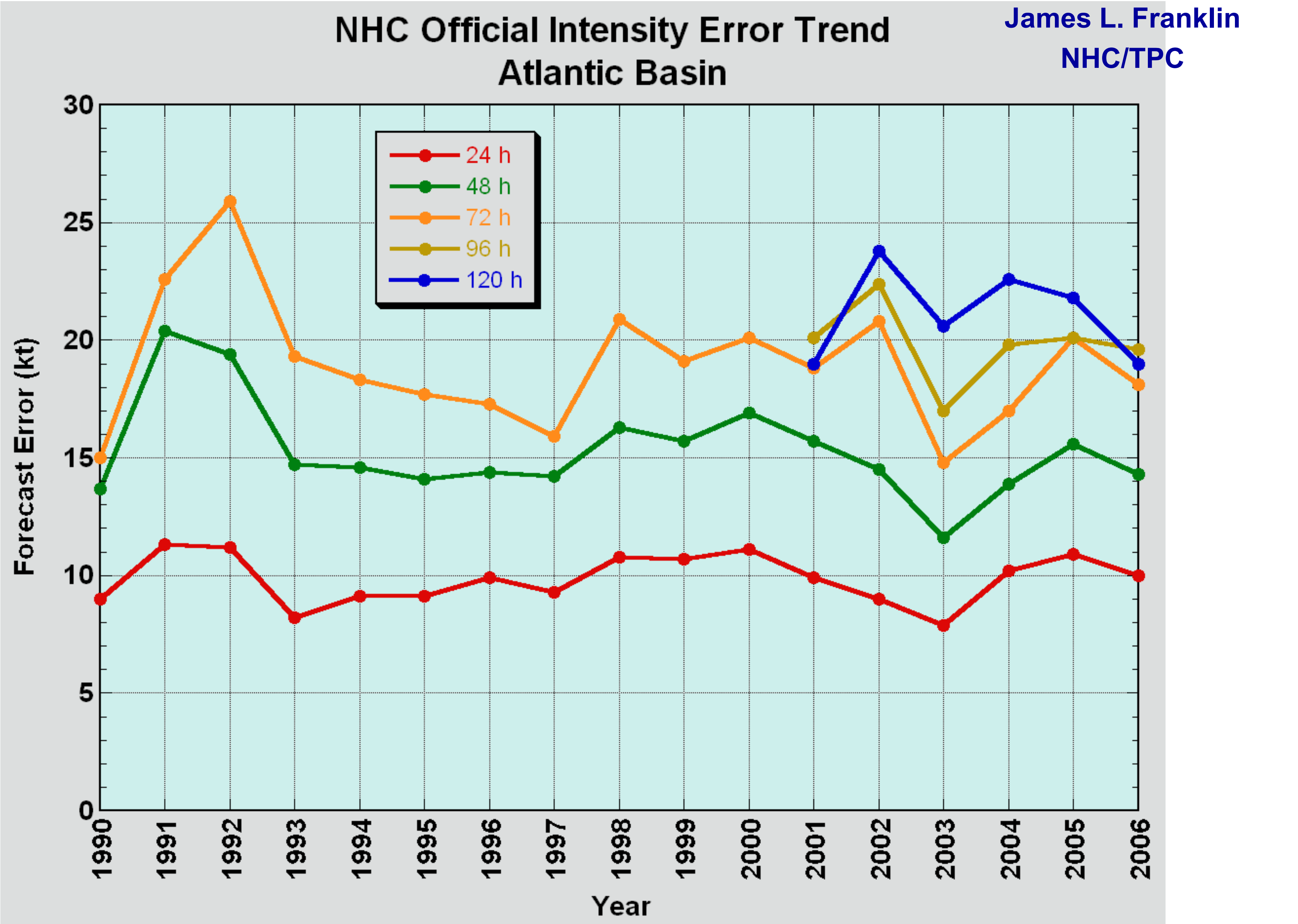

2003.09.01　　杜鵑 颱風

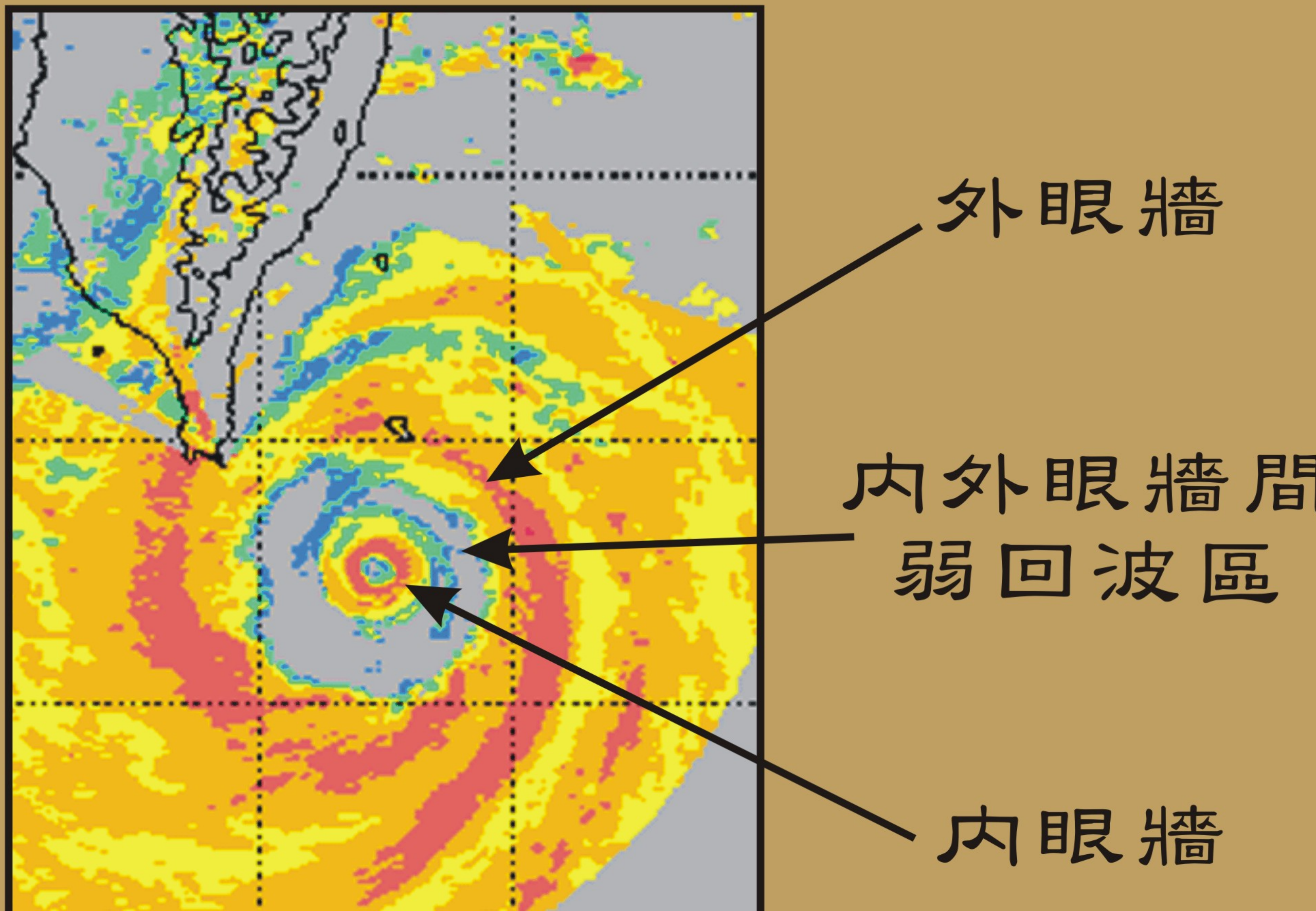

Composite Time Series of the Normalized Intensity

Kuo et al. (2008)

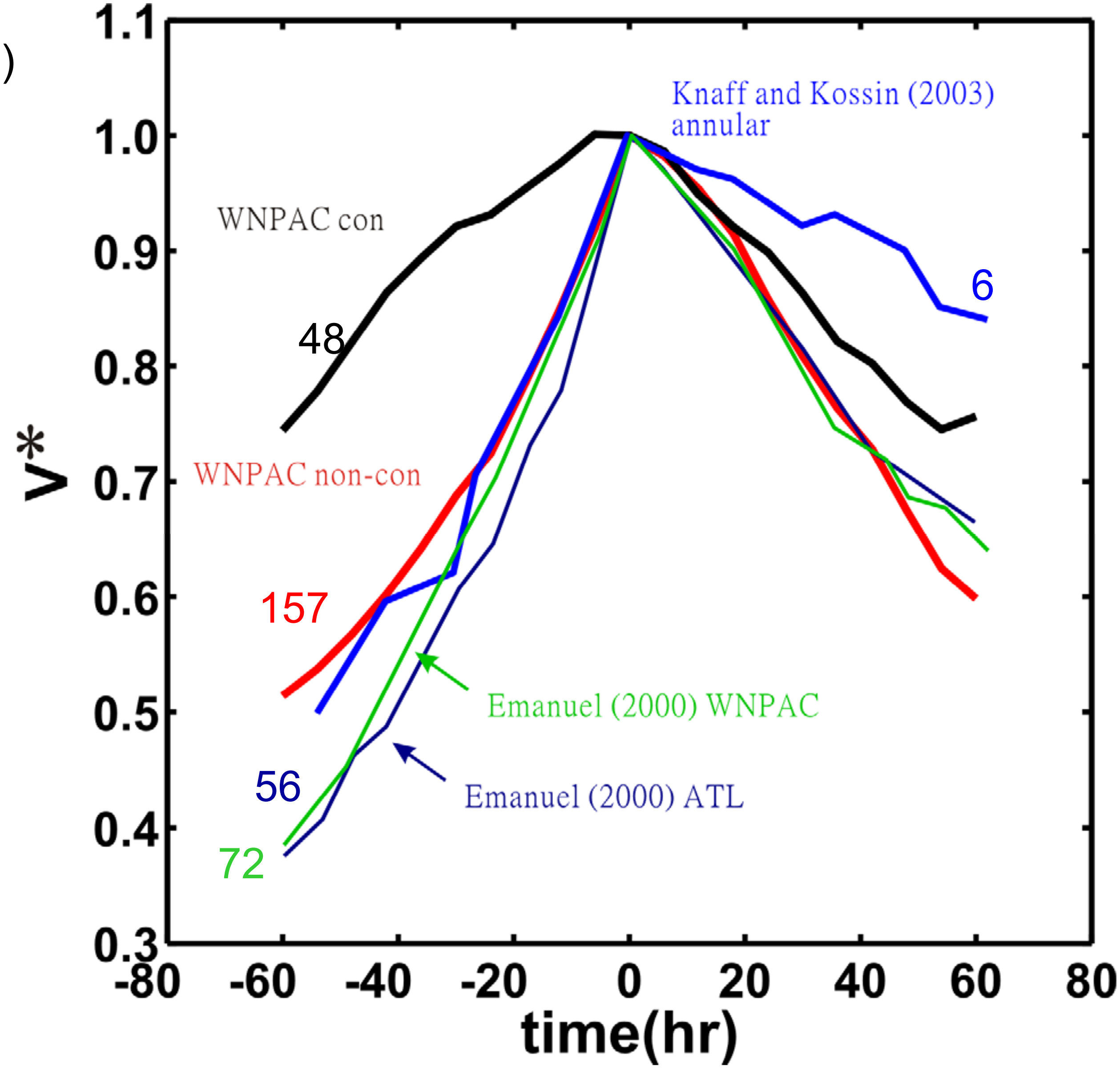

Knaff and Kossin (2003)

- color-enhanced IR image of Hurricane Luis (1995) at 2015 UTC 3 Sep

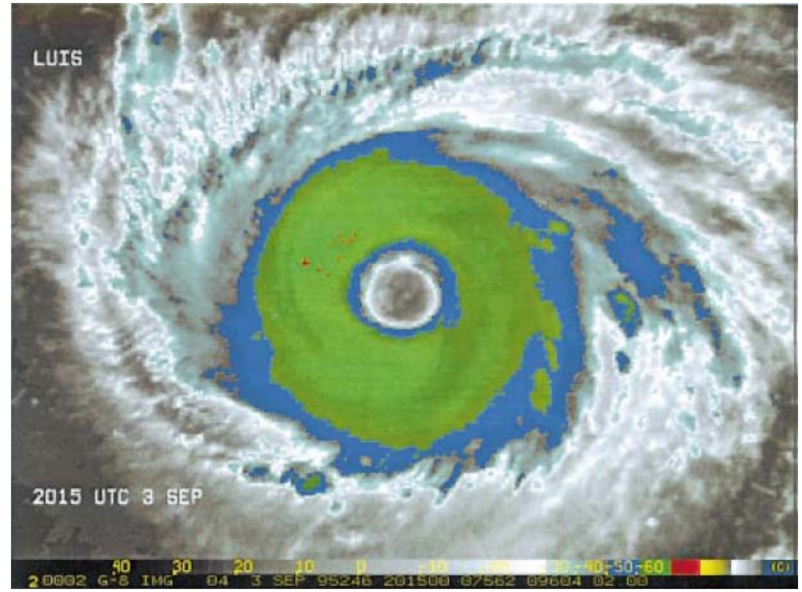

dimensionless	24-h weakening
ATL(56)	0.14
Annular hurricanes(6)	0.05

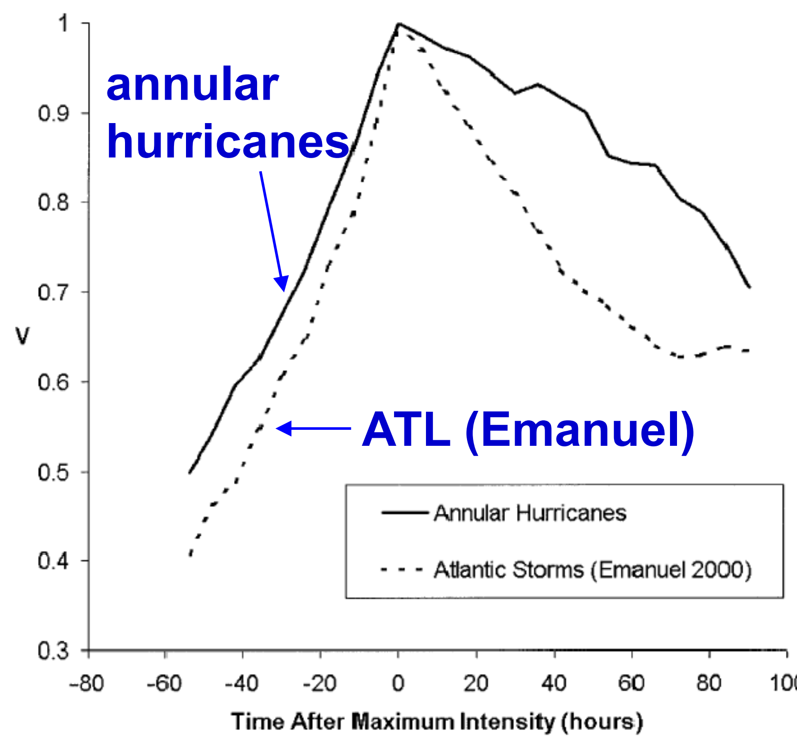

薔蜜颱風
Jangmi

Sep. 2008

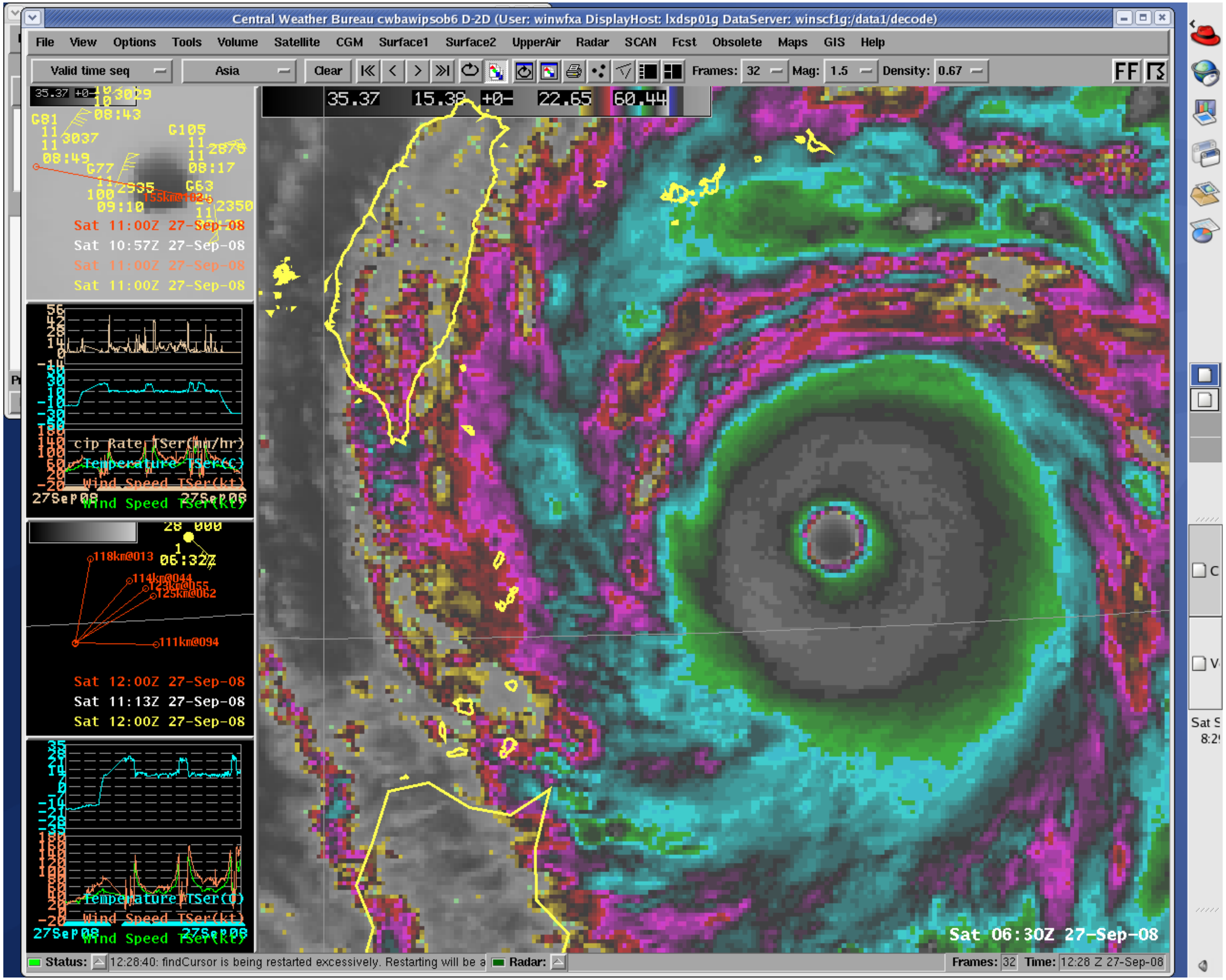

Typhoon Lekima (2001)

0935-1935 LST

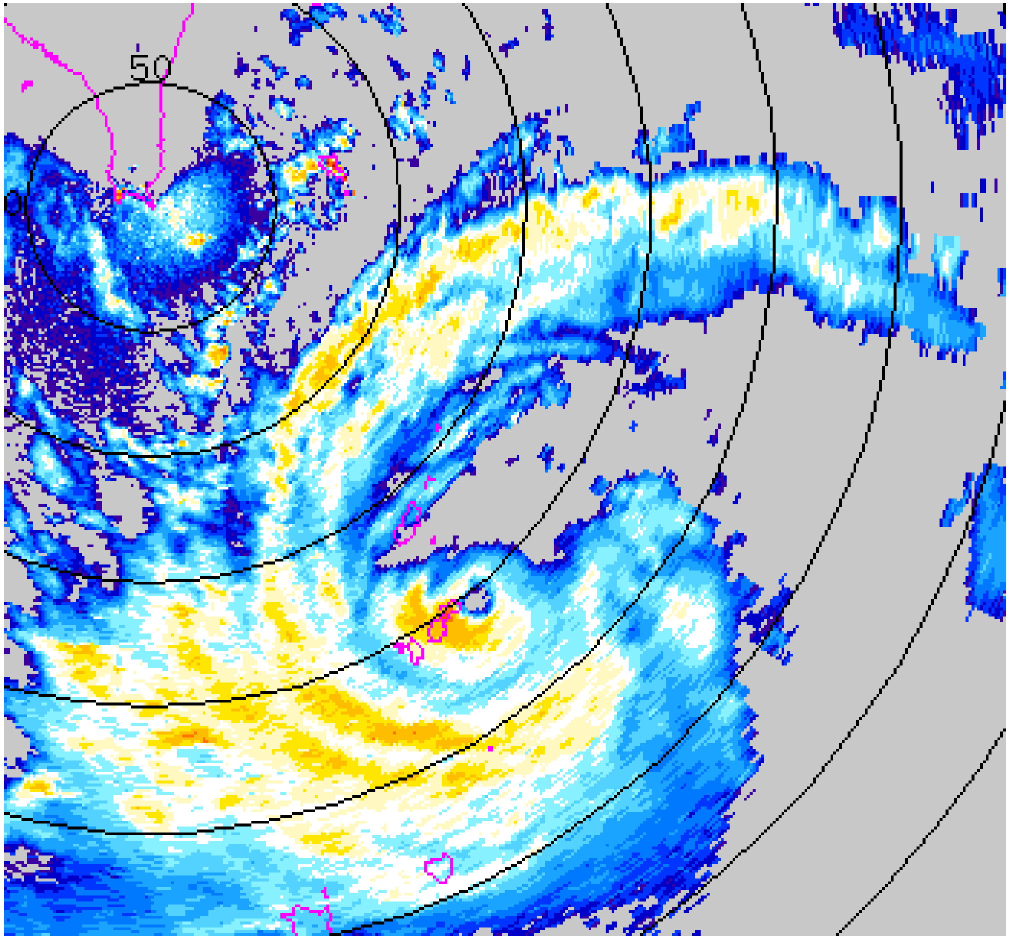

0925 1900LST

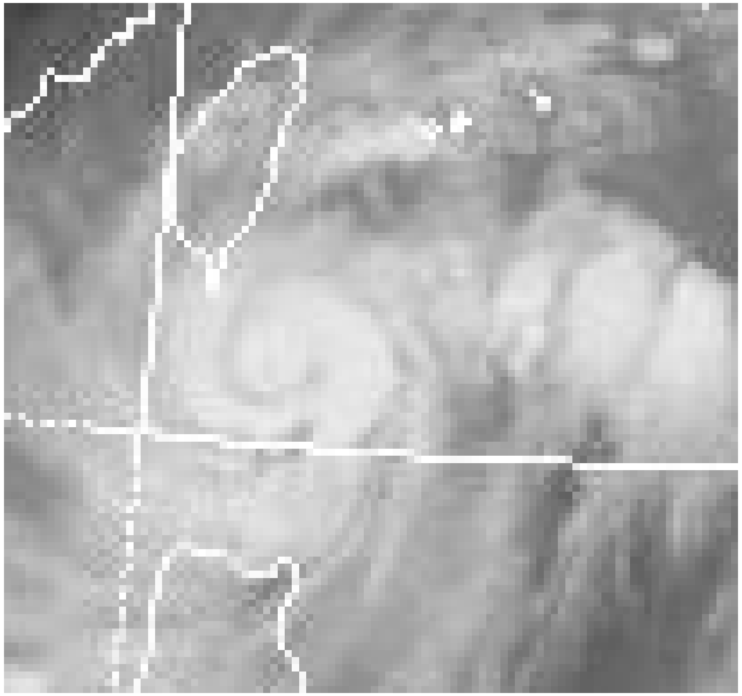

Binary vortex interaction

Kuo et al. (2004)

【Variables】

$$R_1, R_2;\ \Delta;\ \zeta_1, \zeta_2$$

【Parameters】

- Vortex radius ratio $(r) = \dfrac{R_1}{R_2}$
- Dimensionl ess gap $(\dfrac{\Delta}{R_1})$
- Vortex strength ratio $(\gamma) = \dfrac{\zeta_1}{\zeta_2}$

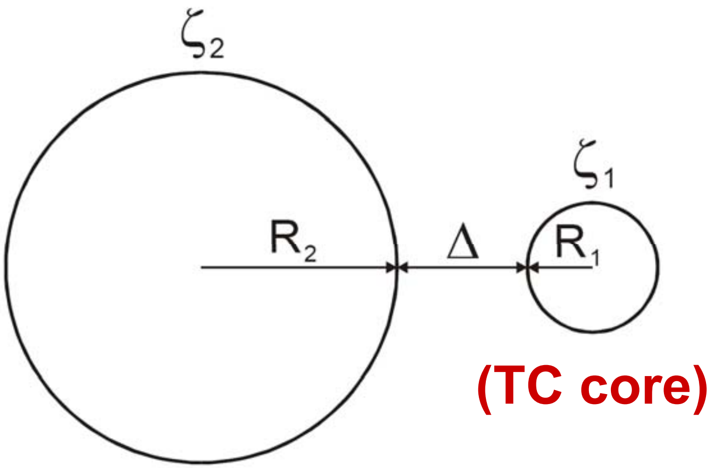

- **An extension of Dritschel and Waugh's (1992) work.**
- **In addition to the radii ratio and the normalized distance between the two vortices, the vorticity ratio is added as a third external parameters.**

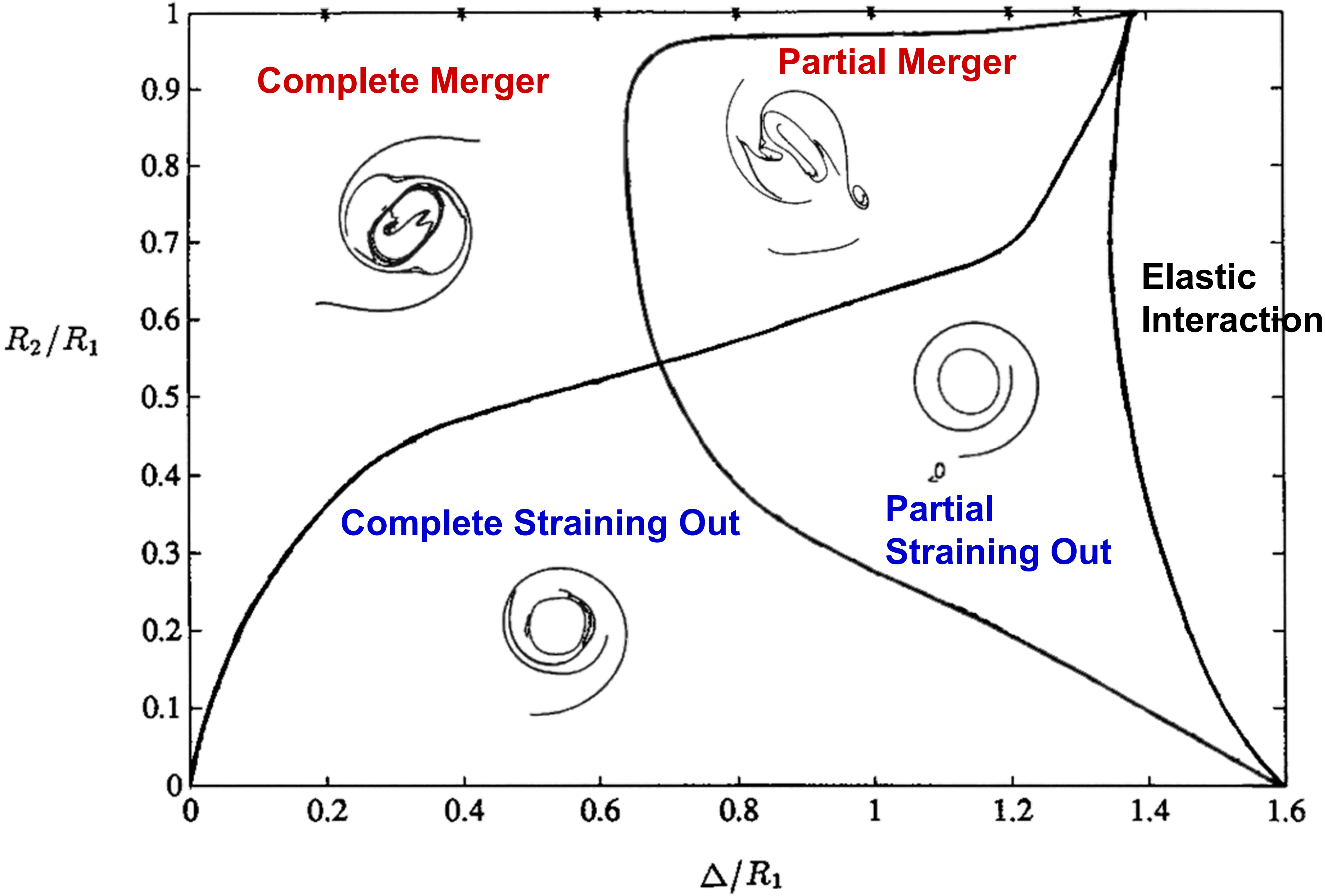

(Adapted from Dritschel and Waugh 1992.)

Examples of the vorticity field at hour 12, showing different classifications of binary vortex interactions involving a skirted core vortex.

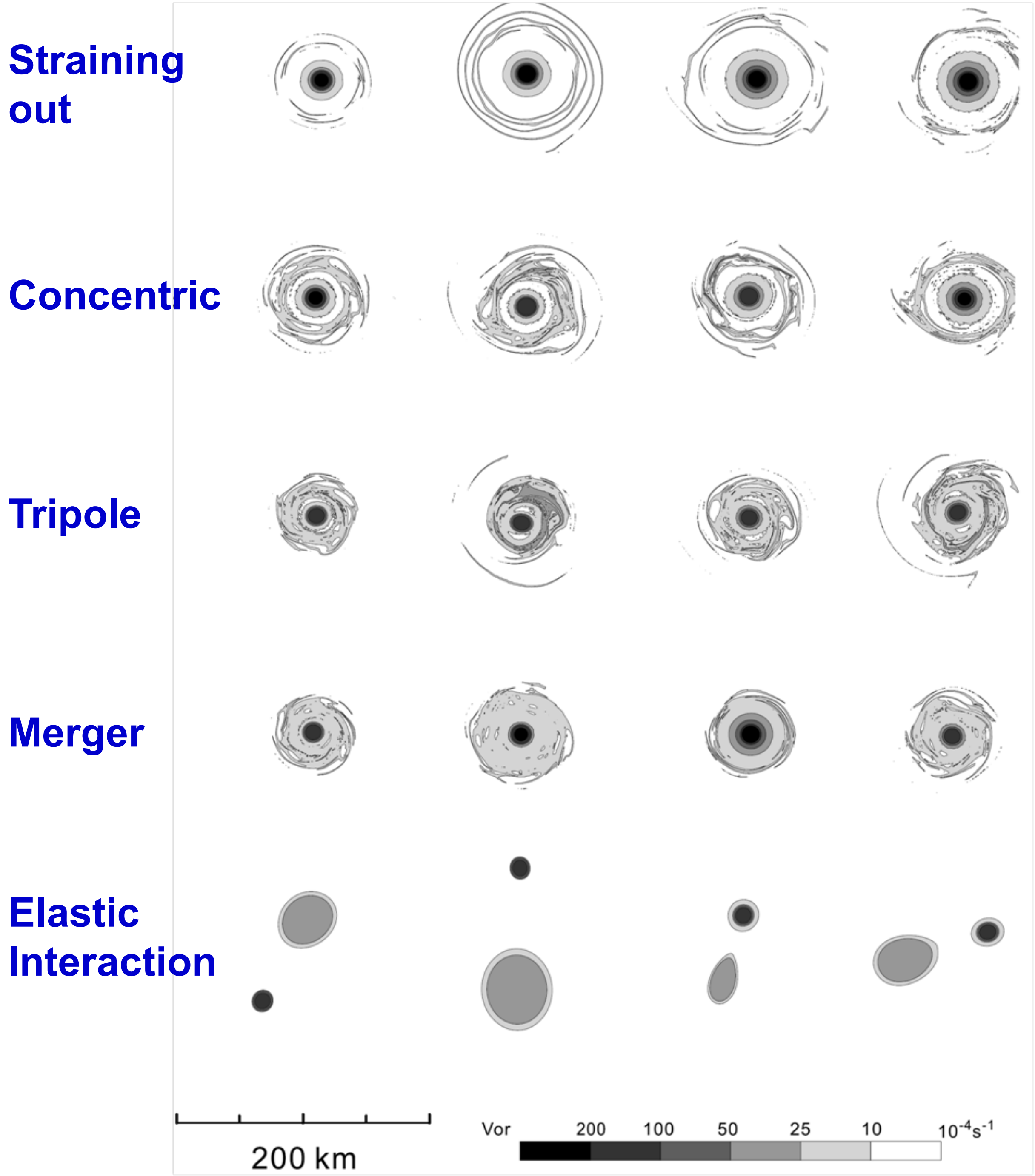

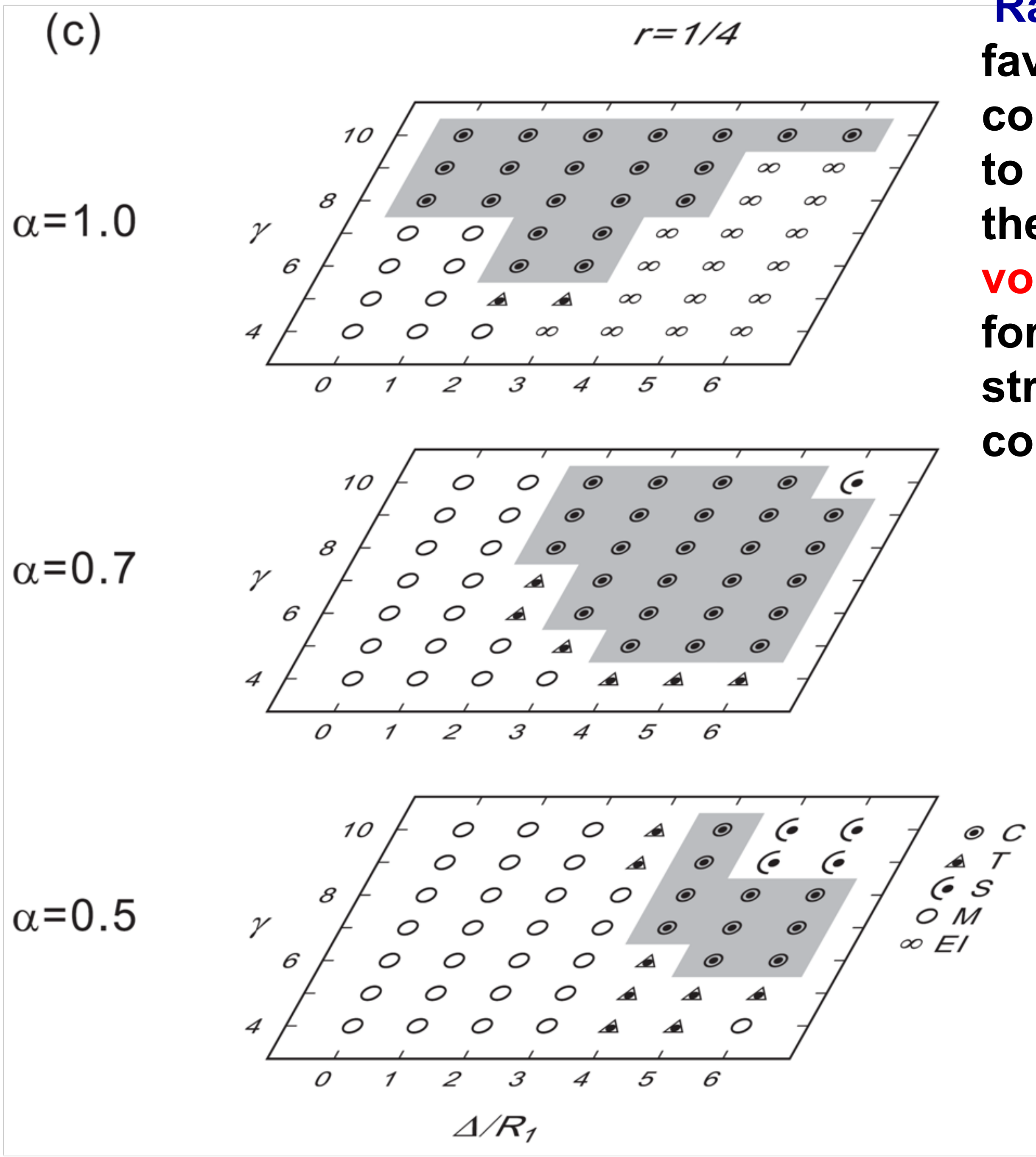

Rankine vortex (α = 1.0) **favors the formation of a concentric structure closer to the core vortex, while the α = 0.7 and α = 0.5 vortices favor the formation of concentric structures farther from the core vortex.**

Examples of asymmetric → symmetric concentric formations.

~ 12 hours.

Initial Δ (outer deep convection region - vortex core distance):

Typhoon Dujuan: nearly 0 km
Typhoon Imbudo nearly 50 km
Typhoon Maemi: nearly 100 km
Typhoon Winnie nearly 260km

A wide range of radii of concentric eyewalls

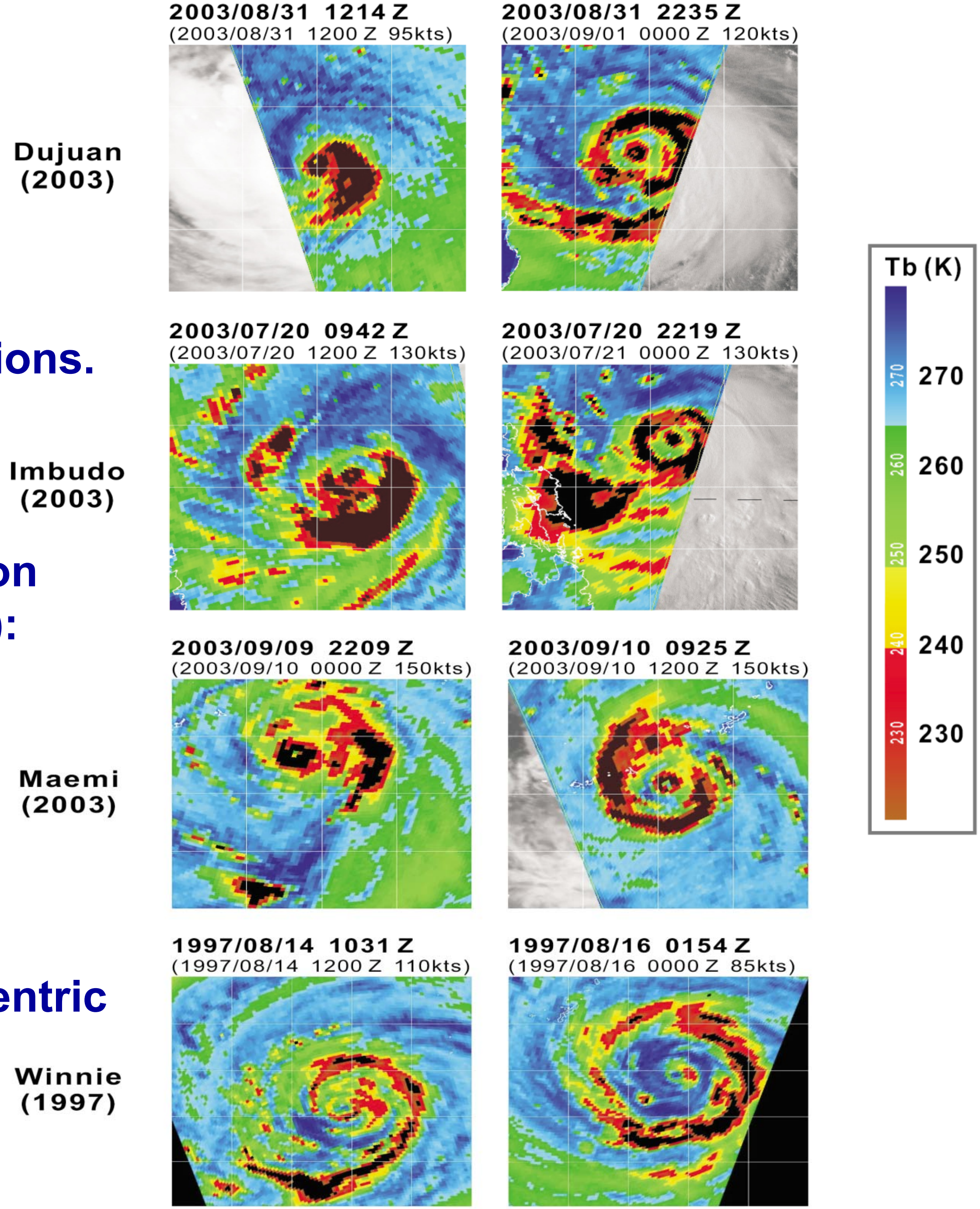

Table 1. List of Secondary Eyewall Formation Hypotheses With Summary of Relevance to our Modeled Hurricanes[a]

Authors	Hypothesis Summary	Relevance to Current Model Results	Type
Willoughby et al. [1982] borrowing from the squall line research of *Zipser* [1977]	Downdrafts from the primary eyewall force a ring of convective updrafts.	Few downdraft-forced updrafts during this time in the simulations.	O
Willoughby [1979]	Internal resonance between local inertia period and asymmetric friction due to storm motion.	No systematic storm motion in the simulated storms.	A
Hawkins [1983]	Topographic effects	No topographic forcing in the simulations.	O
Willoughby et al. [1984]	Ice microphysics	"Warm-rain" (no-ice) sensitivity case also produces secondary eyewall.	A
Molinari and Skubis [1985] and *Molinari and Vallaro* [1989]	Synoptic-scale forcings (e.g., inflow surges, upper-level momentum fluxes)	No synoptic-scale forcings in the simulations	O
Montgomery and Kallenbach [1997], *Camp and Montgomery* [2001] and *Terwey and Montgomery* [2003]	Internal dynamics-axisymmetrization via sheared vortex Rossby wave processes; collection of wave energy near stagnation or critical radii	Possible explanation	N
Nong and Emanuel [2003]	Sustained eddy momentum fluxes and WISHE feedback	Possible explanation	A
Kuo et al. [2004, 2008]	Axisymmetrization of positive vorticity perturbations around a strong and tight core of vorticity.	Possible explanation	N

[a]The type column refers to the type of model or observations that were used to formulate the hypothesis. O stands for observationally-based; A stands for axisymmetric model; N stands for nonaxisymmetric model.

$$\vec{f} = 2\Omega\cos\phi\,\hat{j} + 2\Omega\sin\phi\,\hat{k}$$

$$\vec{f} \cong 2\Omega\sin\varphi\,\hat{k}$$

deep atmosphere
(Jupiter??)

shallow atmosphere
(Earth)

$z << a$

traditional
approximation

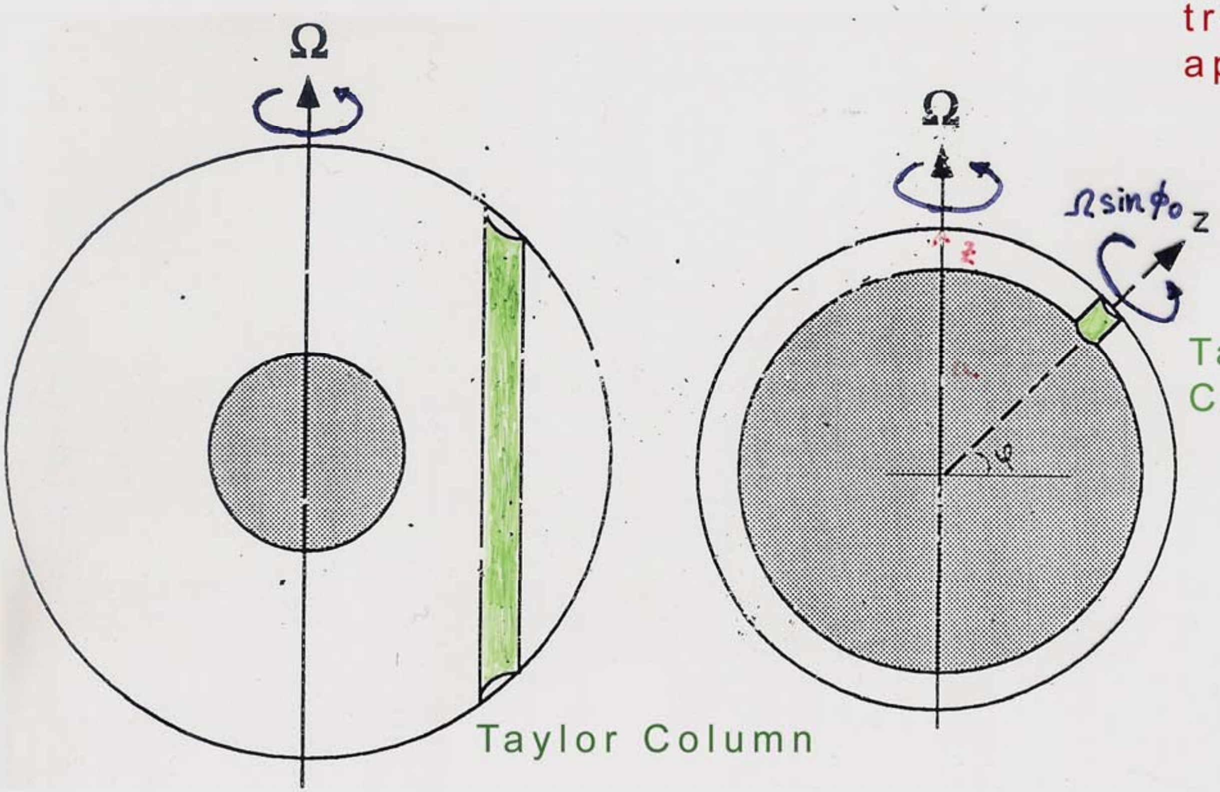

Taylor
Column

ECMWF 資料分析
1980~1987年6.7.8月850mb
平均氣流場與渦度擾動場

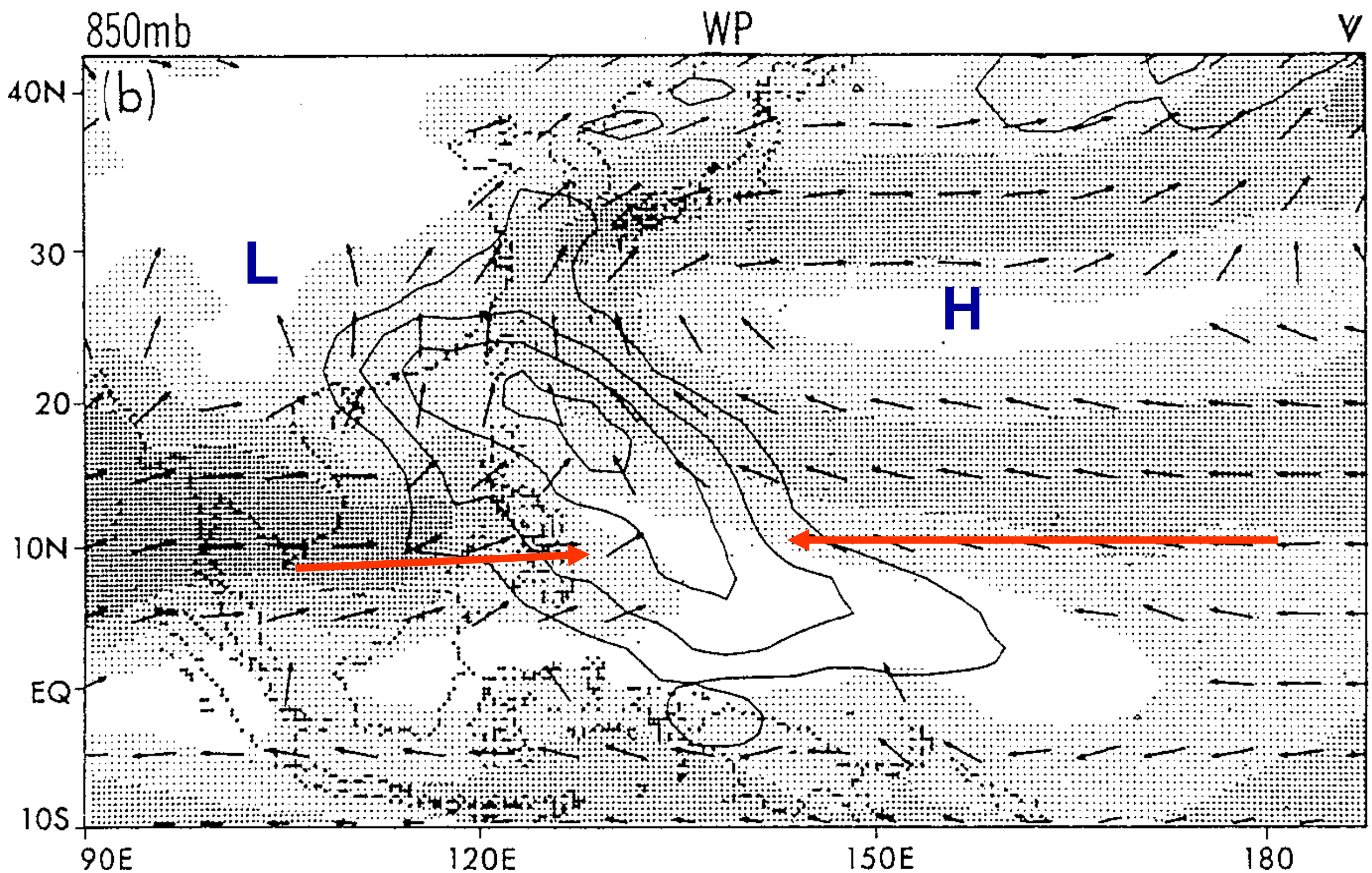

Lau and Lau, 1990

利用NCEP資料分析1994年8月10日~8月20日 850 hPa 絕對渦度

10 August 1994

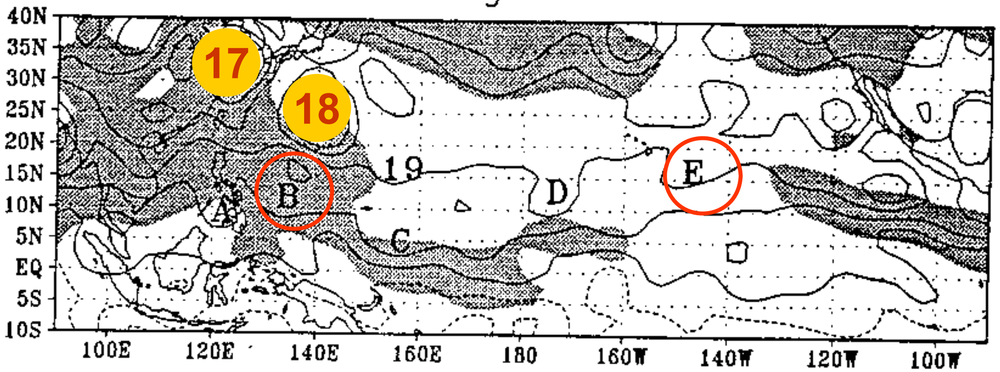

15 August 1994

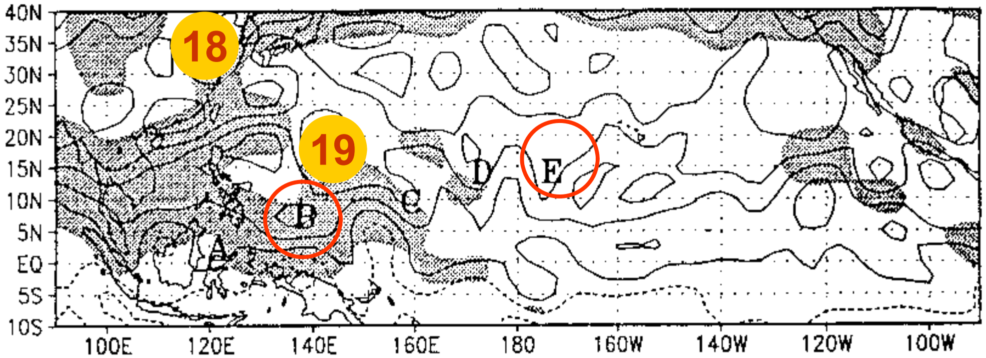

20 August 1994

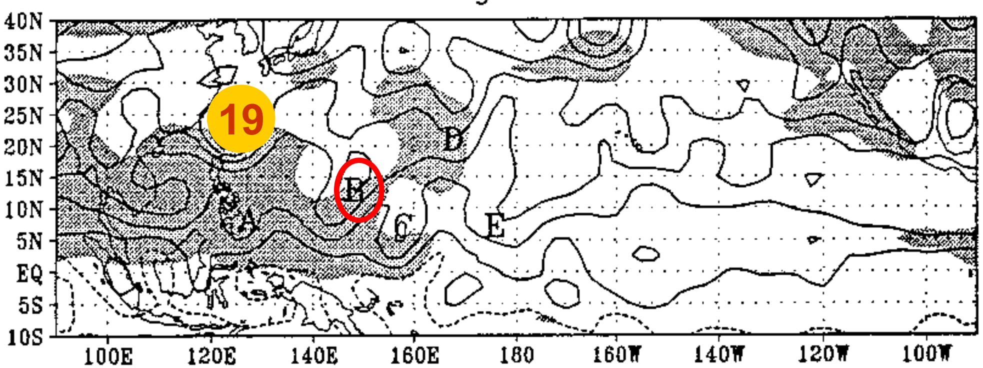

- 波動振幅增加
- 波動在東西方向尺度壓縮
- 颱風有連續生成的現象

Sobel and Bretherton(1998)

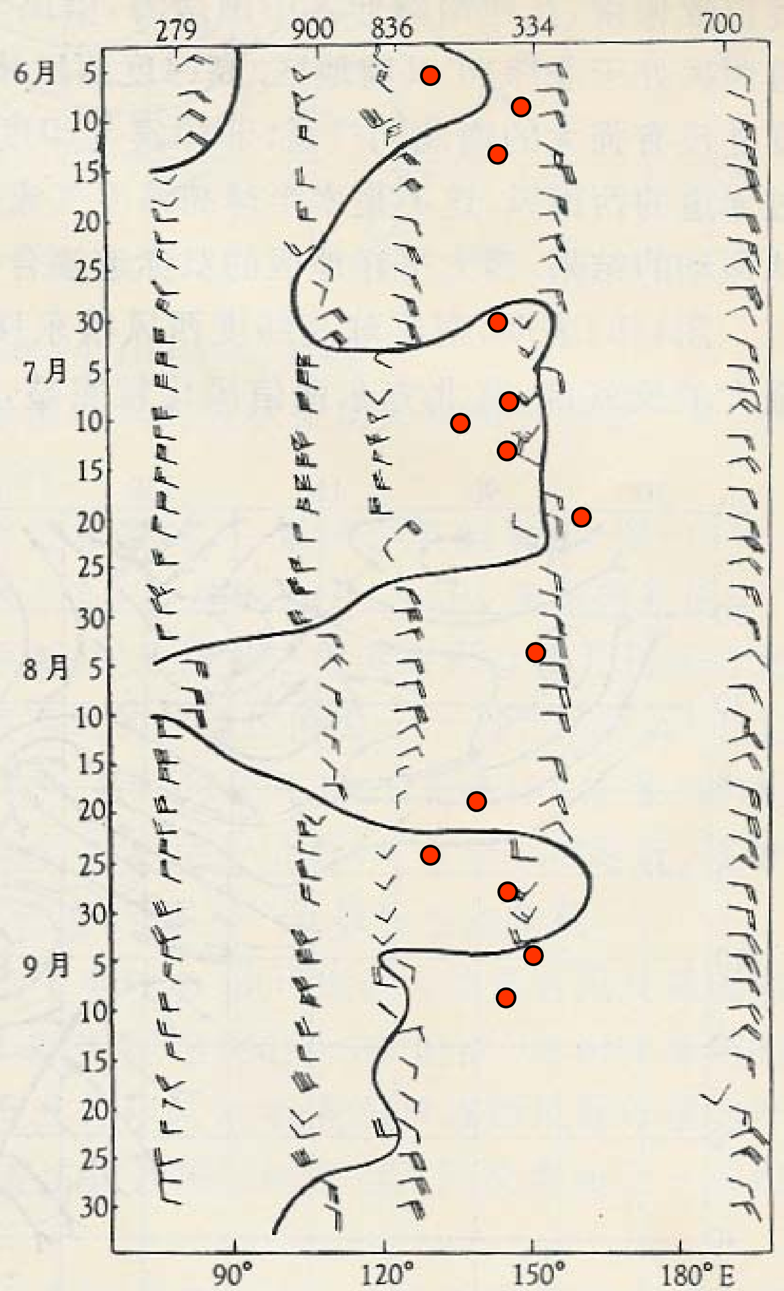

图3　1958年6～9月印度南端到太平洋赤道附近700 hPa东西风分界线与台风发生的关系

- ➢颱風生成有群聚以及連續生成的特性
- ➢Clustering

- ➢東西風分界線有低頻震盪的現象
- ➢Low frequency

謝與陳(1963)

Nondivergent barotropic vorticity model

$$\frac{\partial \zeta'}{\partial t} = -\left(\frac{\partial L_1 + N_1}{\partial x} + \frac{\partial L_2 + N_2}{\partial y} \right) - \beta v' - \hat{D}\zeta' - \gamma\zeta' - F$$

Linear terms

$$L_1 = \bar{u}\zeta' + \bar{\zeta}u'$$

$$L_2 = \bar{v}\zeta' + \bar{\zeta}v'$$

$\gamma\zeta'$:The dissipation timescale of Rayleigh friction term （15 days）

Nonlinear terms

$$N_1 = u'\zeta'$$

$$N_2 = v'\zeta'$$

F :Rossby wave maker

$-\hat{D}\zeta'$:The convergence forcing of ζ' by the large-scale convection

Domain size:24000km×12000km resolution:100km

(I) opposing current :

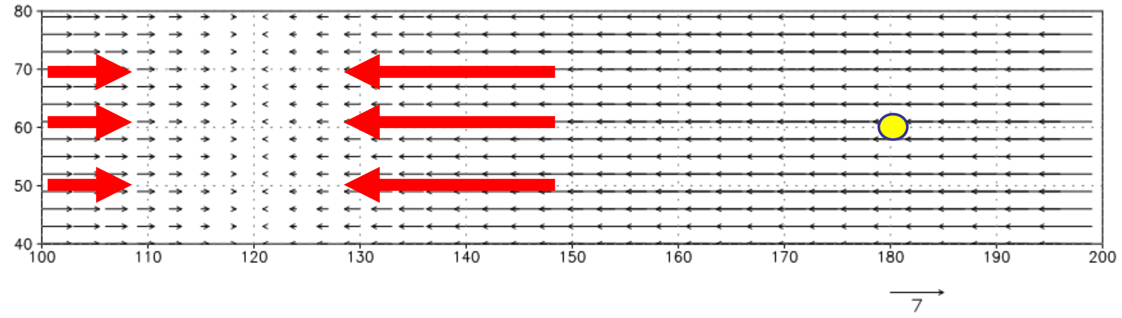

vorticity

linear

non-linear

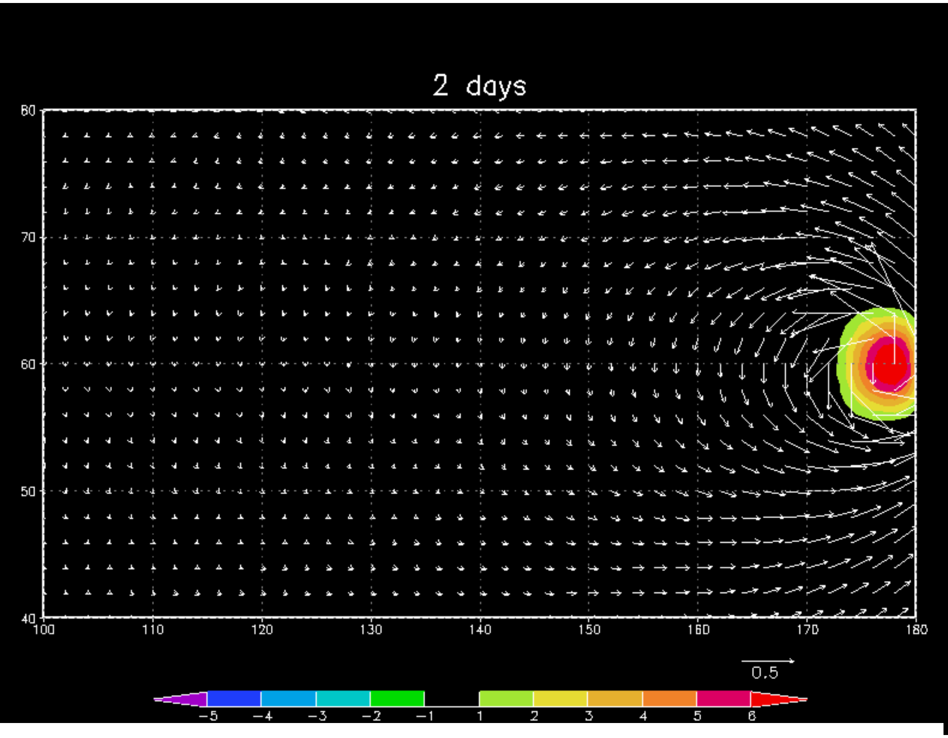

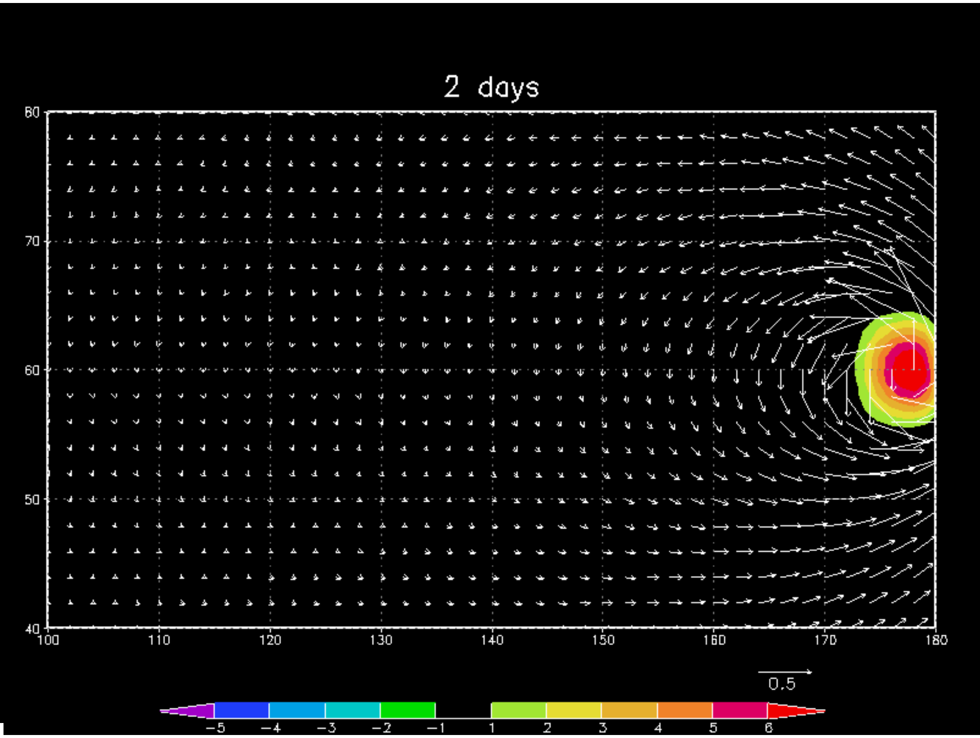

Kuo et. al. *, 2001*

Opposing zonal currents

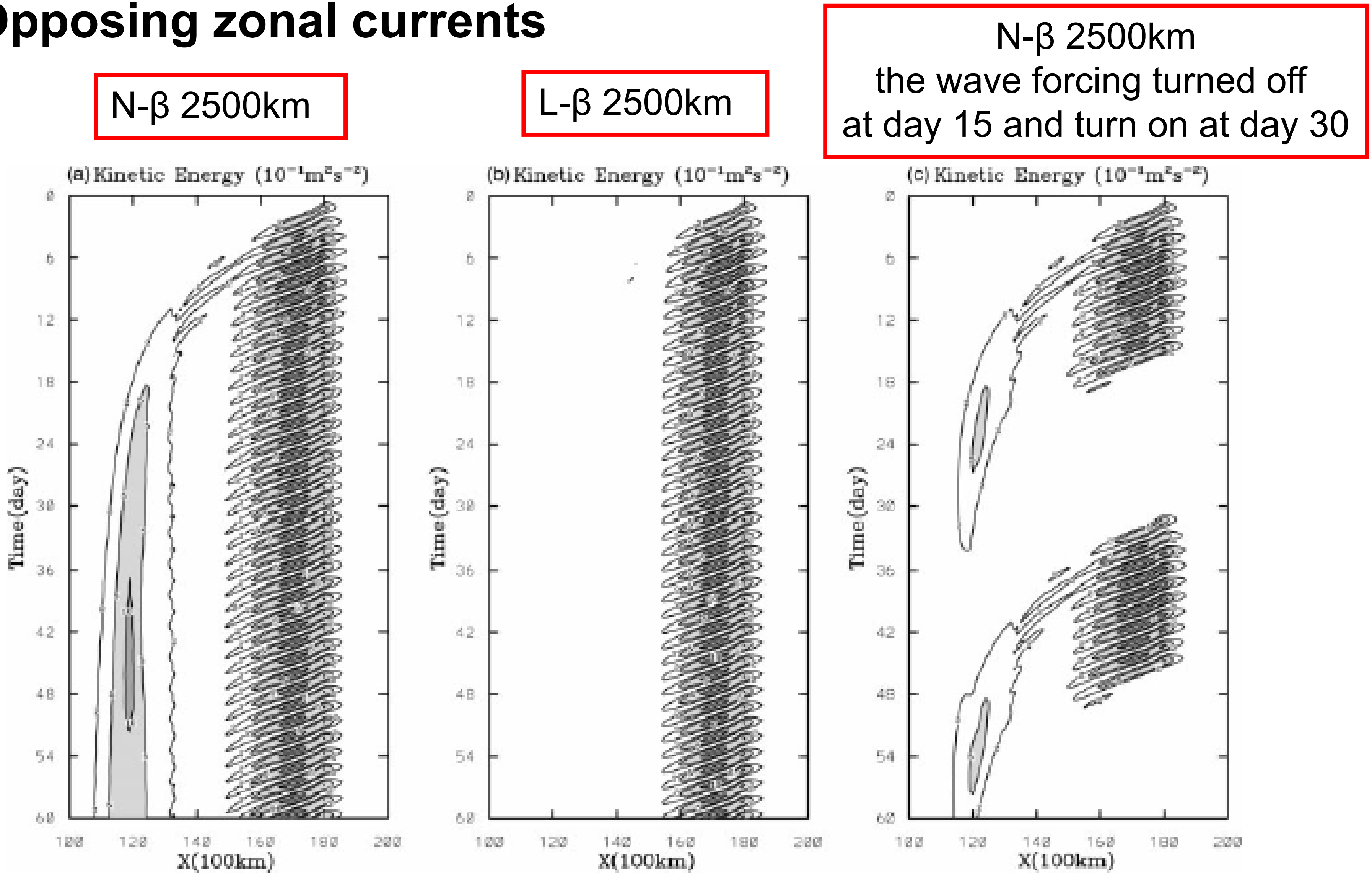

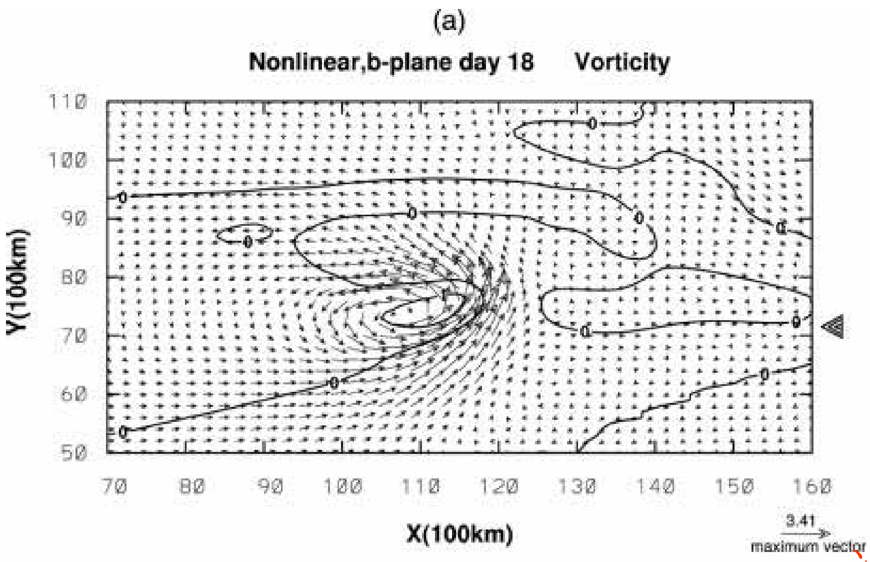

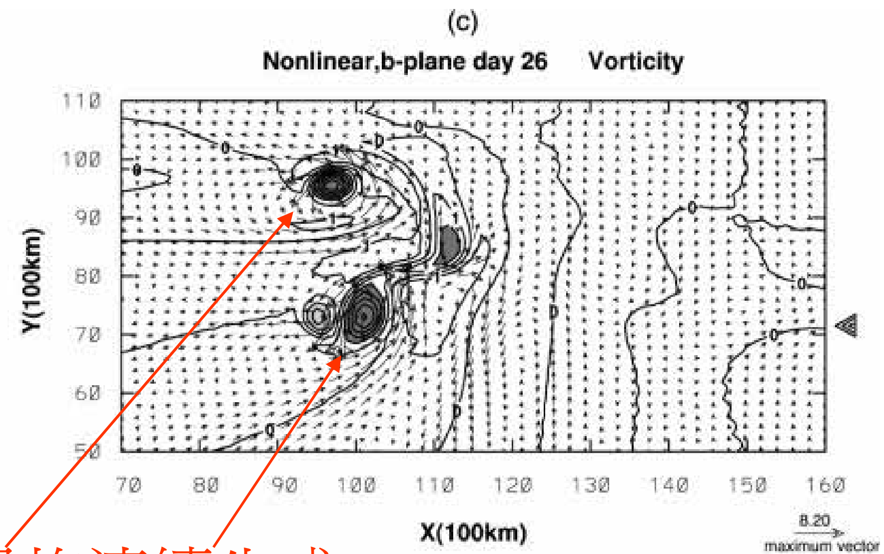

渦旋連續生成

Beta Rossby number (V/ β r ^2) ~ 1

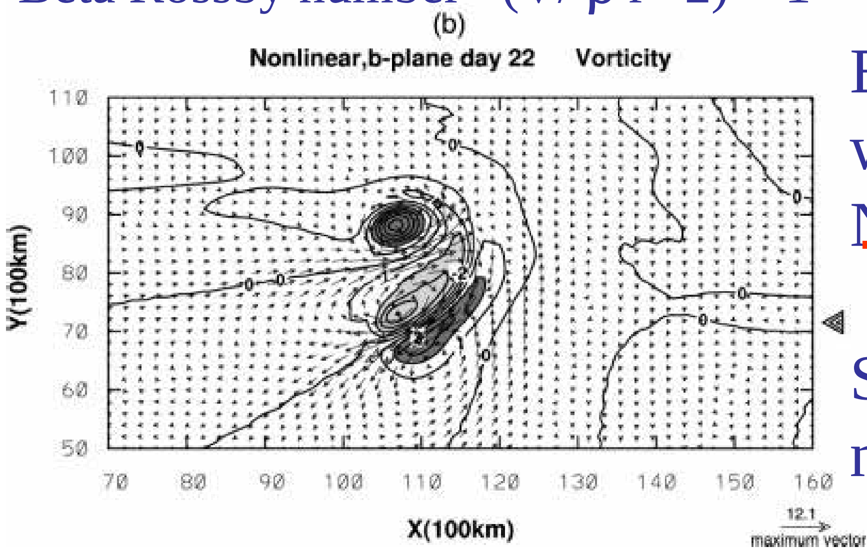

Emergence of vortex from Rossby wave energy dispersion by the Nonlinear dynamics

Sharpening of gradient by the monsoon flow

FIG. 11. Same as in Fig. 10 except for the nonlinear β-plane calculation.

Kuo et al. 2001

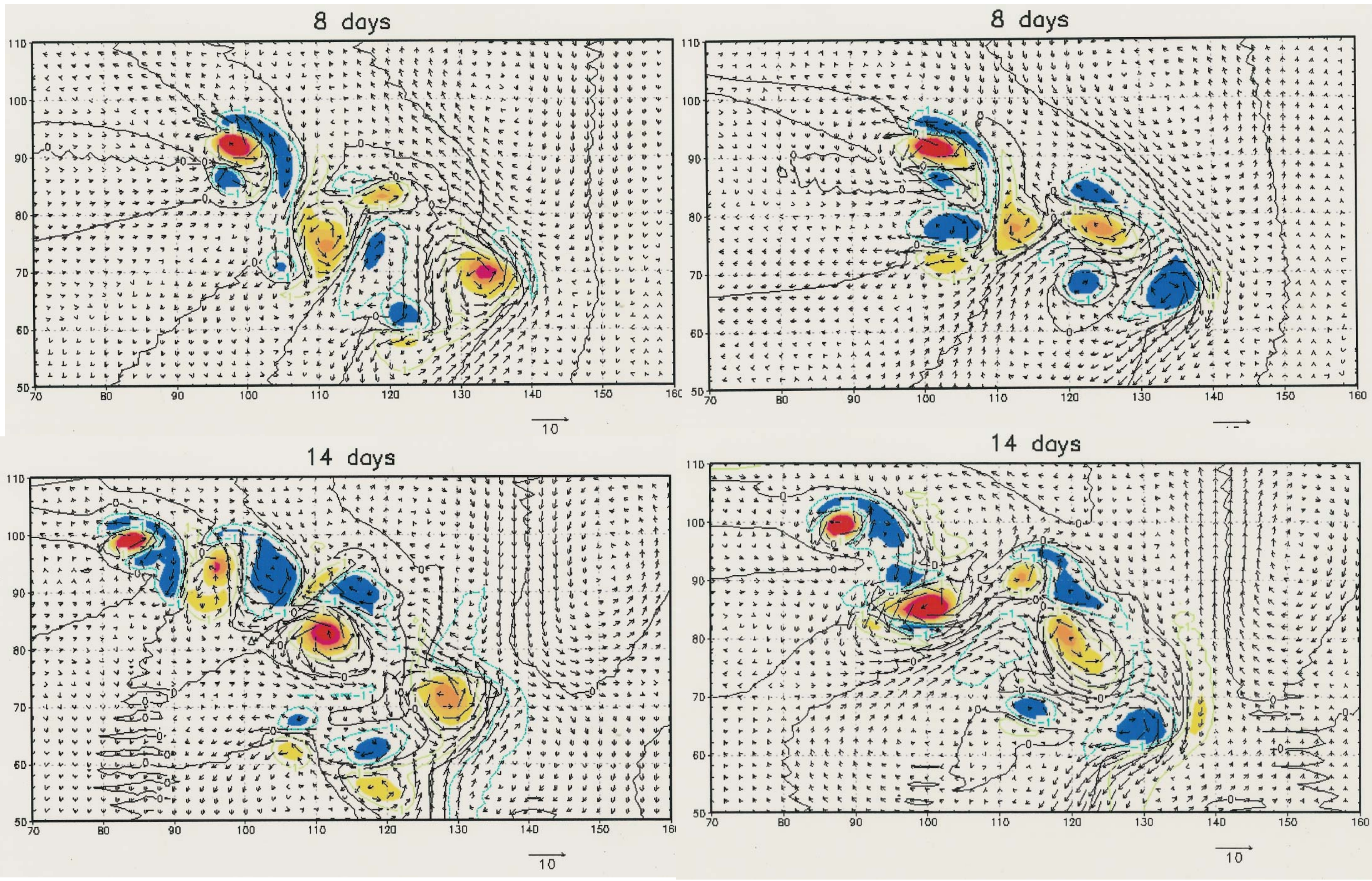

8 days
8 days
14 days
14 days
110
100
90
80
70
60
50
70
80
90
100
110
120
130
140
150
160
10

反聖嬰年九月或十月容易有強颱侵襲中國東南沿海

Tropical Cyclone Track Density

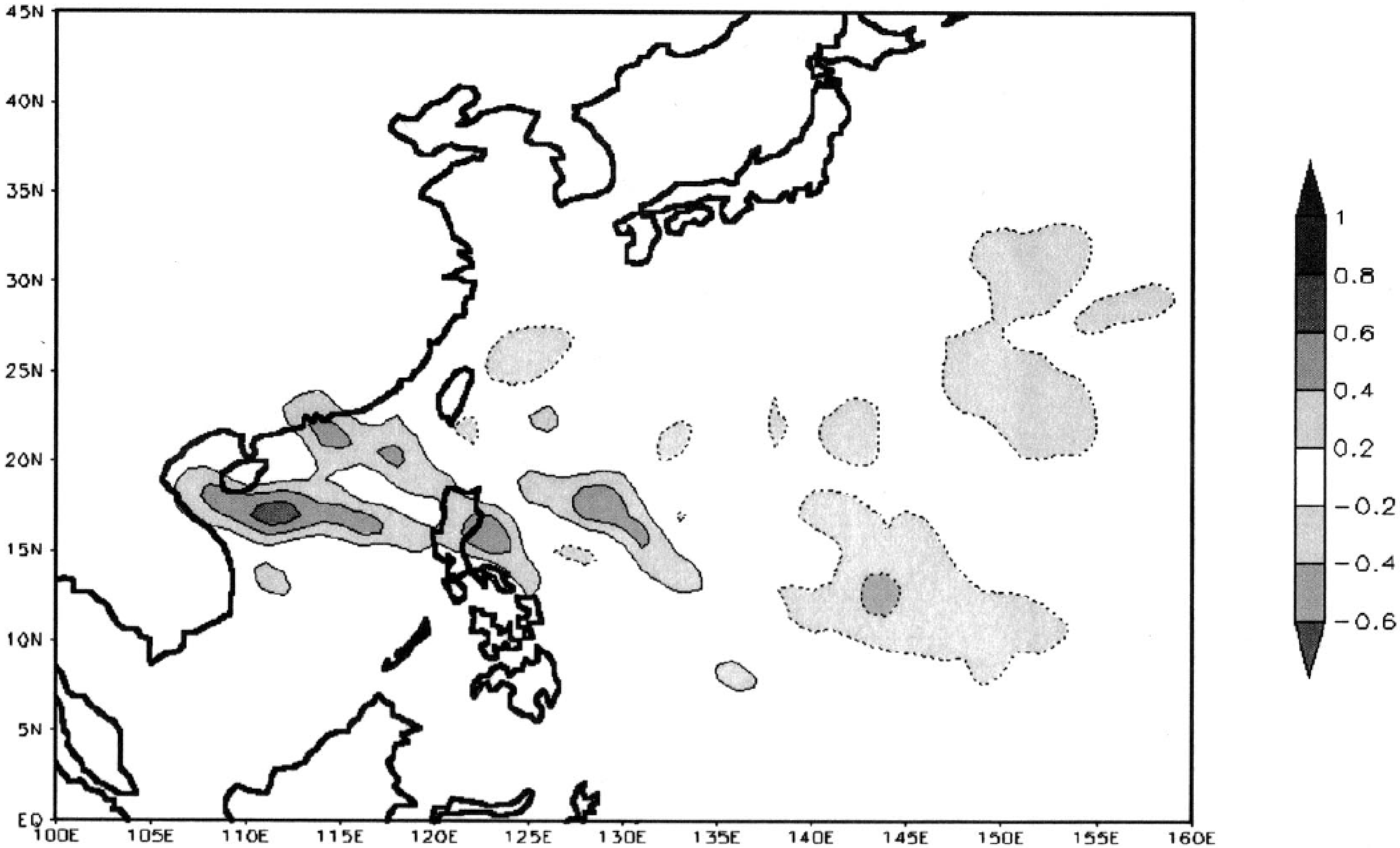

(b) La Niña years

< ***Wu et al. 2004*** >

Efficient Methods：

O(N) operations for O(N) degrees of freedom

- Matrix operation
  $Ax = y$ **$O(N^2)$**
- Inner Product **$\langle u , \phi_n \rangle$** **$O(N^2)$**
  FFT , Chebyshev Transform **$O(N)$**
- Gaussian Elimination
  $A^{-1}b = x$ **$O(N^3)$**
- Relaxation (Gauss-Seidel method)
  $\nabla^{-2} y = x$ **$O(N^4)$** for 2D **$O(N^2)$** degrees of freedom

Accuracy: same CPU time, more accurate solution

Efficiency: same accuracy, less CPU time

Reliable And Efficient Methods Exist

More Issues Need To Be Considered Other Than Efficiency !!

- **Geostrophic Adjusment**

  C-grid for Finite Differences

  Z-grid for Spectral and Finite Element

- **Axisymmetrization Dynamics**

  $\overline{r^2}$ conserved

- **Selective Decay (Statistical Dynamics)**
  - Improvement over simple ∇^2 diffusion in global or regional or hurricane models
    - **Anticipated potential vorticity method**
      - Sadourny and Basdevant 1985
      - Arakawa and Hsu 1990
      - Kazantsev et al. 1998 (Boltzmann mixing entropy maximized under energy conservation constraint)
  - Coherent Structure vs 2D Turbulences

- **Conservations :**
  Enstrophy, Vorticity, Kinetic Energy, Available Potential Energy, Water Substance, angular momentum etc

- **Topography**
  hurricane spin-down, turbulence structure

- **Positive Definite Method**

- **Hybrid $\theta - \sigma$ coordinate**
  (quasi-Lagrangian vertical corrdinate)

High Resolution Direct Simulations
Cumulus Parameterization Abandoned?!
Direct simulations of Micro-states

Collective Effects, Scale Interactions
Statistical Physics, Macro Model
Efficient Numerical Methods

Numerical Method

- Grids Method → Finite Difference; Finite Volume
- Series Method → Finite Element; Spectral Method

Spectral Method

1. Completeness（完整性） → Sufficient condition
2. Orthogonality（正交性）
3. Speed of convergence（收斂速度）
4. Fast Transform（快速轉換）

$\left.\begin{array}{l}2.\\3.\\4.\end{array}\right\}$ Application

Sturm-Liouville equation

$$L\phi(x) = -\frac{d}{dx}(p(x)\phi'(x)) + q(x)\phi(x) = \lambda W(x)\phi(x)$$

Transform Pair

$$u = \sum \hat{u}_k \phi_k$$
$$\hat{u}_k = < u, \phi_k >$$

To get $\hat{u}_k$ **in computer,**

$$\hat{u}_k = < u, \phi_k > = \sum_j u(x_j)\phi_k(x_j)\Delta x_j$$

Let $u(x_j) = \underline{u}$ **and** $\hat{u}_k = \underline{\hat{u}}$

then A **matrix has components** $\phi_k(x_j)$

$\underline{\hat{u}} = A\underline{u}$ **matrix multip** $O(N^2)$

2D model $O(N^3)$

Fast Transform
(FFT, Fast Chebyshev Transform)

$1D \quad O(N \ln N)$

$2D \quad O(N^2 \ln N)$

$\phi_k(x)$ from Sturm-Liouville equations

(1) **orthonormal in the inner product**

$$(\phi_i, \phi_j)_w = \int_a^b \phi_i(x)\phi_j(x)w(x)dx = \delta_{ij}$$

(2) $\phi_k(x)$ **form a complete set**

Example: $$-\frac{d}{dx}(p(x)\frac{d\phi(x)}{dx}) + q(x)\phi(x) = \lambda W(x)\phi(x)$$

If $p(x) = 1 - x^2$ $\quad -1 \le x \le 1$

$q(x) = 0$

$$\rightarrow \frac{d}{dx}((1-x^2)\frac{d\phi}{dx}) + \lambda\phi = 0$$

Lgendre function

If $p(x) = 1$ $\quad 0 \le x \le 2\pi$

$q(x) = 0$

$$\rightarrow \frac{d^2\phi}{dx^2} + \lambda\phi = 0$$

Fourier series

Example: $$-\frac{d}{dx}\left(p(x)\frac{d\phi(x)}{dx}\right)+q(x)\phi(x)=\lambda W(x)\phi(x)$$

If $p(x)=(1-x^2)^{1/2}$

$q(x)=0$ $\qquad -1\le x\le 1$

$w(x)=(1-x^2)^{-1/2}$

$$\Rightarrow \frac{d}{dx}\left[(1-x^2)^{1/2}\frac{d\phi}{dx}\right]+\lambda(1-x^2)^{-1/2}\phi=0$$

Chebyshev series

- **Fourier, Legendre functions have been used in global spectral model**
- **Chebyshev functions are used in the limited area spectral modeling**

$$f = \sum a_k \phi_k$$

$$a_k = < f, \phi_k > w$$

$$= \int_a^b f(x)\phi_n(x)W(x)dx$$

$$= \frac{1}{\lambda_n}\int_a^b f(x)\left\{-[p(x)\phi_n'(x)]' + q(z)\phi_n(x)\right\}dx$$

Speed of convergence

➔ Efficiency

➔ Boundary condition

Integrate by parts twice, we have

$$a_n = \frac{1}{\lambda_n}\left[p(f'\phi_n - f\phi_n')\right]_a^b + \frac{1}{\lambda_n}(\phi_n, \frac{Lf}{w})_w$$ ➔ **Boundary term**

If boundary term not vanish

$$a_n = O(\frac{1}{\lambda_n})$$ ***algebraic convergence***

Nonsingular Problem $P > 0 \quad \text{on}\,[a,b]$

for $P(f'\phi_n - f\phi_n')\big|_a^b = 0$

we need $f'\phi_n - f\phi_n'\big|_a^b = 0$

➔ Periodic domain

➔ Exponential Convergence

※ This is the case for Fourier Series

Singular Problem $P(a) = P(b) = 0$

then $P(f'\phi_n - f\phi_n')\big|_a^b = 0$

<u>**Regardless of the behavior of f(x) near the boundary a, b**</u>

➔Exponential Convergence

※ This is the case for Legendre and Chebyshev polynomials

If $\frac{1}{\lambda_n}\left[p(f'\phi_n - f\phi_n')\right]_a^b = 0$

and ϕ_n **is p times differentiable**

We can do integration by parts p times

$$a_n < O(\frac{1}{\lambda_n^{\,p}})$$

➔ ***Exponential convergence***

When boundary terms vanished,
the speed of convergence
depends on the smoothness of the function.

Pafnuty Lvovich Chebyshev

Wikipedia

Russian mathematician
(1821～1894)

Moscow State University

Saint Petersburg
State University

Main contributions:

Probability
Statistics
Number theory

➜ Chebyshev's inequality

➜ Bertrand-Chebyshev theorem

Chebyshev polynomials

➜ Chebyshev filter

Cornelius Lanczos

Wikipedia

Hungarian mathematician & physicist
(1893～1974)

1928 ～ 1929: He served as an assistant to Albert Einstein.

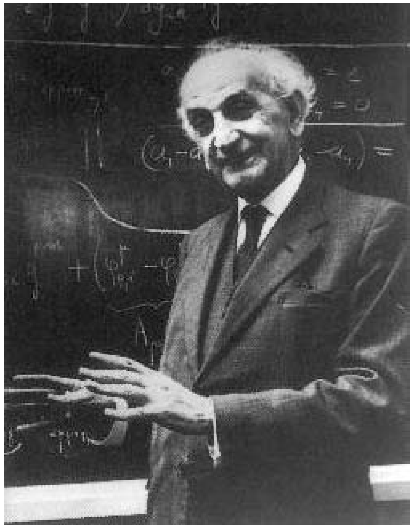

Main Contributions:

- General relativity
- Quantum mechanics
- Applied and computational mathematics

→ Fast Fourier Transform (FFT)
→ Chebyshev Tau method
→ ill-posed problems

Technical University of Budapest → University of Freiburg → Purdue University → Theoretical Physics Department at the Dublin Institute (1952 ~ 1974)

Chebyshev Polynomials

$$\begin{cases} T_n(\cos\theta) = \cos n\theta \\ x = \cos\theta \end{cases}$$

Recurrence Formula:

$$T_{n+1}(x) + T_{n-1}(x) = 2xT_n(x)$$

$$T_n(-1) = (-1)^n$$

$$T_n(1) = 1$$

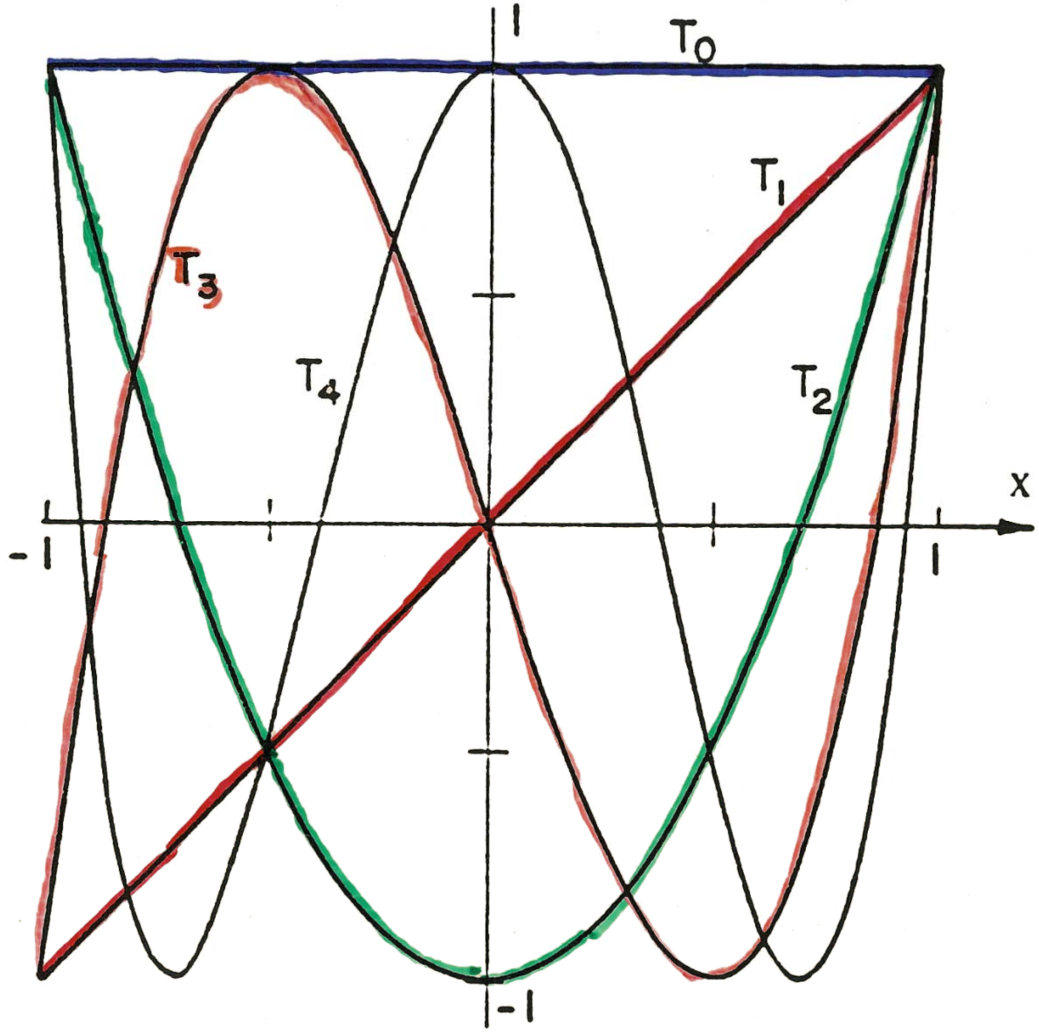

Orthogonality of Chebyshev series

$$(u,v)=\int_{-1}^{1}\frac{u(x)v(x)}{(1-x^2)^{1/2}}\,dx \qquad \textit{as inner product}$$

In particular

$$(T_m,T_n)=\int_{-1}^{1}\frac{T_m(x)T_n(x)}{(1-x^2)^{1/2}}\,dx$$

$$T_m(x)=\cos m\phi \quad T_n=\cos n\phi \quad x=\cos\phi$$

$$\begin{aligned}dx&=-\sin\phi\,d\phi=-(1-\cos^2\phi)^{1/2}\,d\phi\\&=-(1-x^2)^{1/2}\,d\phi\end{aligned}$$

$$(T_m,T_n)=\int_0^{\pi}\cos m\phi\cos n\phi\;\,d\phi$$

Coefficients for the Chebyshev Polynomials $T_n(x)$ and for x^n in terms of $T_m(x)$

$$T_n(x) = \sum_{m=0}^{n} C_m x^m \qquad x^n = b_n^{-1} \sum_{m=0}^{n} d_m T_m(x)$$

	x^0	x^1	x^2	x^3	x^4	x^5	x^6	x^7	x^8	x^9	x^{10}	x^{11}	x^{12}	
b_n	1	1	2	4	8	16	32	64	128	256	512	1024	2048	
T_0	1 1		1		3		10		35		126		462	T_0
T_1		1 1		3		10		35		126		462		T_1
T_2	−1		2 1		4		15		56		210		792	T_2
T_3		−3		4 1		5		21		84		330		T_3
T_4	1		−8		8 1		6		28		120		495	T_4
T_5		5		−20		16 1		7		36		165		T_5
T_6	−1		18		−48		32 1		8		45		220	T_6
T_7		−7		56		−112		64 1		9		55		T_7
T_8	1		−32		160		−256		128 1		10		66	T_8
T_9		9		−120		432		−576		256 1		11		T_9
T_{10}	−1		50		−400		1120		−1280		512 1		12	T_{10}
T_{11}		−11		220		−1232		2816		−2816		1024 1		T_{11}
T_{12}	1		−72		840		−3584		6912		−6144		2048 1	T_{12}
	x^0	x^1	x^2	x^3	x^4	x^5	x^6	x^7	x^8	x^9	x^{10}	x^{11}	x^{12}	

$$T_6(x) = 32x^6 - 48x^4 + 18x^2 - 1 \qquad x^6 = \frac{1}{32}\left[10T_0 + 15T_2 + 6T_4 + T_6\right]$$

Chebyshev Polynomials $T_n(x)$

$$\theta(x) = \sin[M\pi(x+a)] = \sum_{n=0}^{\infty} \hat{\theta}_n T_n(x)$$

Define L2 error as

$$\left\{ \int_{-1}^{1} \left[\theta(x) - \sum_{n=0}^{N} \hat{\theta}_n T_n(x) \right]^2 dx \right\}^{1/2}$$

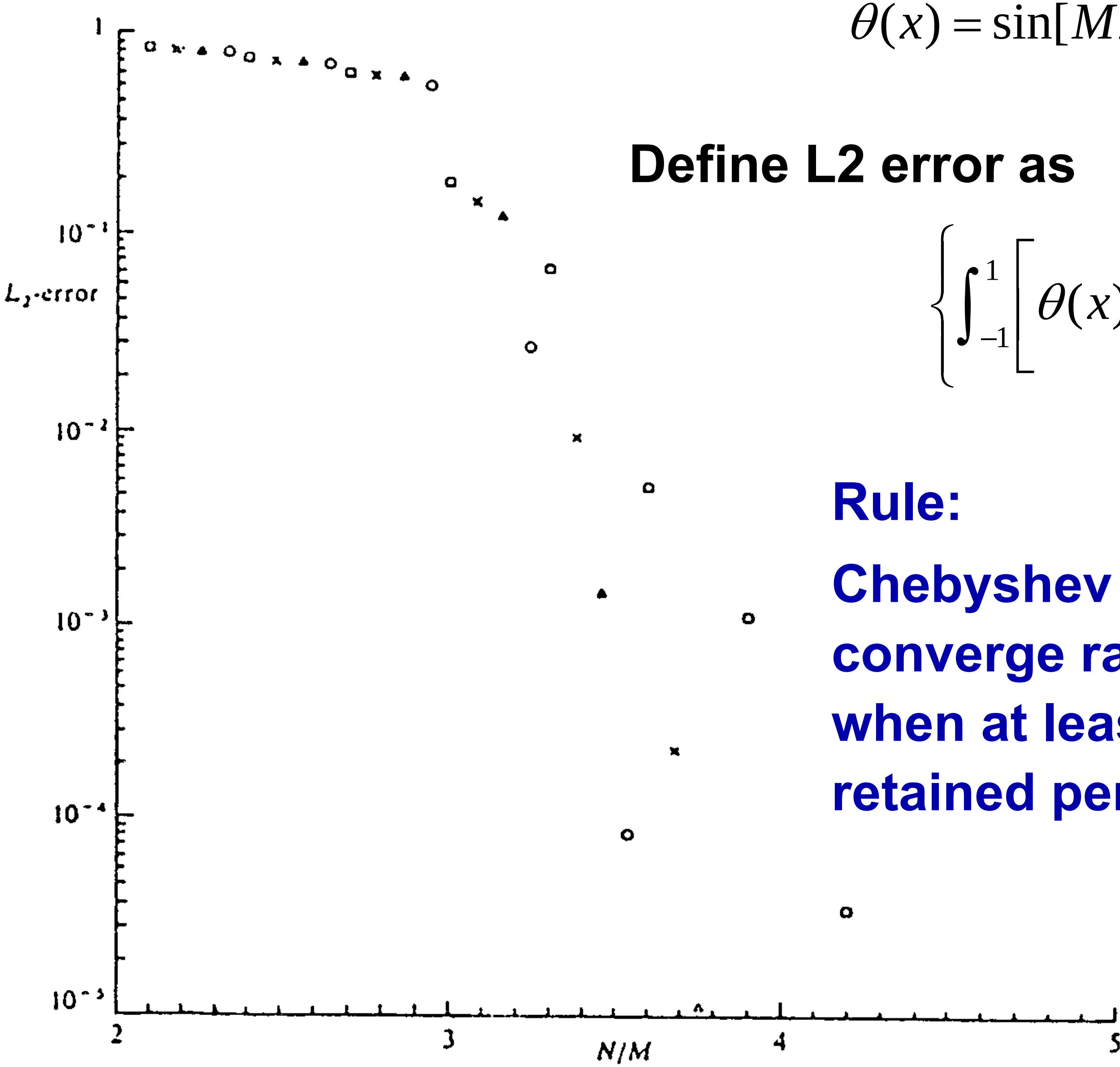

FIG. 3.7. *A plot of the L_2-error in the Chebyshev series expansion* (3.41) *of* sin $(M\pi x)$ *truncated after* $T_N(x)$ *versus* N/M. *The various symbols represent:* □ $M = 10$; × $M = 20$; △ $M = 30$; ○ $M = 40$. *Observe that the L_2-error approaches zero rapidly when* $N/M > \pi$.

Rule:

Chebyshev expansions converge rapidly when at least π polynomial are retained per wavelength

Define $C_n = \begin{Bmatrix} 2 & n=0 \\ 1 & n>0 \end{Bmatrix}$ **then** $\frac{2}{\pi C_n}(T_m, T_n) = \begin{Bmatrix} 1 & m=n \\ 0 & m \neq n \end{Bmatrix}$

$$\theta(x,t) = \sum_{m=0}^{\infty} \hat{\theta}_m(t) T_m(x)$$

$$< \theta(x,t),\ T_n(x) \ > = \sum_{m=0}^{\infty} \hat{\theta}_m(t) < T_m(x),\ T_n(x) \ >$$

$$= \frac{\pi C_n}{2} \hat{\theta}_n(t)$$

Transform pair is

$$\theta(x,t) = \sum_{n=0}^{\infty} \hat{\theta}_n(t) T_n(x)$$ ***spectral space to physical space***

$$\hat{\theta}_n(t) = \frac{2}{\pi C_n} < \theta(x,t), T_n(x) >$$ ***physical space to spectral space***

Speed of Convergence -- Efficiency

$$f = \sum a_n \phi_n$$

$$\begin{aligned} a_n &= < f, \phi_n > w \\ &= \int_a^b f(x)\phi_n(x)W(x)dx \\ &= \frac{1}{\lambda_n}\int_a^b f(x)\{-[p(x)\phi_n'(x)]' + q(z)\phi_n(x)\}\,dx \end{aligned}$$

Integration by parts twice, we have

$$a_n = \underbrace{\frac{1}{\lambda_n}\left[p(f'\phi_n - f\phi_n')\right]_a^b}_{\text{Boundary term}} + \frac{1}{\lambda_n}\left(\phi_n, \frac{Lf}{w}\right)_w$$

If boundary term does not vanish

$$a_n \propto O\left(\frac{1}{\lambda_n}\right)$$ *algebraic convergence*

Exponential Convergence

$$a_n = \cancelto{0}{\frac{1}{\lambda_n}\left[p(f'\phi_n - f\phi_n')\right]_a^b} + \frac{1}{\lambda_n}\left(\phi_n, \frac{Lf}{w}\right)_w$$

If f is $\boldsymbol{p}$ times differentiable,
we can do integration by parts $\boldsymbol{p}$ times.

$$a_n \propto O\left(\frac{1}{{\lambda_n}^p}\right) \quad , \; p \text{ sufficiently large}$$

→ Exponential Convergence

Chebyshev Equation – Sturm-Liouville Singular Problem

$$P(a) = P(b) = 0 \longrightarrow P(f'\phi_n - f\phi_n')\Big|_a^b = 0$$

the speed of convergence depends
only on the smoothness of the function.

Fast Chebyshev Transform

Transform pair is:

$$\begin{cases} \hat{u}_k = < u, \phi_k > & \text{physical space to spectral space} \\ u = \sum \hat{u}_k \phi_k & \text{spectral space to physical space} \end{cases}$$

Chebyshev Polynomials $\begin{cases} T_n(\cos\theta) = \cos n\theta \\ x = \cos\theta \end{cases}$

- Could take advantage of Fast Fourier Transform (FFT)
(Cooley and Tukey, 1965)

$$\begin{cases} \textbf{General Transform} & \begin{cases} 1D & O(N^2) \\ 2D & O(N^3) \end{cases} \\ \textbf{Fast Transform} & \begin{cases} 1D & O(N \ln N) \\ 2D & O(N^2 \ln N) \end{cases} \end{cases}$$

Chebyshev Collocation & Tau Method

- Chebyshev Collocation Method: Doing derivation in spectral space, then inverse transform to physical space to do integration, applying boundary conditions in physical space.
(*pseudospectral*)

- Chebyshev Tau Method: Doing all derivation, integration, and applying boundary conditions in spectral space, after all, inverse transform to physical space.
(Lanczos, 1938b, 1952c,d, 1956)

Finite Difference Method

FD-1

$$v_j = \frac{u_{j+1} - u_j}{\Delta x}$$

FD-2

$$v_j = \frac{u_{j+1} - u_{j-1}}{2\Delta x}$$

FD-4

$$v_j = \frac{4}{3}\frac{u_{j+1} - u_{j-1}}{2\Delta x} - \frac{1}{3}\frac{u_{j+2} - u_{j-2}}{4\Delta x}$$

FD-6

$$v_j = \frac{3}{2}\frac{u_{j+1} - u_{j-1}}{2\Delta x} - \frac{3}{5}\frac{u_{j+2} - u_{j-2}}{4\Delta x} + \frac{1}{10}\frac{u_{j+3} - u_{j-3}}{6\Delta x}$$

Advection Equation

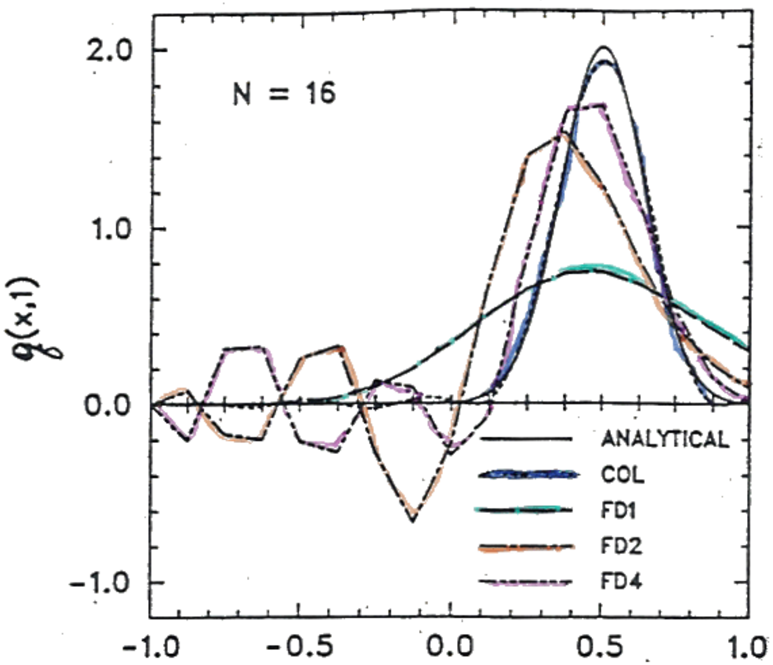

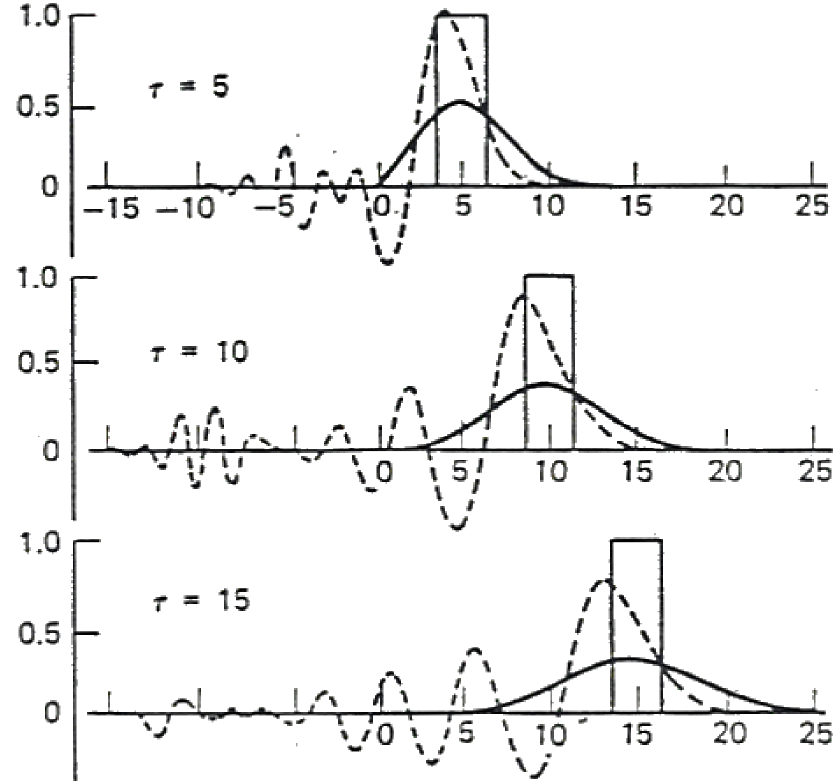

Table 1

	$\frac{c\Delta t}{\Delta x}$:	$2\Delta x$	$4\Delta x$	$6\Delta x$	$8\Delta x$	$10\Delta x$	$12\Delta x$
Second order	0.2	0	0.64	0.83	0.91	0.94	0.96
	0.4	0	0.66	0.84	0.92	0.95	0.96
	0.6	0	0.68	0.87	0.93	0.96	0.97
	0.8	0	0.74	0.92	0.96	0.97	0.98
Fourth order	0.2	0	0.86	0.97	0.99	1.00	1.00
	0.4	0	0.89	0.99	1.00	1.01	1.01
	0.6	0	0.98	1.03	1.03	1.02	1.01
	0.8	0	Unstable	1.11	1.07	1.04	1.03

Performance of Chebyshev Collocation Method

Fulton & Schubert (1987 a)

Linear Advection Equation

$$\frac{\partial u}{\partial t}+\frac{\partial u}{\partial x}=0$$

- Finite Difference Method:
  Algebraic convergence（代數收斂）
  誤差隨網格點增加呈算數減少

- Chebyshev Collocation Method:
  Exponential convergence（指數收斂）
  誤差隨網格點增加呈指數減少

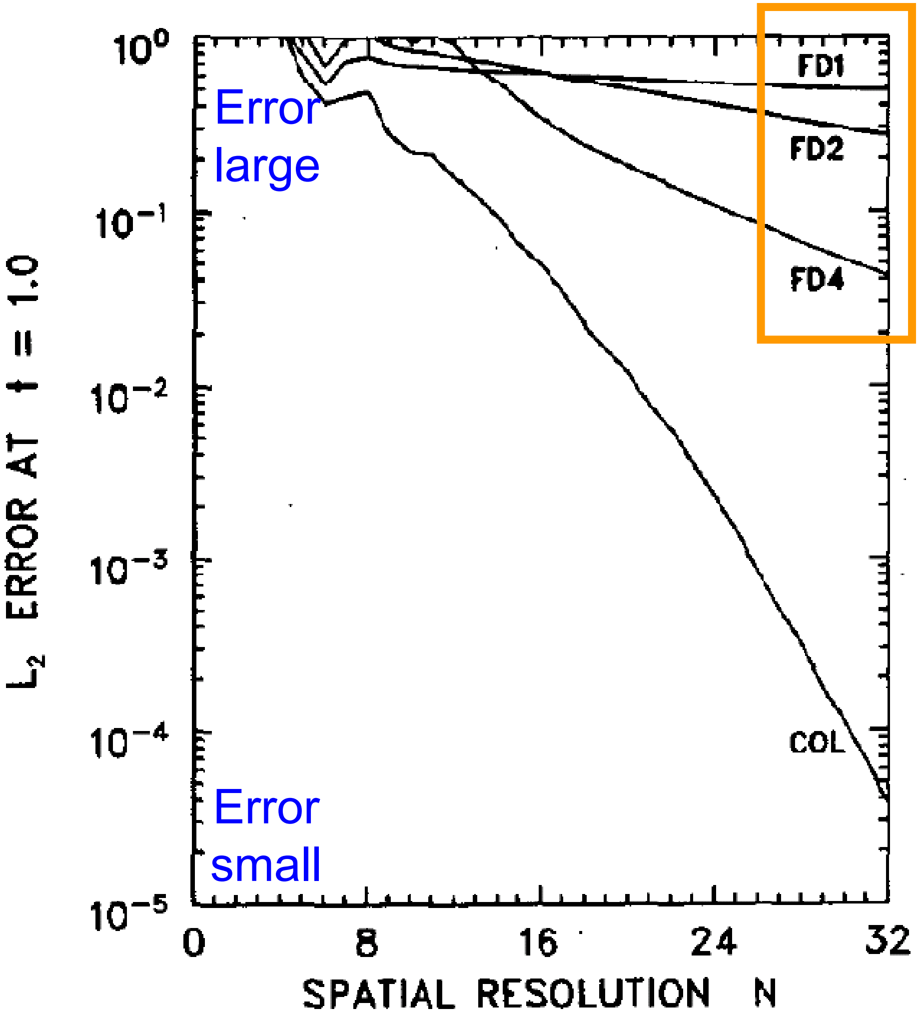

Error exponential convergence

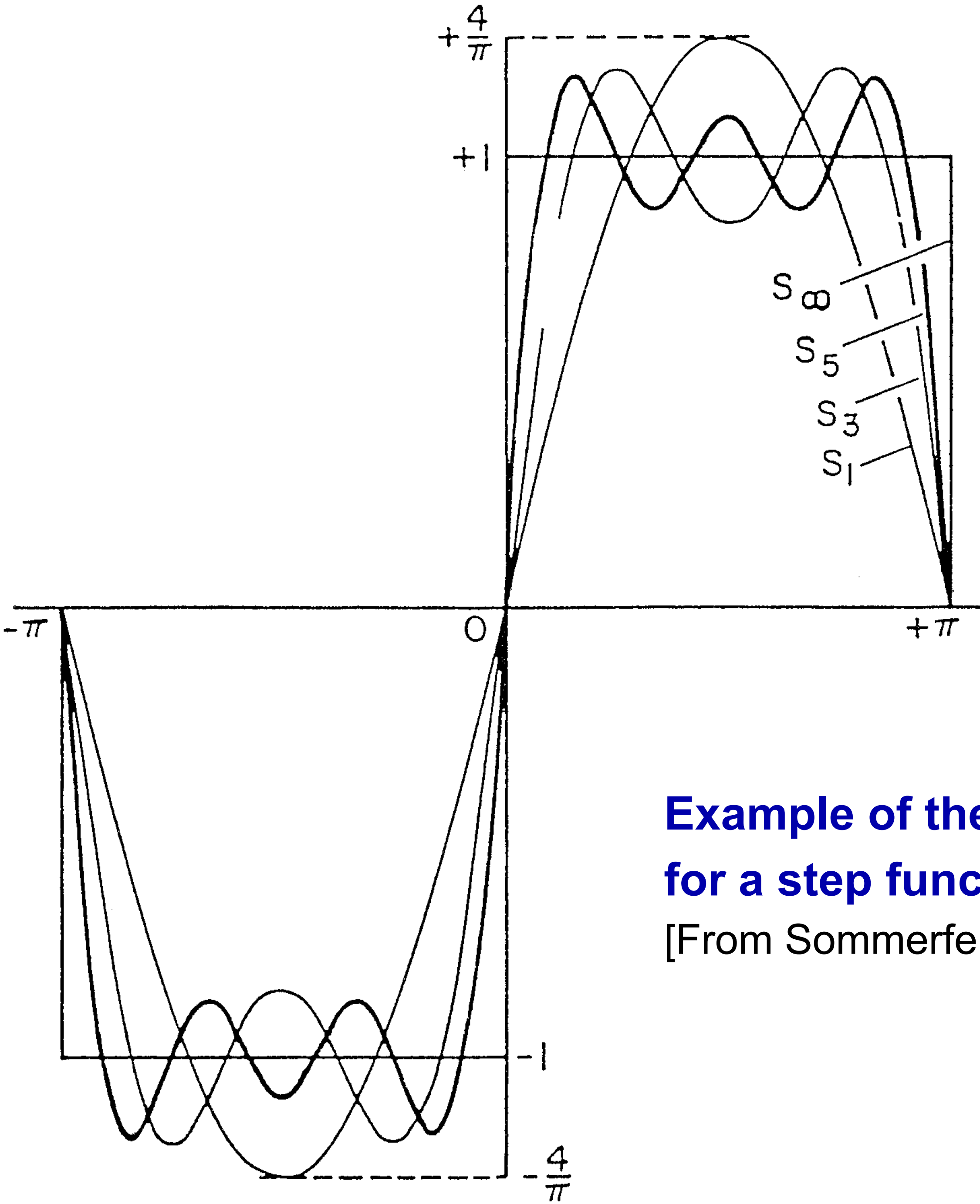

Example of the Gibbs phenomenon for a step function.

[From Sommerfeld (1949).]

Chebyshev Transform *vs.* FFT

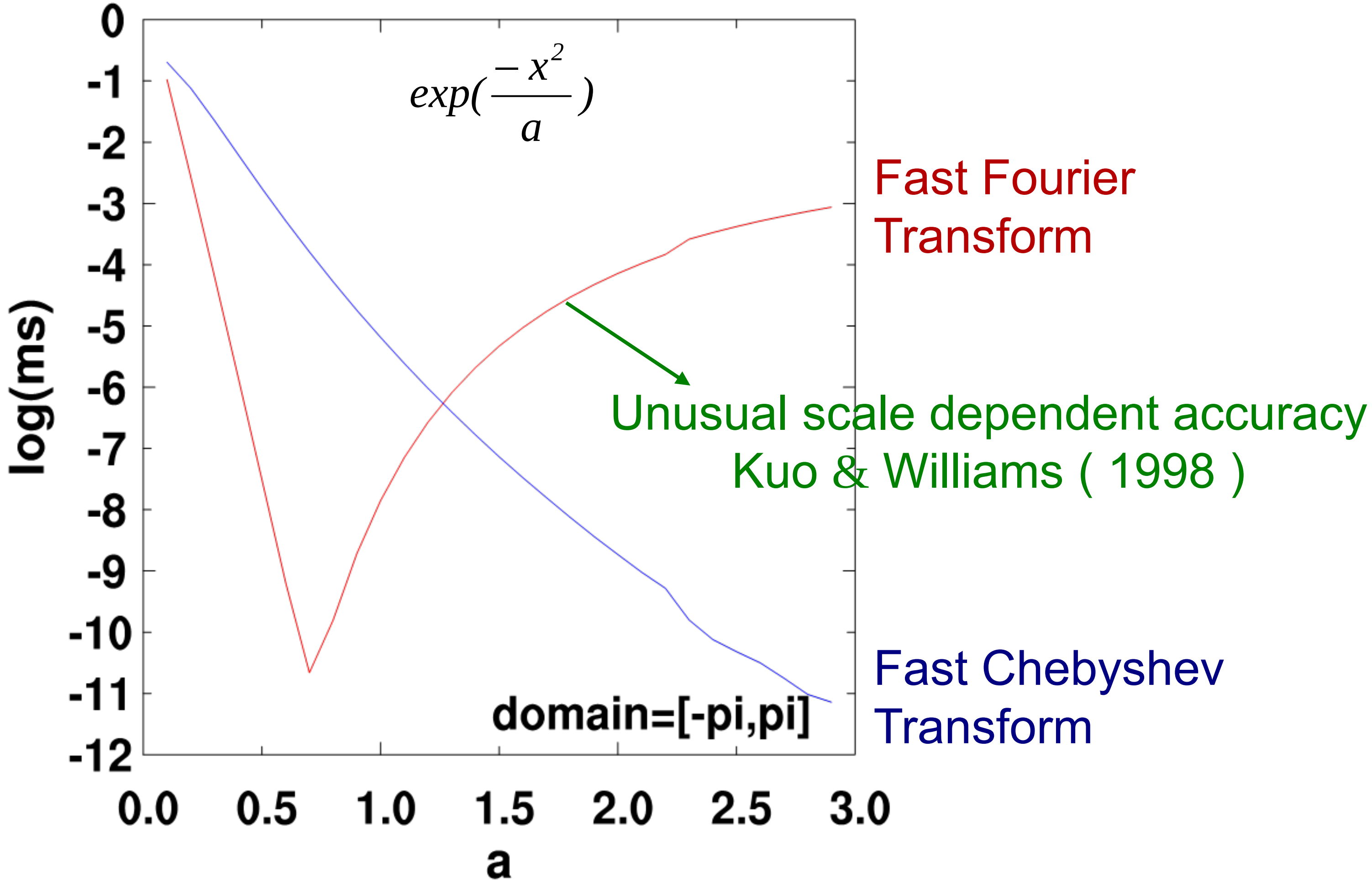

Domain Decomposition

Original Problem:

N

Domain Decomposition:

1) Same degree of freedom
   less time
   increase ***Efficiency***

$\frac{N}{4}$ $\frac{N}{4}$ $\frac{N}{4}$ $\frac{N}{4}$

2) Same time
   more degree of freedom
   increase ***Accuracy***

N N N N

PC cluster

Theoretical Speedup

$$SP(n) = \frac{s+p}{s+p/n} = \frac{{}^{s}\!/_{p}+1}{{}^{s}\!/_{p}+{}^{1}\!/_{n}}$$

n: number of working processors

s: time spent by the sequential portion of the code

p: time spent by the parallel portion of the code

$$SP(n)$$

$$\left\{\begin{array}{ll} {}^{s}\!/_{p} \to 0 & n \\ {}^{s}\!/_{p} \to 1 & \dfrac{2n}{n+1} \\ {}^{s}\!/_{p} \to \infty & 1 \end{array}\right.$$

Domain Decomposition MPI

Application of Chebyshev Spectral Method in Oceanic Modeling

- Haidvogel (1976)

With pseudospectral method, employing an orthogonal expansion in Fourier and Chebyshev functions, to investigate the sensitivity and predictability of <u>mesoscale eddies</u> in an idealized model ocean.

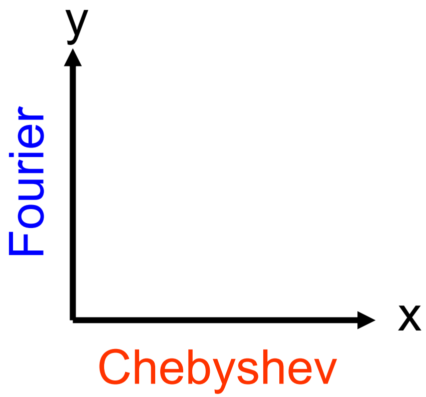

Stream function

Mean

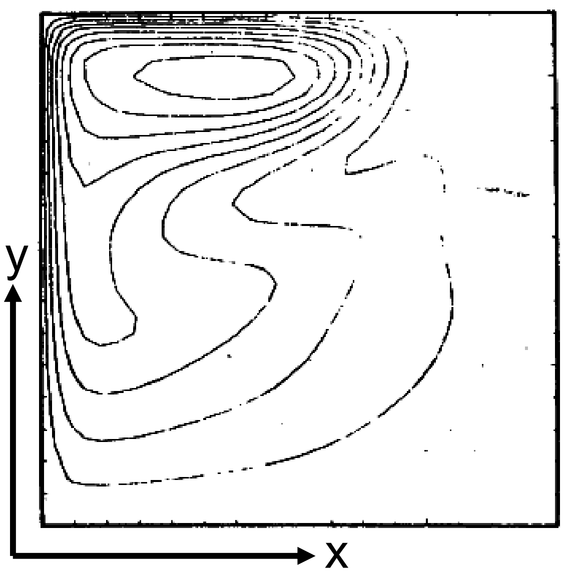

Eddy

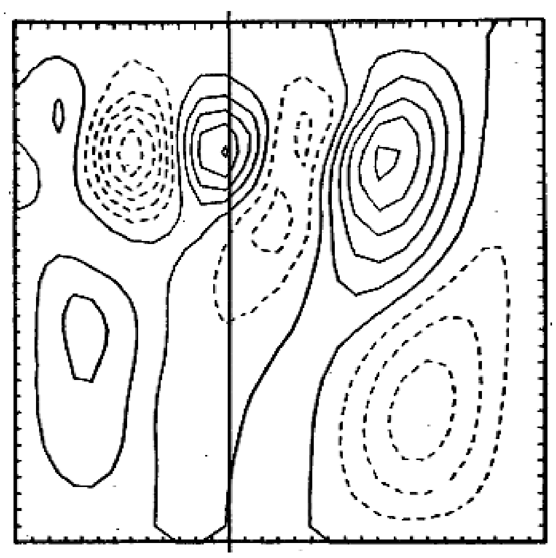

Application of Chebyshev Spectral Method in Atmospheric Modeling

- Kuo & Schubert (1988)

Applied the Fourier-Chebyshev method in a Boussinesq nonhydrostatic model to study the <u>entrainment instability</u> of marine boundary layer stratocumulus.

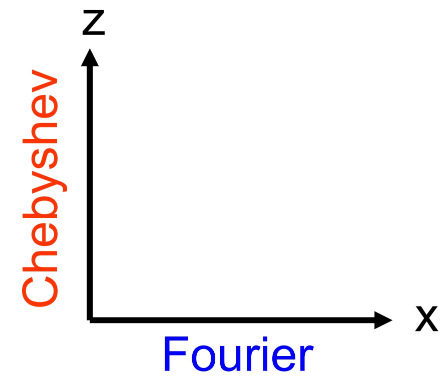

Initial field

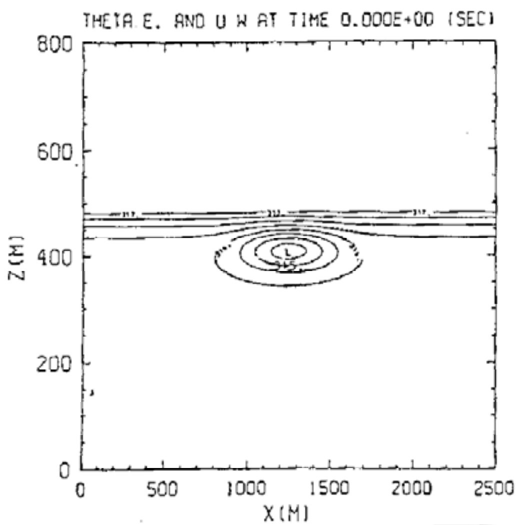

20 mins

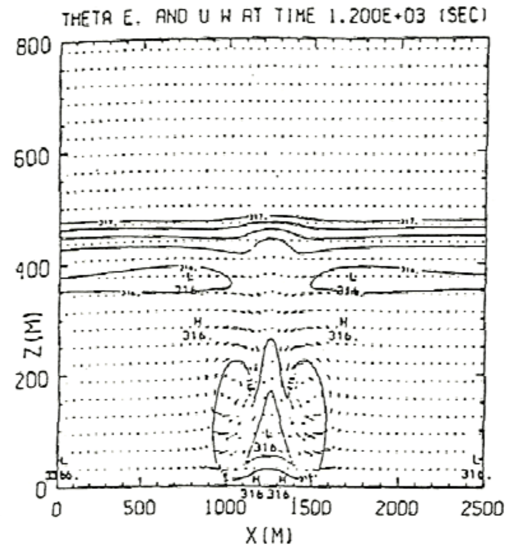

40 mins

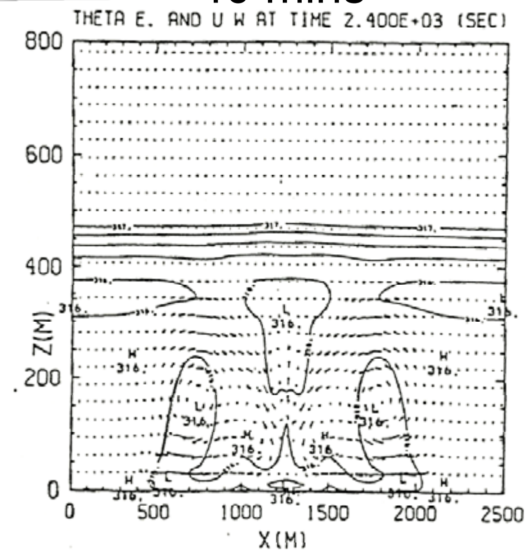

Domain Decomposition

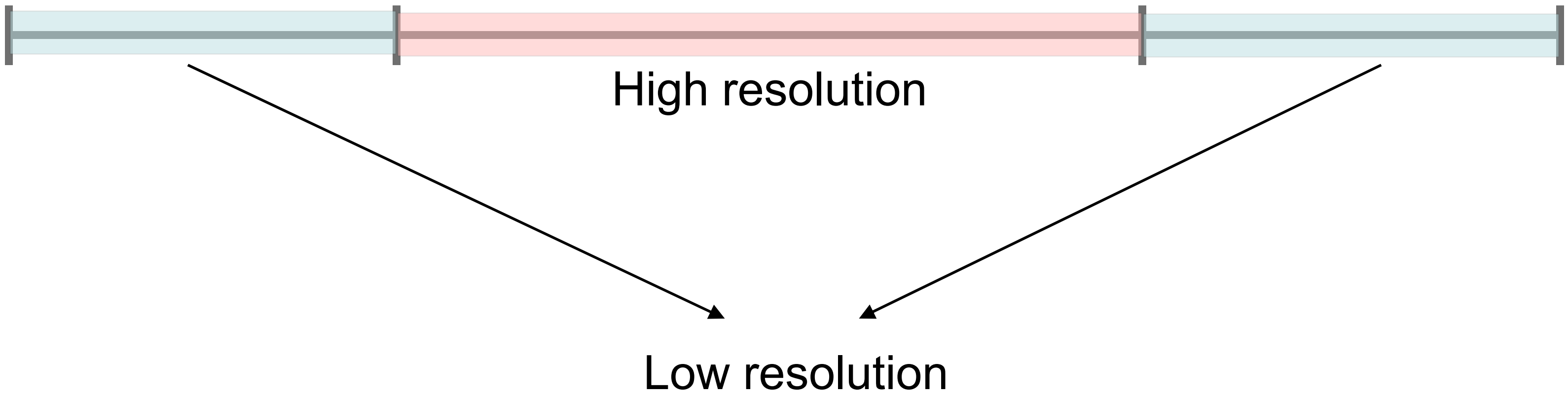

Chebyshev polynomials

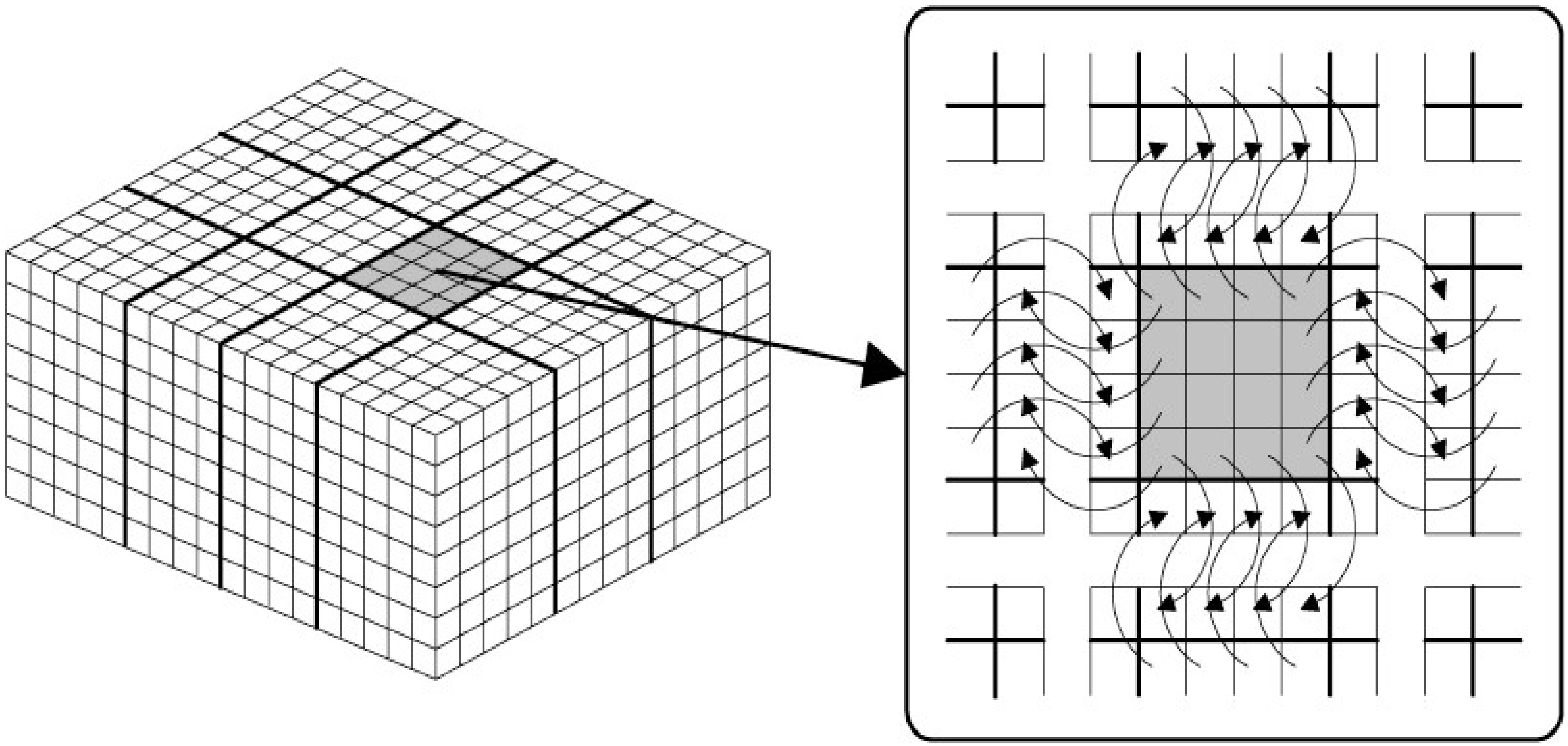

Coupling CReSS with GCM

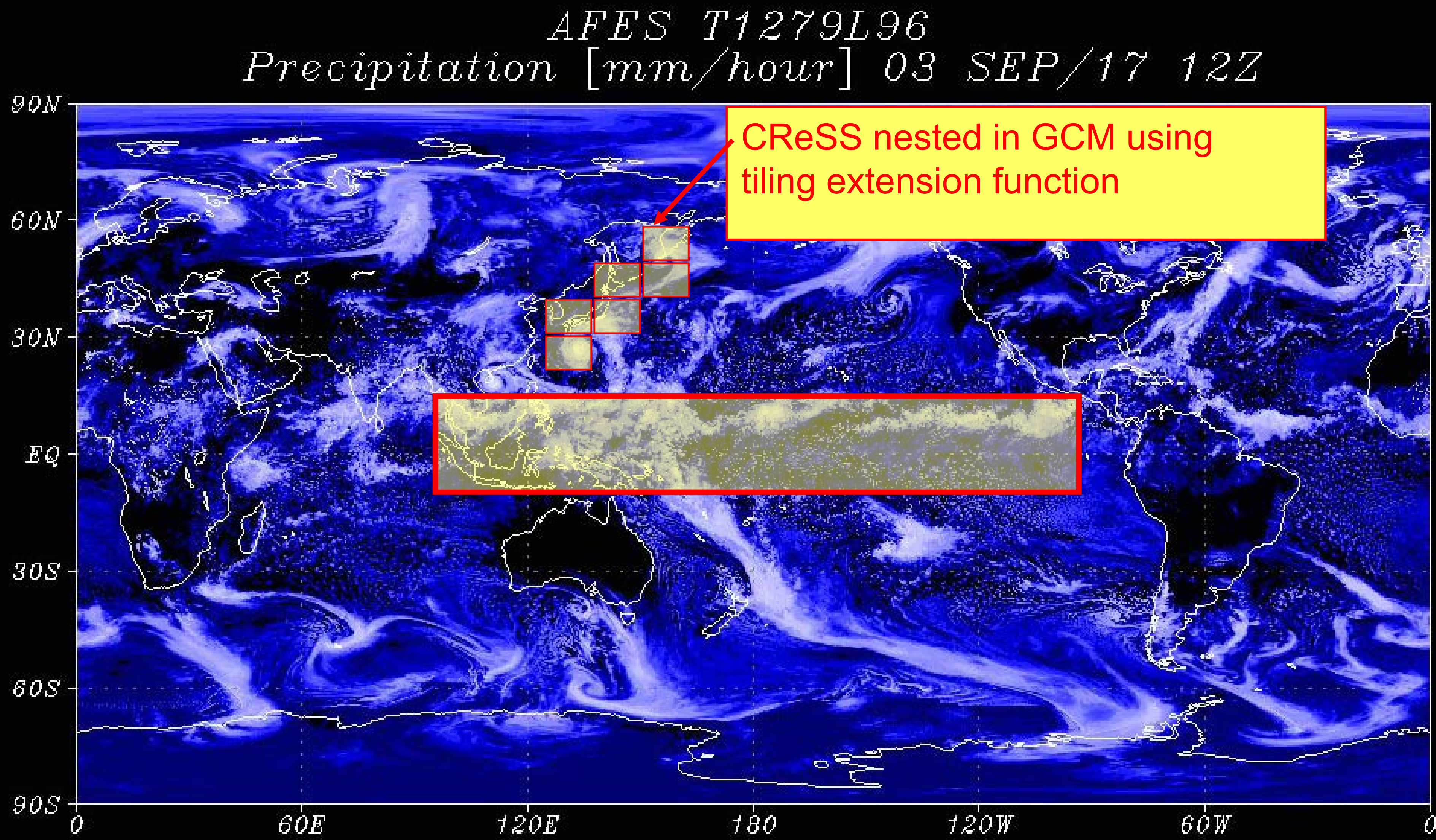

AFES (Atmospheric general circulation model For Earth Simulator)

7 days simulation of T0418

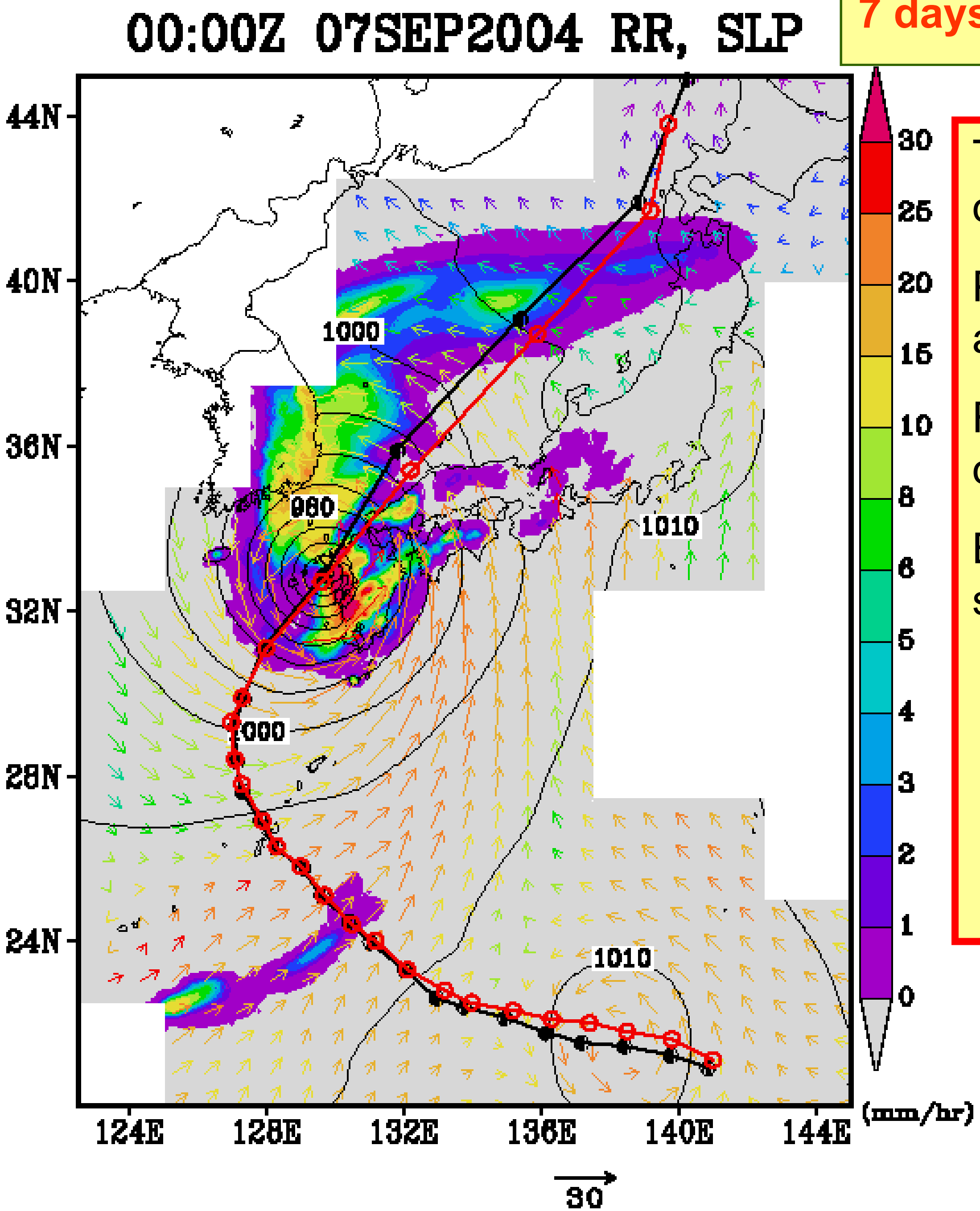

Tiling extension function of CReSS ver.3

Precipitation rate (mm/hr) at 5 days from initial time.

Red line: JMA best track of Typhoon 18.

Black line: CReSS simulation result.

Interior BCs

- Physical BCs are treated by collocation method
- Ie, replace the numerical sol. at boudaries by BCs
- What about points at sub-domain boundaries?
- Patching! [David A. Kopriva 1989]
- Continuation of derivatives in desired order.

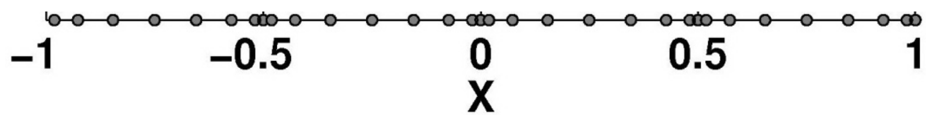

Other methods?

Overset

- Sub-domains overlap with each other
- March one step
- Exchange!
- Use Chebyshev interpolation if sub-domain layout is different

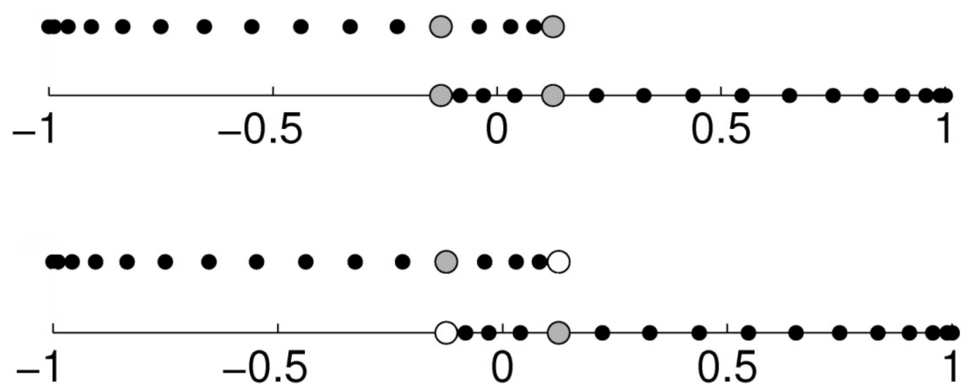

Auxiliary Sub-domains

- Apply additional domains
- Initialize as other sub-domains
- March forward one step
- Exchange!
- Regional and global models interaction
- n_A and L_A

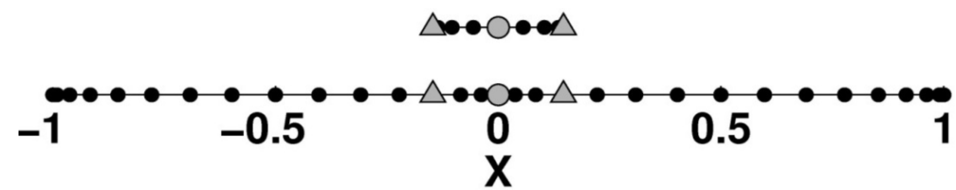

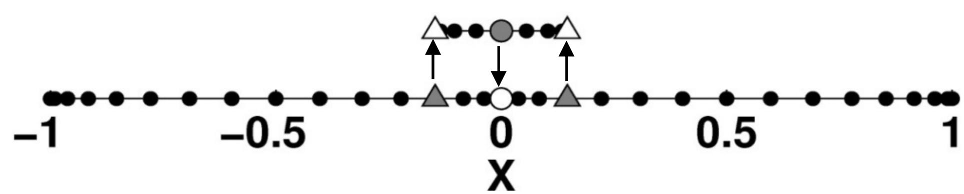

Burger’s equation:

Advection, Diffusion, Non-linear shock formation

$$\boxed{\frac{\partial u}{\partial t} + (\bar{u} + u)\frac{\partial u}{\partial x} = \frac{\partial^2 u}{\partial x^2}}$$

MODEL PROBLEMS

Advection Equation

- Gaussian IC with various width
- u'_j obtained by discrete chebyshev transform and recursive formula
- RK-4 ODE solver
- Aim to find additional speed-up factor

$$\begin{cases} \frac{\partial u}{\partial t} + c\frac{\partial u}{\partial x} = 0 \quad (c = 1 \text{ during all tests}) & (3.1a) \\ u(-1,t) = \exp\left[\left(\frac{-0.5 - ct}{\sigma}\right)^2\right] & (3.1b) \\ u(x,0) = \exp\left[\left(\frac{x + 0.5}{\sigma}\right)^2\right] & (3.1c) \end{cases}$$

$$u(x,t) = \exp\left[\left(\frac{x - t + 0.5}{\sigma}\right)^2\right] \quad (3.2)$$

$$\begin{cases} \frac{du_j}{dt} = -cu'_j \quad (j = 0,1,\dots,N-1) & (3.3a) \\ u_N(t) = \exp\left[\left(\frac{-0.5 - ct}{\sigma}\right)^2\right] & (3.3b) \end{cases}$$

$$\sigma = 0.01 \text{ and } 0.04$$

$$u_N^i(t) = u_1^{i-1}(t) \quad (i = 2,3,\dots,M)$$

Diffusion Equation

- Gaussian IC with various width
- Analytic sol. obtained by Fourier integral
- BCs are give as analytic sol. at boundaries
- RK-4 ODE solver, $\Delta t = 10^{-5}$
- Aim to test Aux. sub-domains schemes

$$\begin{cases} \dfrac{\partial u}{\partial t} = \kappa \dfrac{\partial^2 u}{\partial x^2} \quad (\kappa = 0.01\ ) & (5.6a) \\ u(-\infty, t) = 0 & (5.6b) \\ u(\infty, t) = 0 & (5.6c) \\ u(x, 0) = \exp\left[\left(\dfrac{x}{\sigma}\right)^2\right] & (5.6d) \end{cases}$$

$$u(x,t) = \exp\left[\frac{-x^2}{(4\kappa t + \sigma^2)\sqrt{\dfrac{4\kappa t}{\sigma^2} + 1}}\right] \qquad (5.7)$$

$$\begin{cases} u(-1,t) = \exp\left[\dfrac{-1}{(4\kappa t + \sigma^2)\sqrt{\dfrac{4\kappa t}{\sigma^2} + 1}}\right] & (5.8a) \\ u(1,t) = \exp\left[\dfrac{-1}{(4\kappa t + \sigma^2)\sqrt{\dfrac{4\kappa t}{\sigma^2} + 1}}\right] & (5.8b) \end{cases}$$

$\sigma = 0.1\ and\ \ 1/\sqrt{500}$

Inviscid Burger's Equation

- Atan IC
- Analytic sol. obtained by fixed point iteration (tol. = 10^{-12})
- BCs are give as analytic sol. at boundaries
- Scale collapse at t=1
- Aim to find error confinement

$$\begin{cases} \dfrac{\partial u}{\partial t} + u\dfrac{\partial u}{\partial x} = 0 \quad (c = 1 \text{ during all tests}) & (3.1a) \\ u(-1,t) = \bar{u} - \tan^{-1}(x - u(-1,t)t - x_0) & (3.1b) \\ u(1,t) = \bar{u} - \tan^{-1}(x - u(1,t)t - x_0) & (3.1c) \\ u(x,0) = \bar{u} - \tan^{-1}(x - x_0) & (3.1d) \end{cases}$$

$$u(x,t) = \bar{u} - \tan^{-1}(x - u(x,t)t - x_0) \quad (3.2)$$

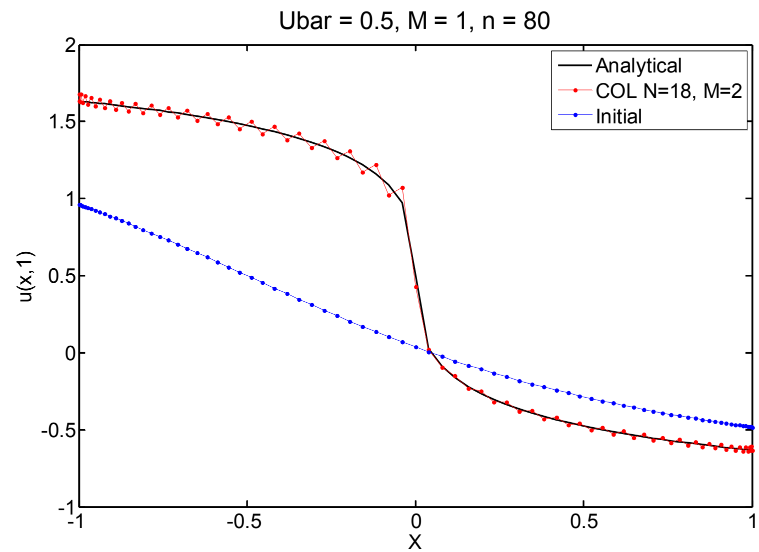

Burger’s equation:

Advection, Diffusion, Non-linear shock formation

NUMERICAL RESULTS

Advection Equation

- Much better than FD4
- Exhibits no oscillation
- Correct peak location and value
- Domain decomposition did not spoil accuracy

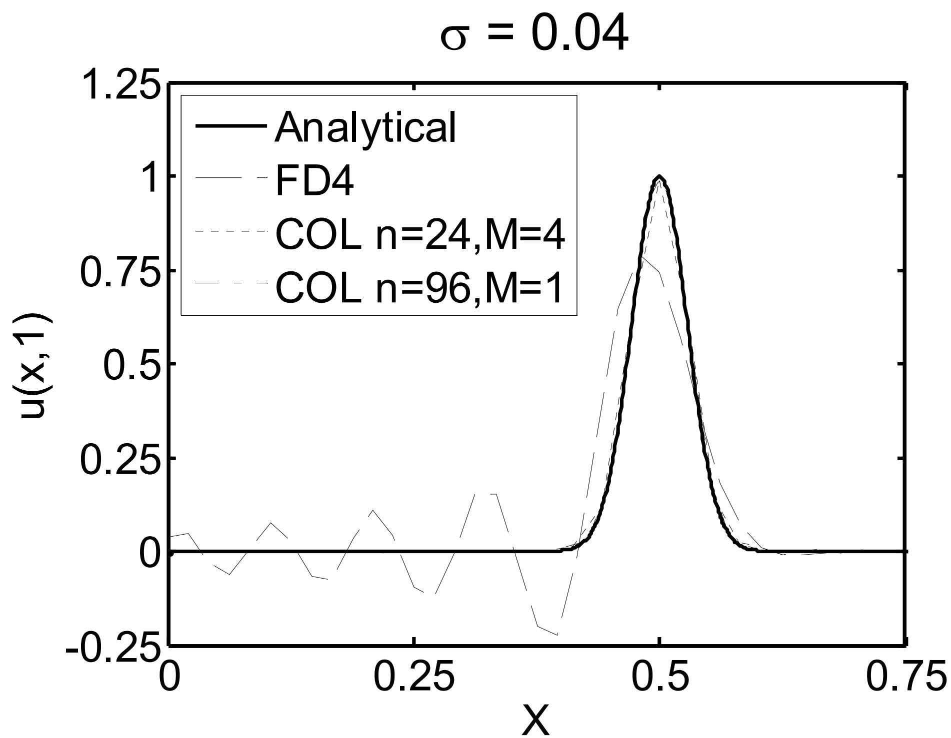

Exponential Convergence

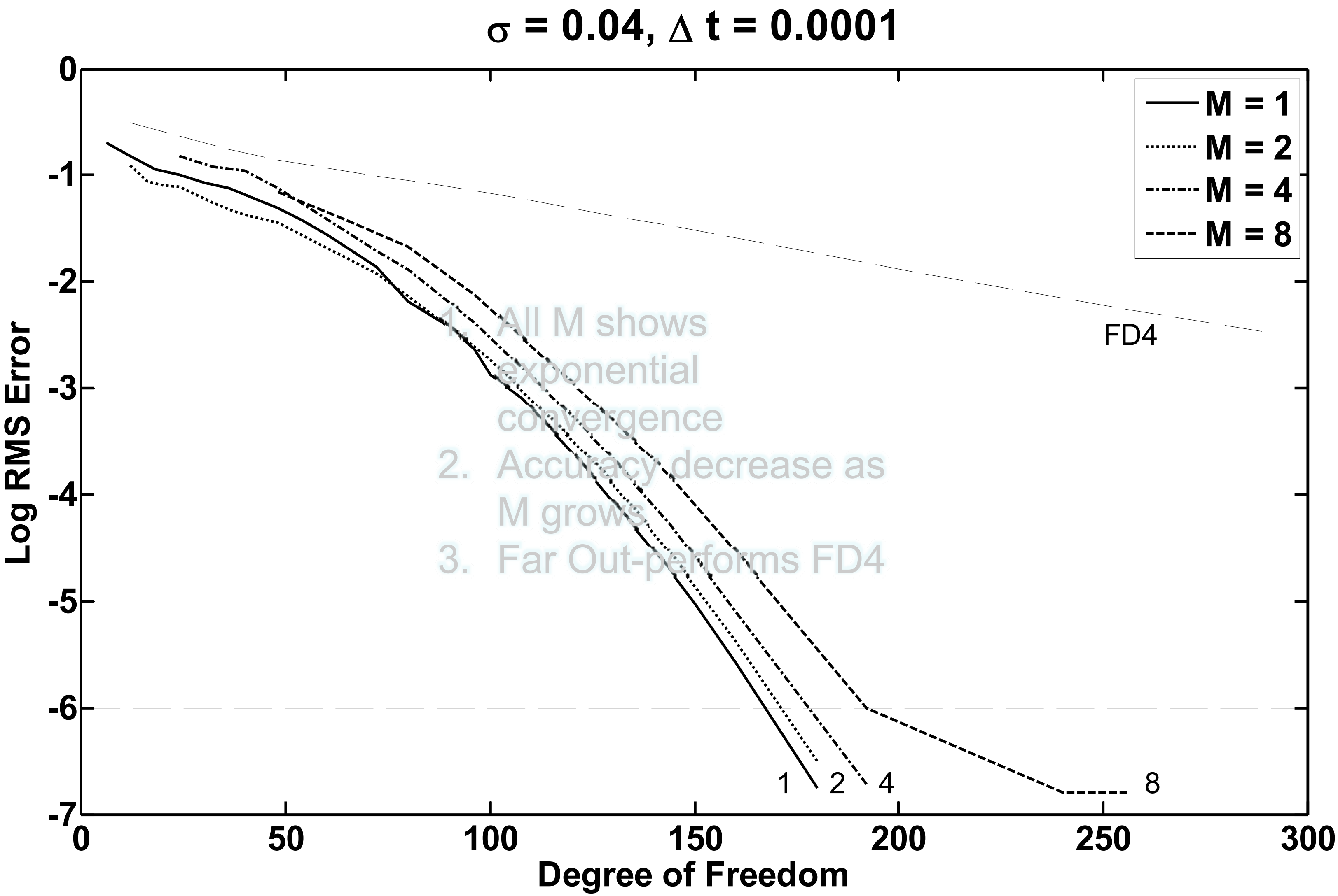

1. All M shows exponential convergence
2. Accuracy decrease as M grows
3. Far Out-performs FD4

Additional Speed-up Factor

$$\text{SpeedUp} = M\frac{N_1}{N_M}\frac{\Delta t_M}{\Delta t_1} = M \times \text{Additional SpeedUp Factor} \qquad (4.1)$$

- Speed-up
- N_M/N1 as x
- $\Delta t_M/\Delta t_1$ as y
- Slope = Additional Sp!
- As large as 6!!
- Max. 48 times faster!!

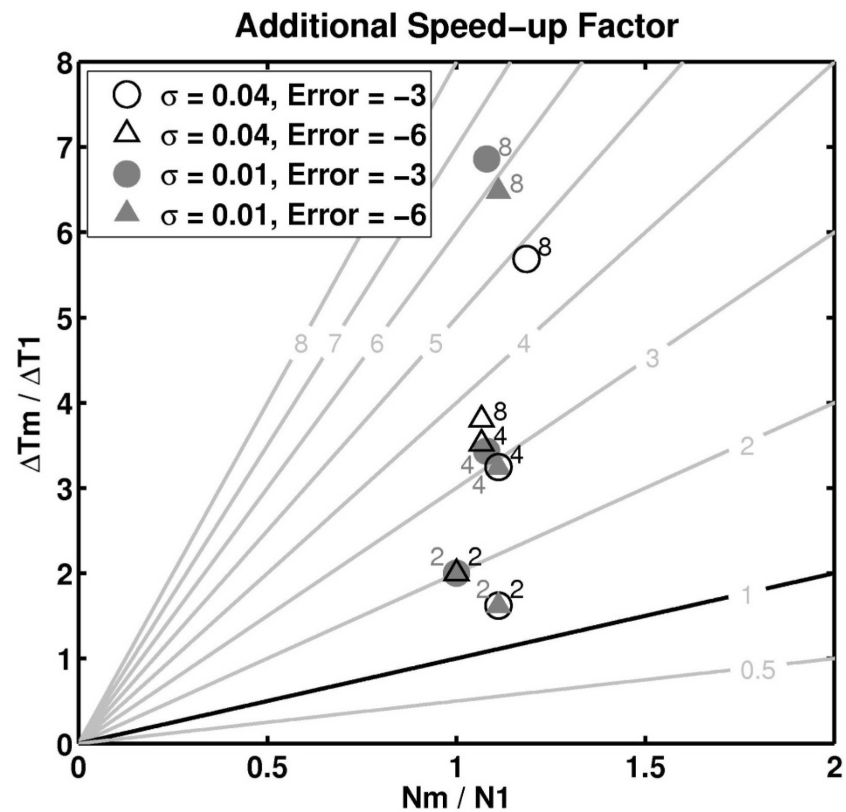

Diffusion Equation

- Similar with FD4
- Very smooth
- Can be simulated very accurately (N=32)
- Domain decomposition is similar

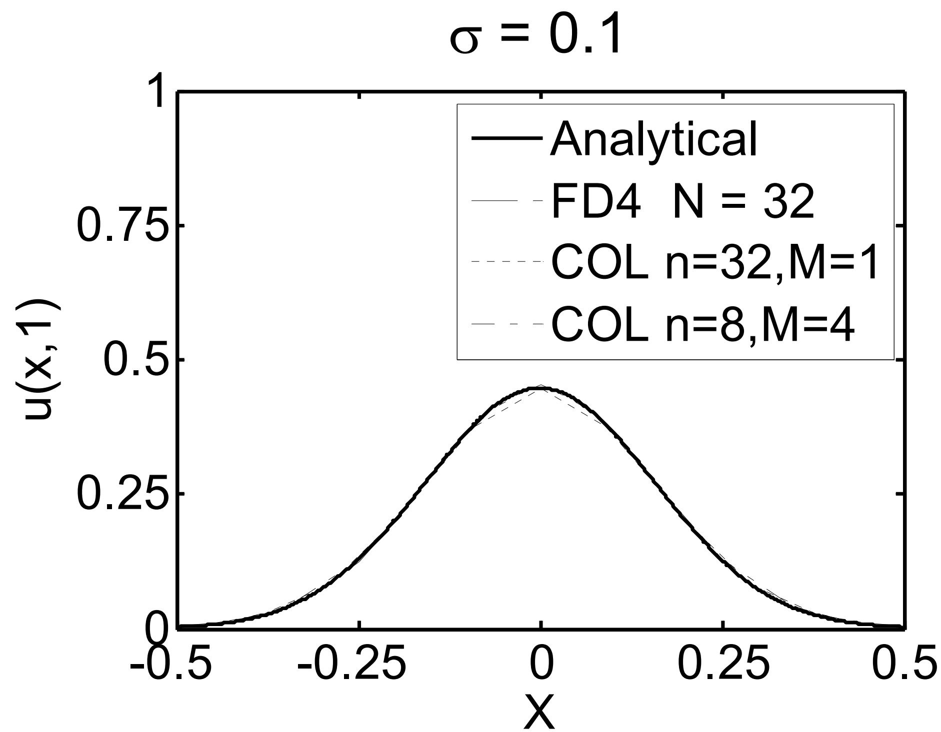

Difference Between Schemes

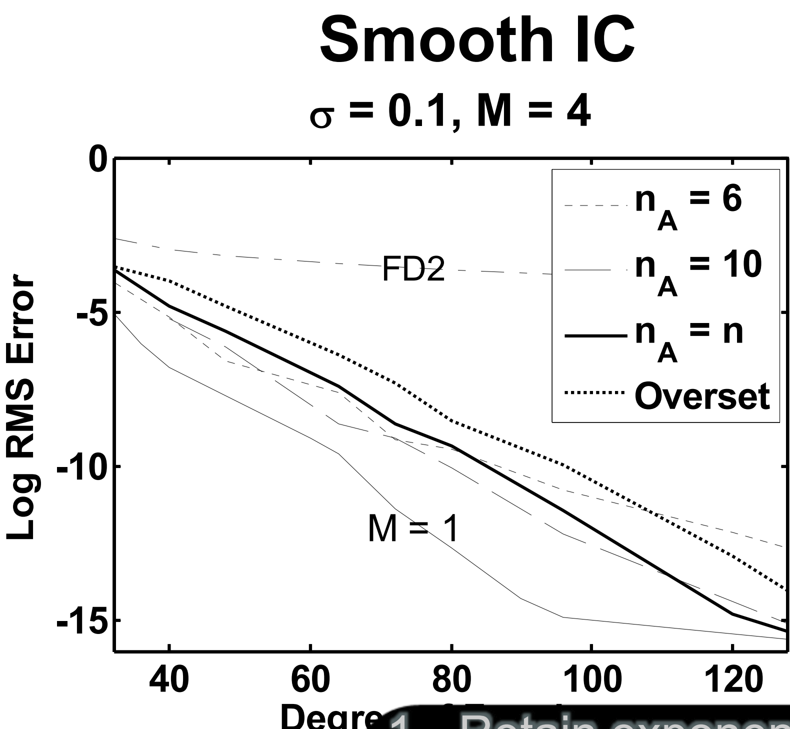

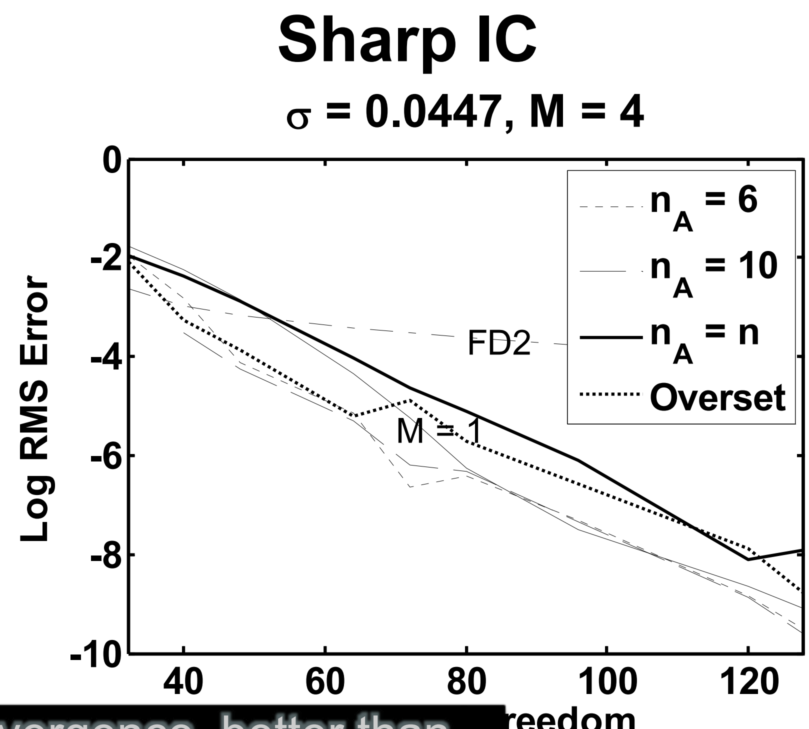

1. Retain exponential convergence, better than FD2
2. In sharp IC D.D. may out-perform single domain Chebyshev method
3. Schemes affect performance, n_A=10 is the best
4. More FLOPs does not guarantee accuracy

Inviscid Burger’s Equation

Stationary Shock formation

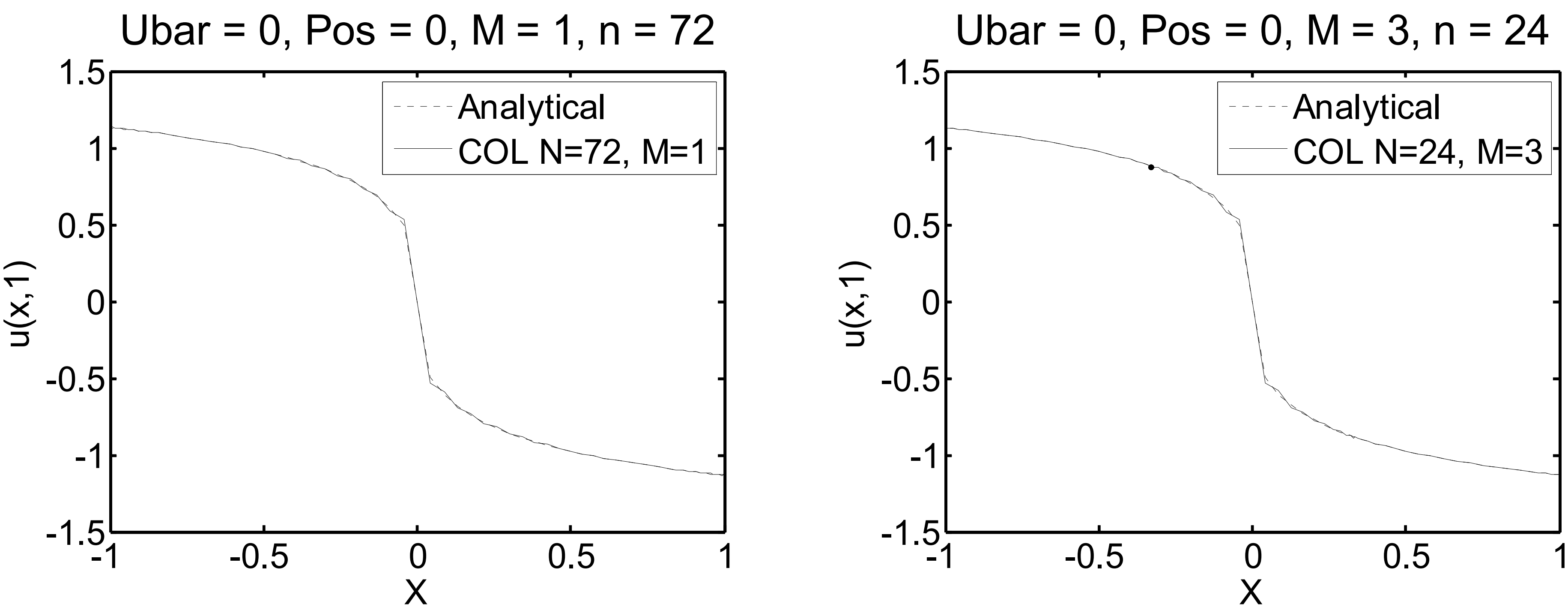

Inviscid Burger's Equation

Shock formation with advection

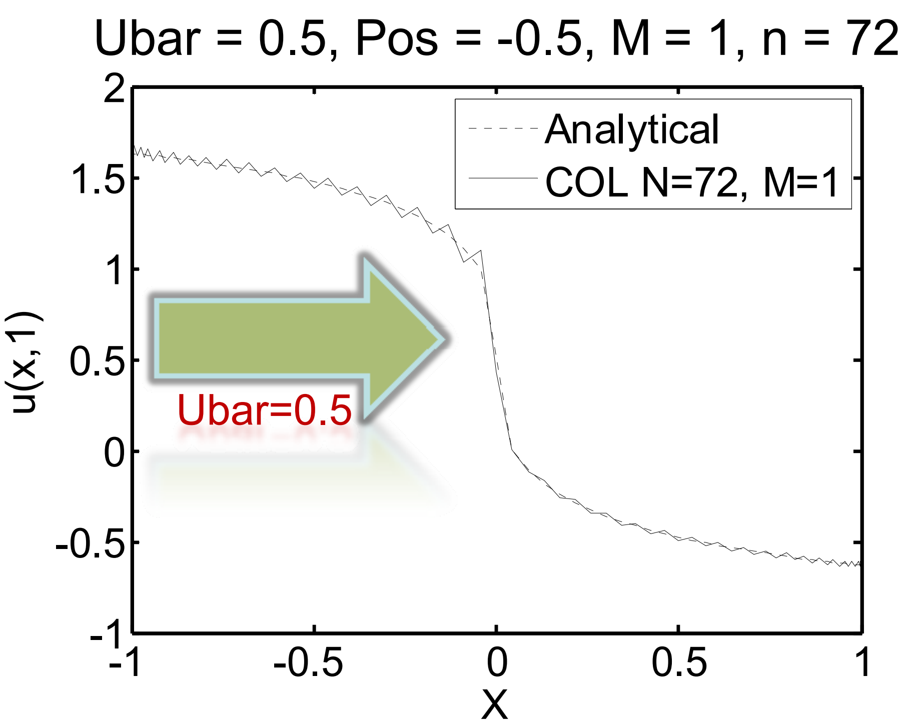

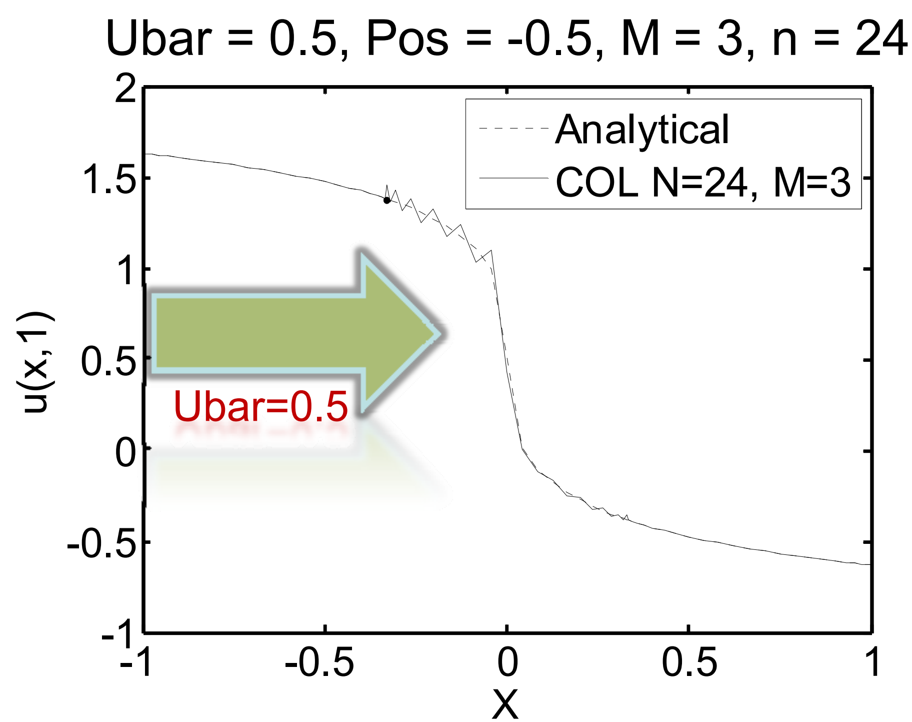

Error Confinement

M = 1

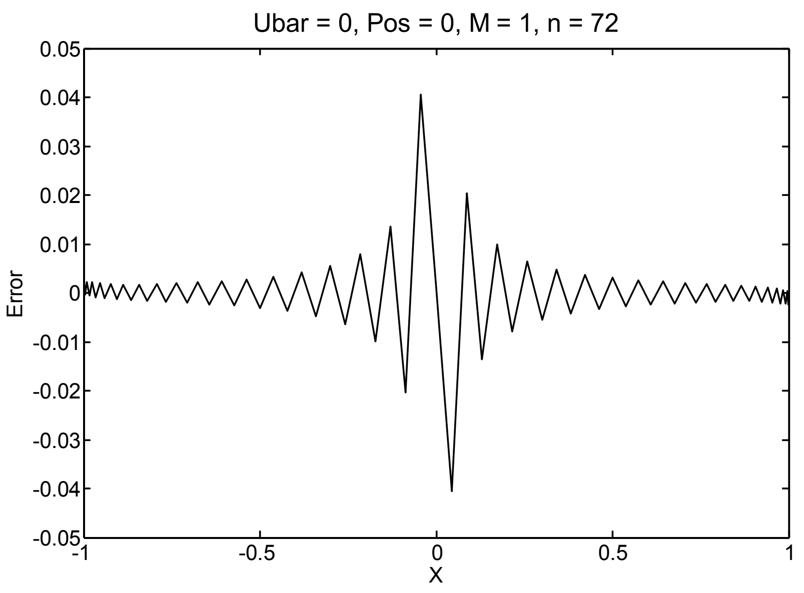

M = 4

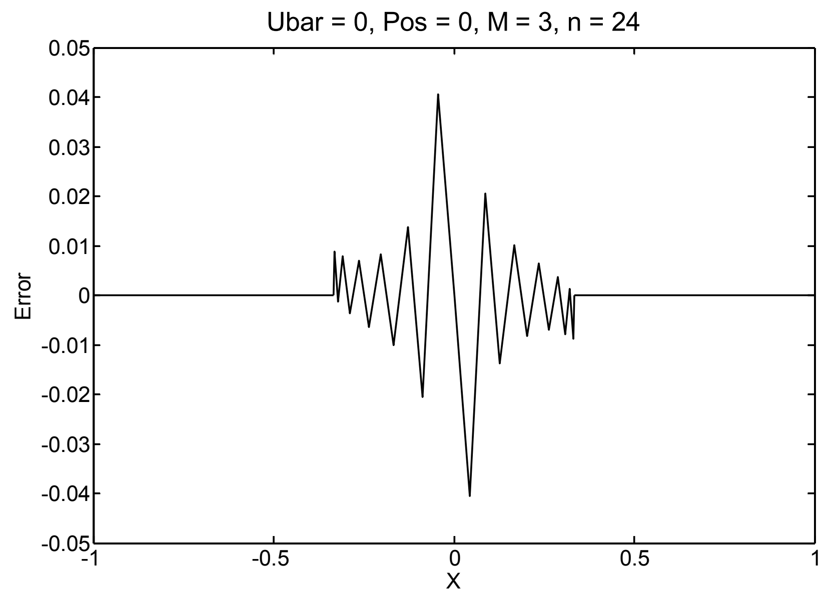

Error Confinement

M = 1

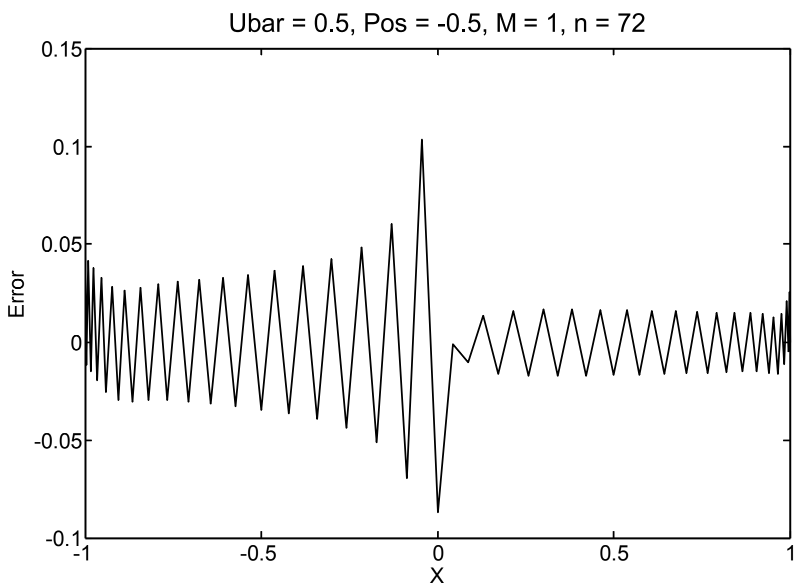

M = 4

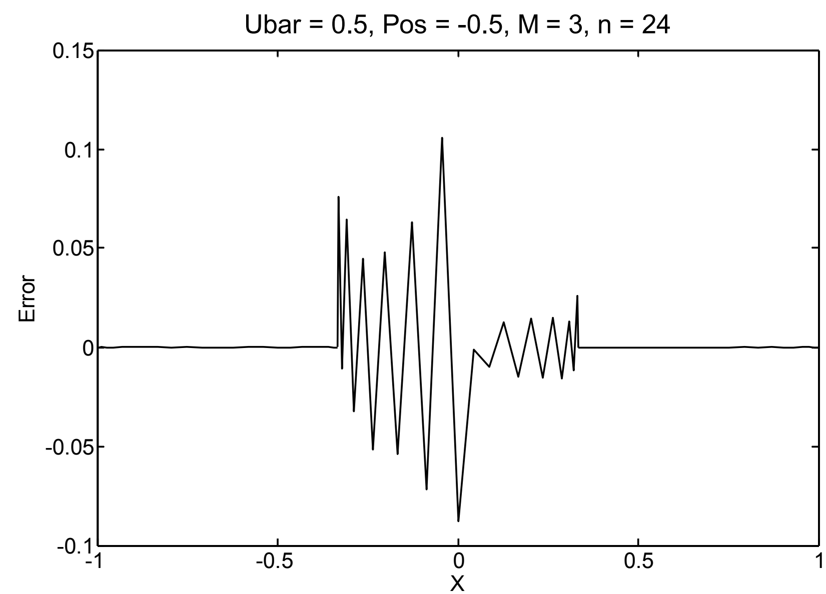

1. The oscillation is confined
2. Max. error remains the same, but L_2 decreased
3. This can be useful in multi-scale model (Front genesis in atmospheric)

A coffee lover's dream:
The best part of waking up, is the vortex in your cup!

$$\frac{D\theta}{Dt} = \frac{\partial\theta}{\partial t} + \vec{V}\cdot\nabla\theta = \nu\nabla^2\theta$$

$$C = \frac{1}{2}\int \nabla\theta\cdot\nabla\theta \; dV$$

$$\frac{dC}{dt} = \int (\vec{V}\cdot\nabla\theta)\nabla^2\theta \; dV - \nu\int(\nabla^2\theta)\, dV$$

Stirring **Mixing**

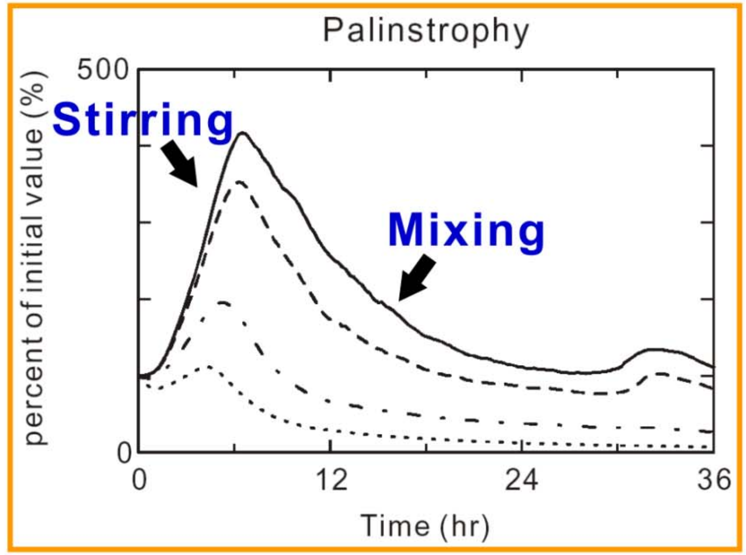

Coffee with white

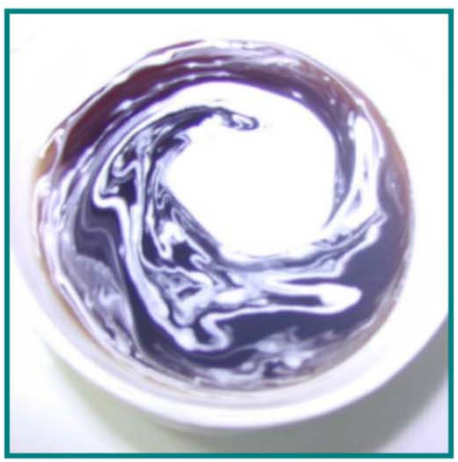

12 hr

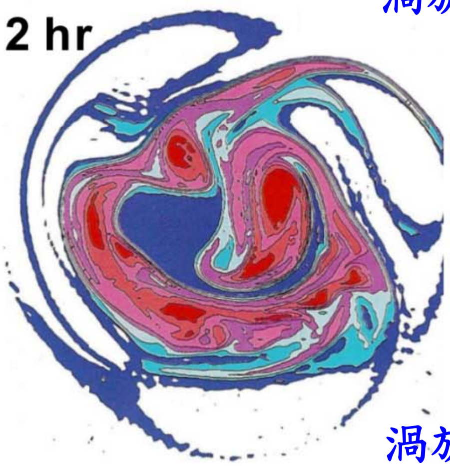

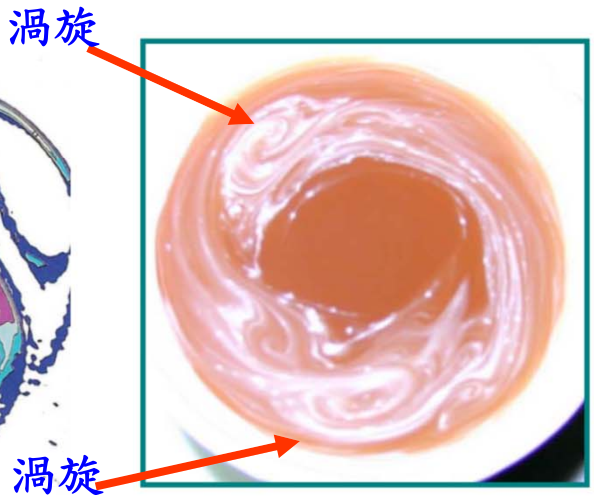

Conclusion

- Chebyshev domain decomposition enlarges min. grid spacing
- Exponential convergence retains after domain decomposition regardless of schemes
- Domain decomposition enlarges Δt as well as accuracy => Bring additional speed-up
- Additional speed-up is determined with L_2 error keep constant
- Can be as large as 48 max. speed-up for 8 CPUs!!

Conclusion Cont.

- Overset and aux. sub-domain may tackle interior BCs
- Aux. sub-domain schemes affect accuracy
- $n_A = 10$ is the best, large n_A does not guarantee accuracy
- Aux. sub-domain confines error in down stream regions in case of scale collapse

Determining n_A and L_A

- Total FLOPs increased!
- n_A as small as possible!
- What about L_A?

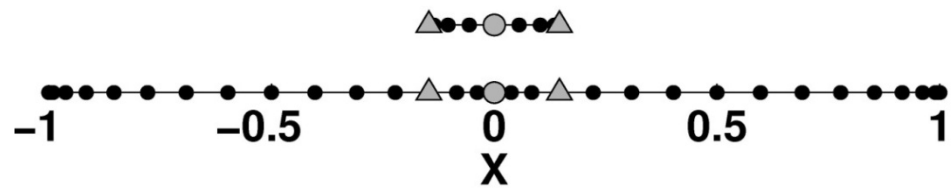

$$\text{Total FLOPs} = \text{FLOPs}_{\text{Sub}} + \text{FLOPs}_{\text{Aux}} \propto [N + n_A \times (M - 1)] \times \frac{\text{Time Span}}{\Delta t} \qquad (5.1)$$

$$L_A = 2 \times \frac{L}{2M} \times \left[1 - \cos\left(\frac{j\pi M}{N}\right)\right] \qquad (5.2)$$

$$\Delta x^A_{\min} = \frac{L_A}{2}\left(1 - \cos\frac{\pi}{n_A}\right) \qquad (5.3)$$

$$\Delta x^A_{\min} \geq \Delta x^{\text{Sub}}_{\min} = \frac{L}{2M}\left(1 - \cos\frac{\pi M}{N}\right) \qquad (5.4)$$

$$j \geq \frac{n}{\pi}\cos^{-1}\left[1 - \frac{\cos\frac{\pi}{n}}{\cos\frac{\pi}{n_A}}\right] \qquad (5.5)$$

- Must overlap with sub-domains: jth point
- ΔX_{min} larger than sub-domains
- $j_{min}(n,n_A)$

Minimum j

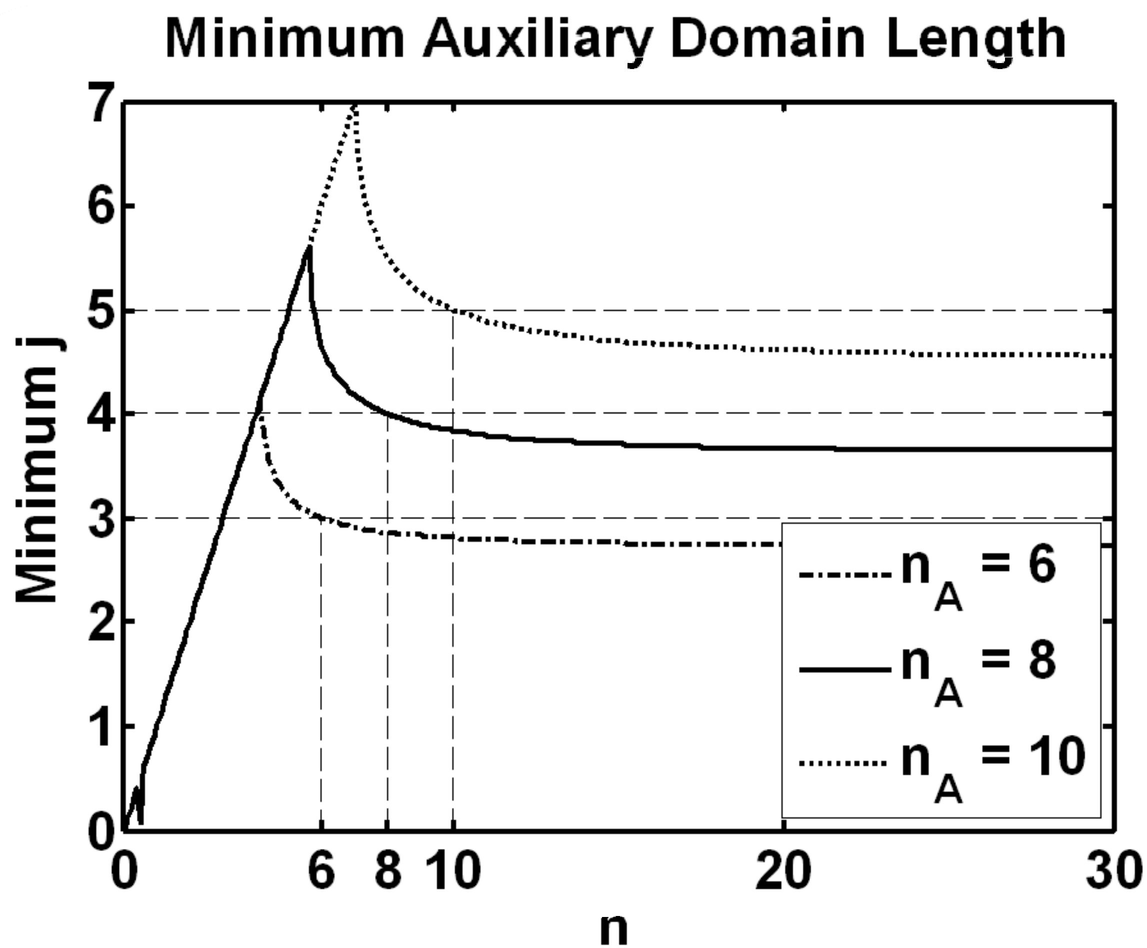
Minimum Auxiliary Domain Length
Minimum j
n
0
1
2
3
4
5
6
7
0
6
8
10
20
30
$n_A = 6$
$n_A = 8$
$n_A = 10$

Auxiliary Sub-domains

- Performance between schemes (n_A)?
- Not too much cost:
  - In a typical large scale computing
  - $N = 1024$, $M = 8$, $n_A = 10$
  - 7% increase only!!
- Confine error

$$\text{Total FLOPs} = \text{FLOPs}_{\text{Sub}} + \text{FLOPs}_{\text{Aux}} \propto [N + n_A \times (M - 1)] \times \frac{\text{Time Span}}{\Delta t} \quad (5.1)$$

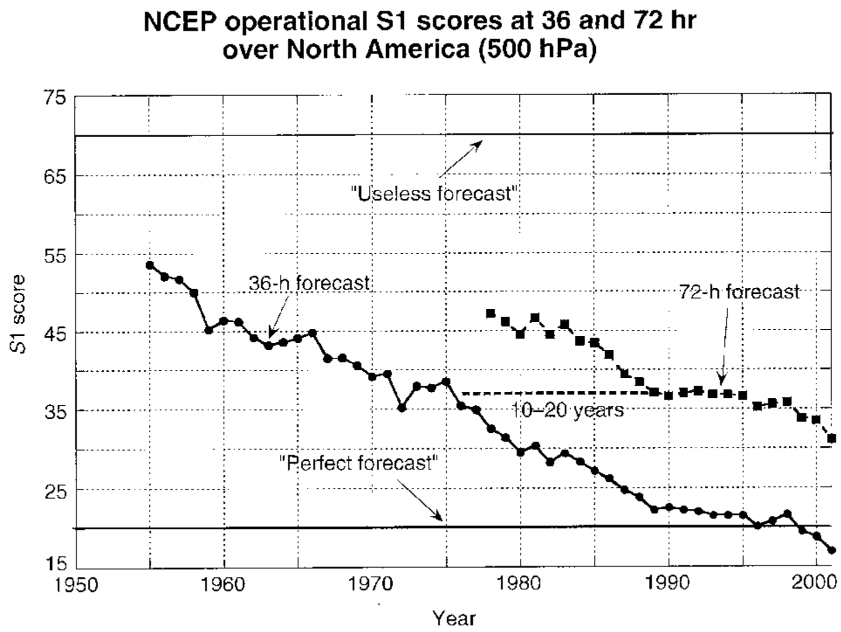

(a)

Numerical Weather Prediction

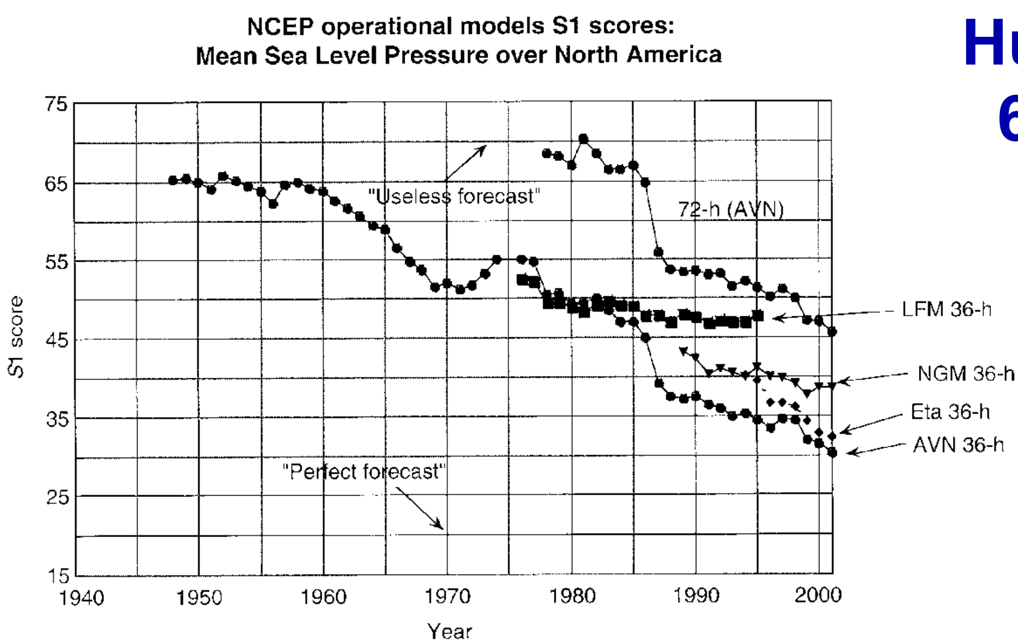

(b)

Hurricane Katrina
60 hrs的預警撤退

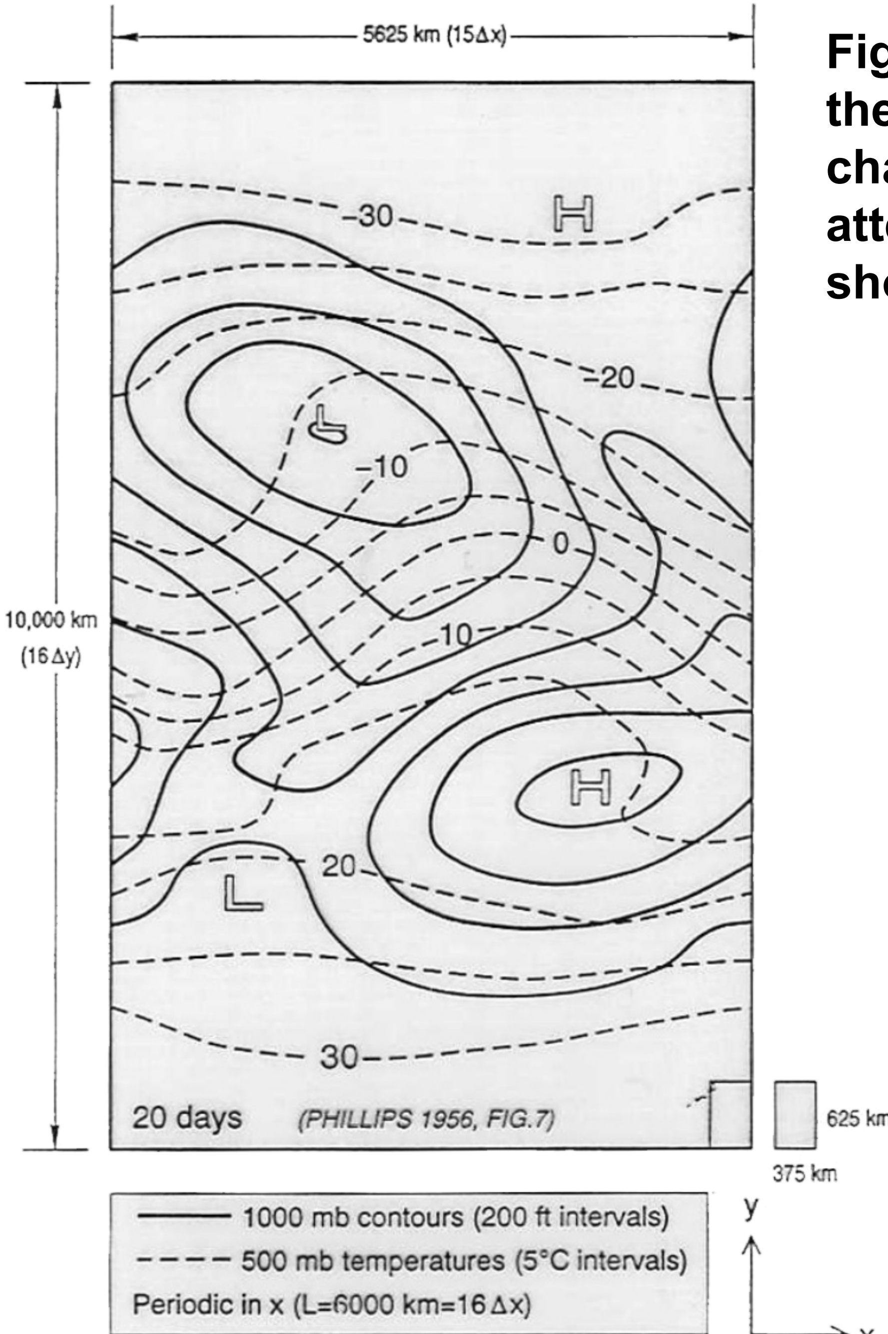

Fig. 5. On day 20 of the simulation, the synoptic-scale disturbance exhibits the characteristics of a developing cyclone with attendant frontogenesis. The mesh size is shown beside the model's horizontal domain.

The model used a rectangular domain on a β-plane given by $0 \le x \le L$ with the cyclic boundary condition and $-W \le y \le W$ with the rigid-wall boundary condition. Here x and y are eastward and northward coordinates respectively.
The heating Q was *prescribed* as $-2H(y/W)$.
Numerical values used are $A = 10^5$ m sec^{-1}, $k = 4*10^{-6}$ sec^{-1}, $H = 2*10^{-3}$ kj ton^{-1} sec^{-1}, W = 5,000 km and L = 6,000 km. The grid size is $\Delta x = 375$ km and $\Delta y = 625$ km.

1960 Magnificent Second Phase 1990 Great-Challenge Third Phase

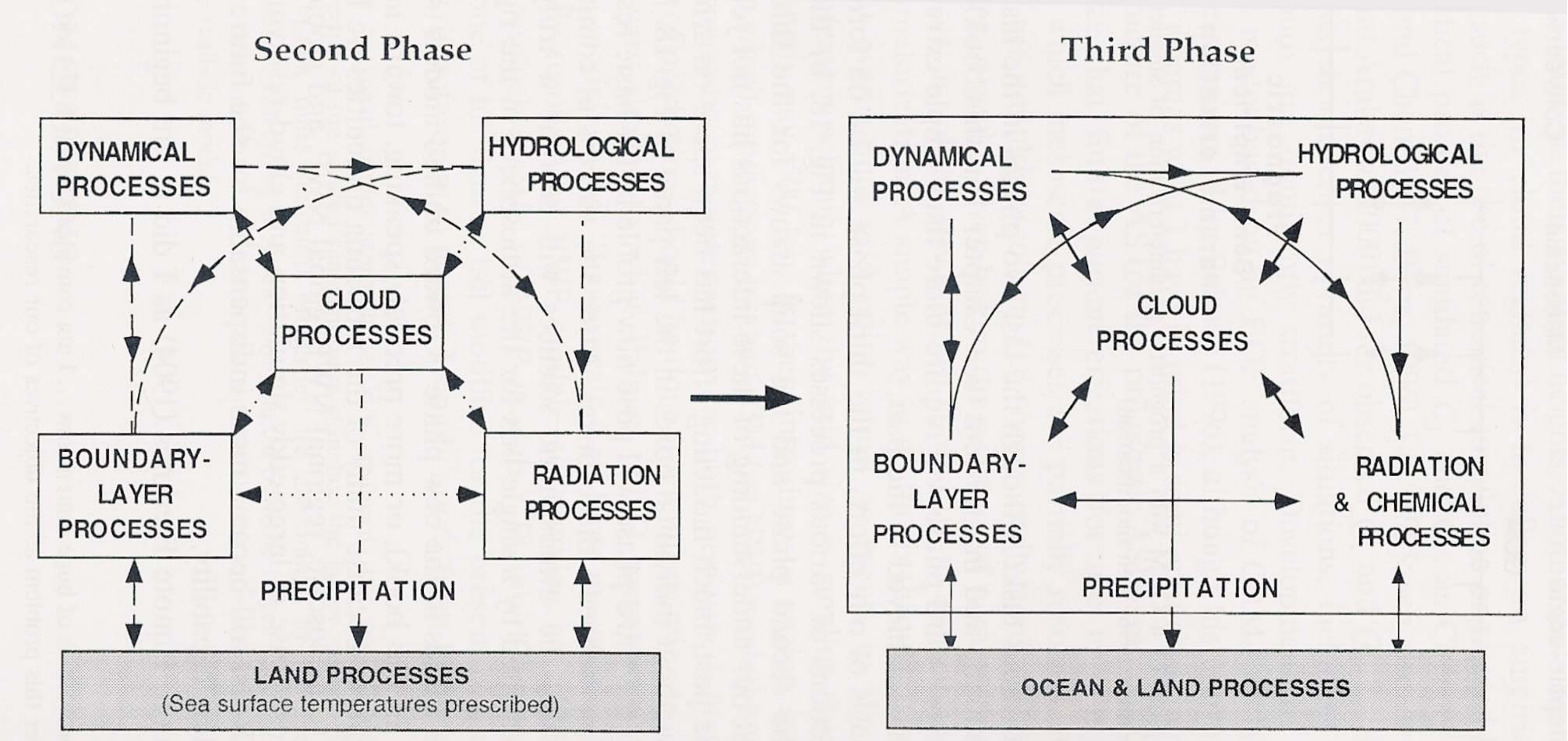

Figure 18 Interactions of various processes. See text for explanation.

All coupled together!
Cloud Processes are the core!

The Atmosphere is Moist 濕的大氣

Water vapor is an efficient absorber and emitter of Long-wave radiation. [Green House Effect.]

溫室效應 大氣輻射

Water vapor stores energy in the form of “latent heat” [Evaporative cooling of surface.]

地球表面蒸發冷卻

Water vapor can condense release latent heat.
[A variety of cloud and associated processes.]

雲過程

Numerical Model

Manmade laboratory on supercomputers using mathematics and physical laws. 高效率計算數學 +大氣運作物理規律 +超級電腦

- **Help Raising Questions**
- **Suggest or Verify Relationship**
- **Data Assimilation**

Research

- 因果之澄清
- 因果之探討
- 資料同化
- 銓釋資料
- 預報

- **Forecast**

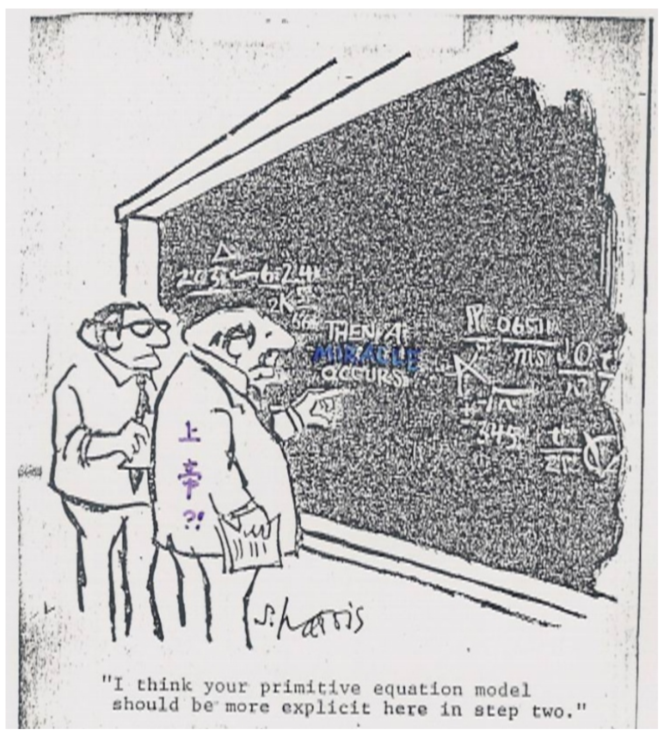

THEN A MIRACLE OCCURS!!

Small viscosity led to
large palinstrophy and the
large enstrophy cascade

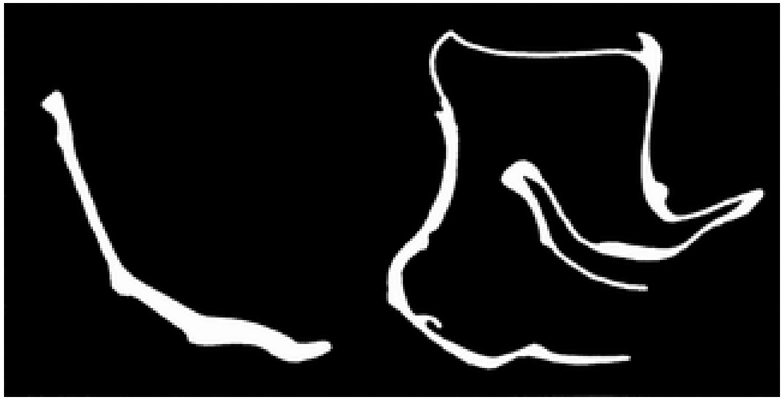

Stirring

Typhoon Herb (1996)

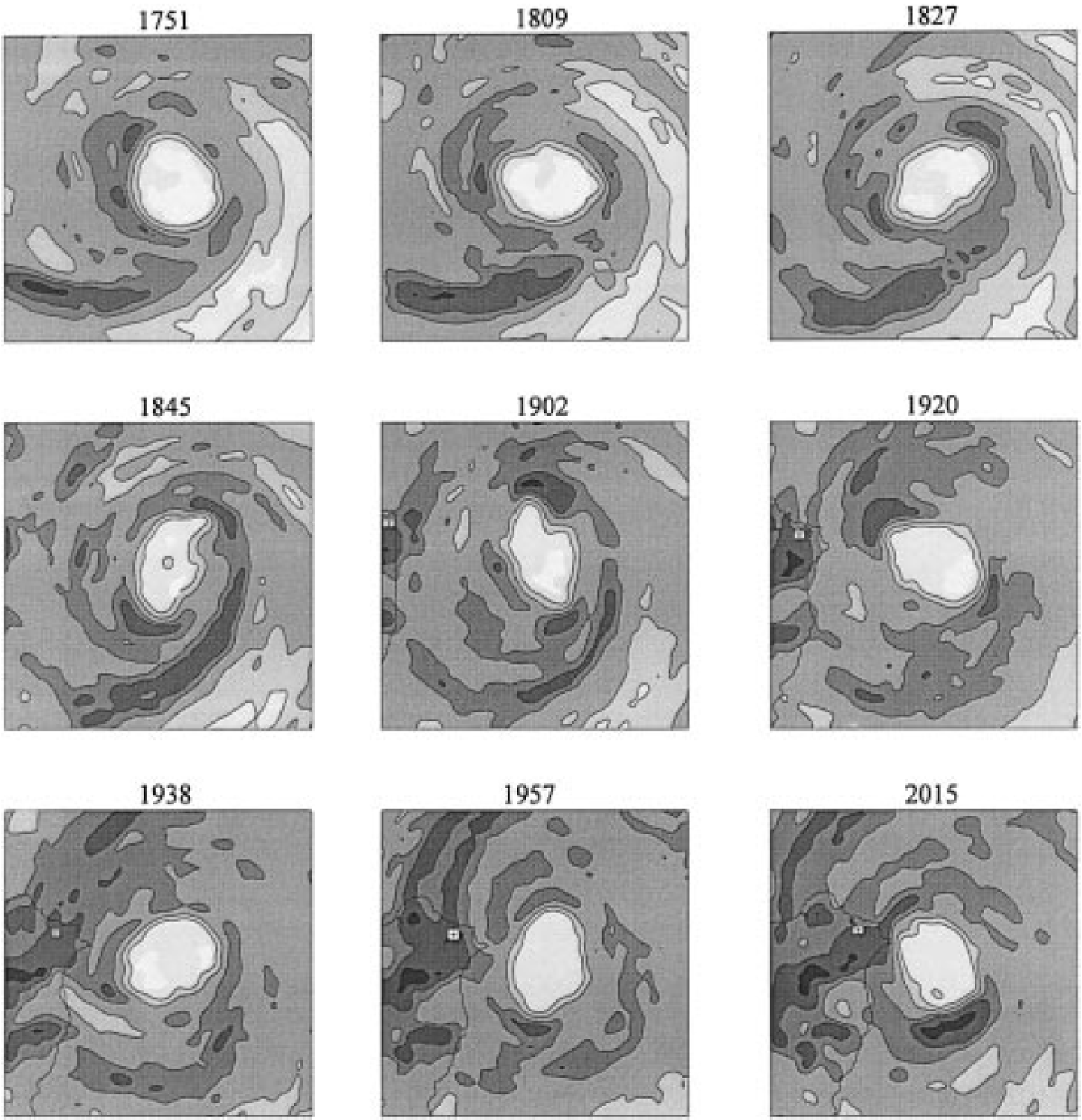

Eye Rotation Period: 144 mins

Kuo et al. 1999

Spiral Band in Hurricane and Galaxy

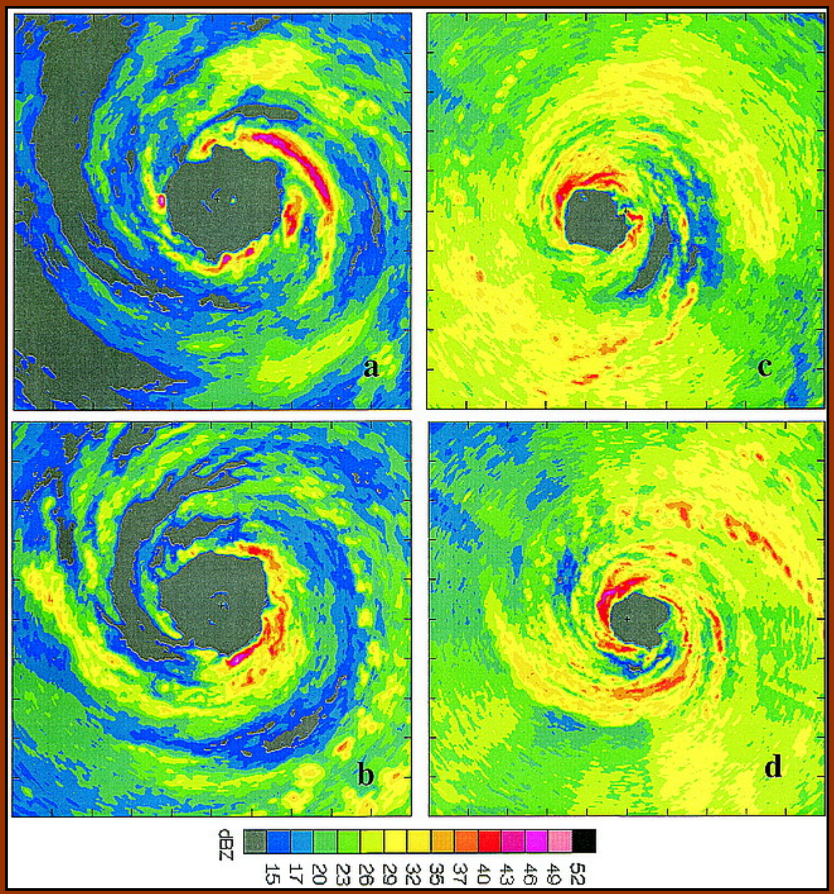

Airborne-radar reflectivity in Hurricanes
Guillermo (1997) (left panels) and Bret (1999) (right panels).

Kossin and Schubert 2001

Waves, turbulence, and coherent vortex

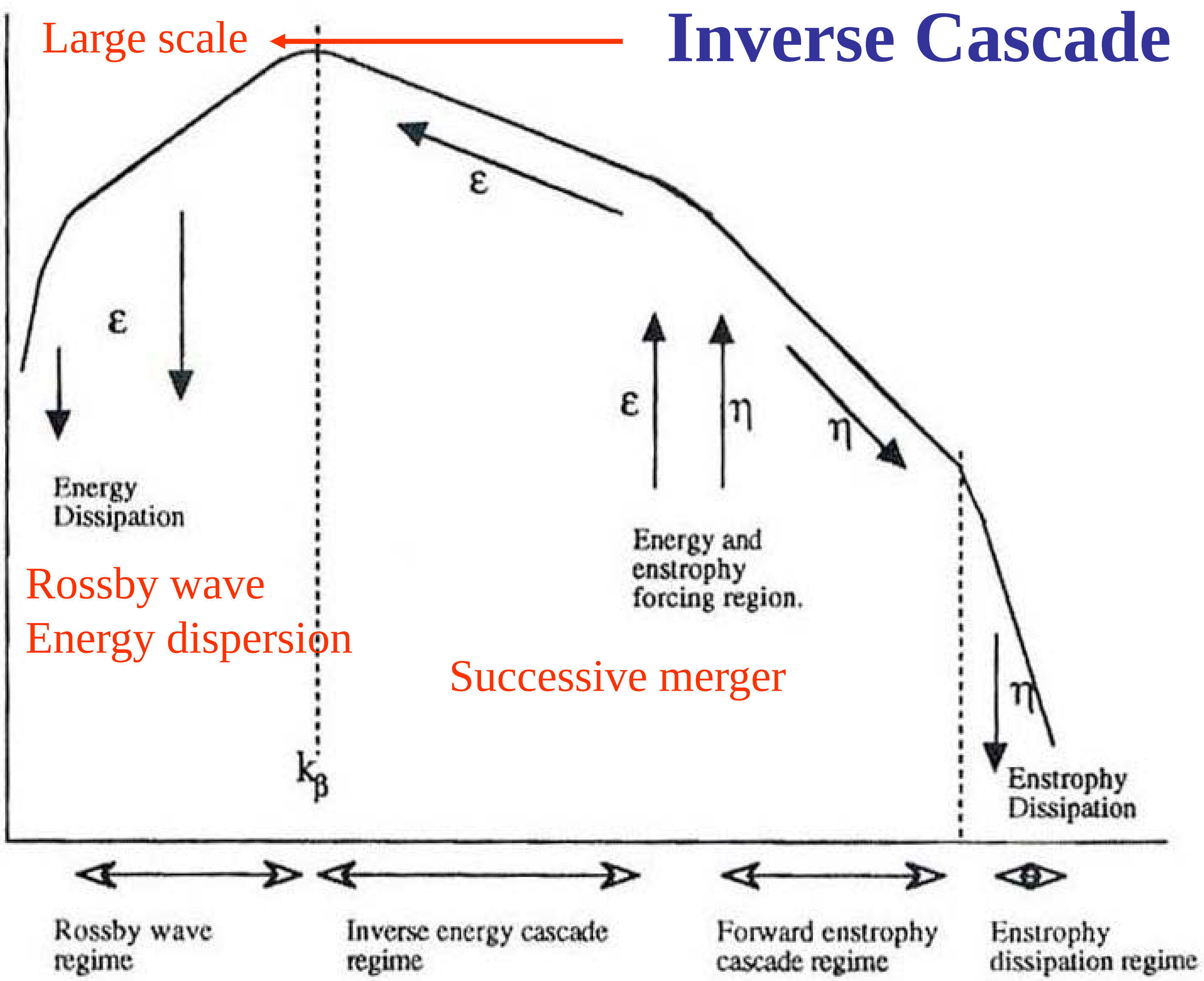

mid 50 — Observational study of eddy transport UCLA,MIT
Haboratory study U of Chicago, MIT
NWP — Charney, Fjortoft and Neumarn (1950) E Barotropic
Charney and Phillips (1953) 2 level QG model

Phillips' numerical experiment

Phillips (1956)

two-level
Quasi-Geostrophic model

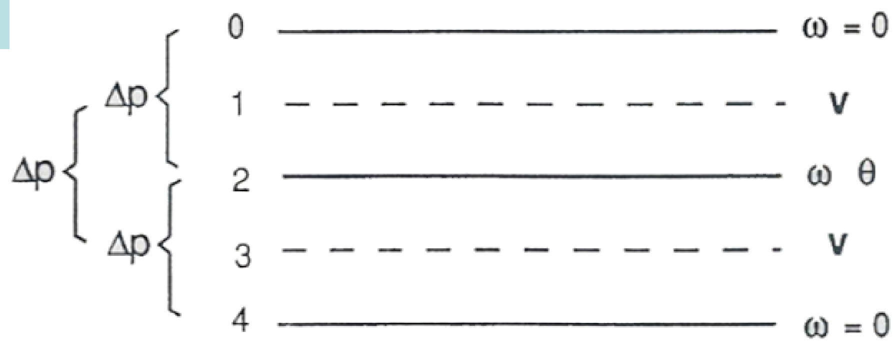

Corresponding to (IV.3.1) for $\ell = 1, 2$ and (IV.3.2) for $\ell = 1$ but with a ew vertical index as shown in Fig. IV.8, the equations of his model are

$$\left(\frac{\partial}{\partial t} + \mathbf{v}_{g1} \cdot \nabla\right)(\zeta_{g1} + f) - f_0 \frac{\omega_2}{\Delta p} = A\nabla^2 \zeta_{g1}, \qquad \text{(IV.4.1)}$$

$$\left(\frac{\partial}{\partial t} + \mathbf{v}_{g3} \cdot \nabla\right)(\zeta_{g3} + f) + f_0 \frac{\omega_2}{\Delta p} = A\nabla^2 \zeta_{g3} - k\zeta_{g4}, \qquad \text{(IV.4.2)}$$

$$\left(\frac{\partial}{\partial t} + \mathbf{v}_{g2} \cdot \nabla\right)(\psi_1 - \psi_3) - \frac{1}{\mu^2}\frac{f_0}{\Delta p}\omega_2 = A\nabla^2(\psi_1 - \psi_3) + \frac{R}{c_p}\frac{1}{f_0}Q, \qquad \text{(IV.4.3)}$$

to study meteorology as an experimental science

Questions:

(1) Unrealistic initial condition, that is, starting the simulation from a state of rest (P. Sheppard and R. Sutcliffe);

(2) Excessive strength of the indirect cell (P. Sheppard)

(3) Absence of condensation processes (B. Mason and R. Sutcliffe);

(4) questionable physical significance of the transformation of energy between K' and K (G. Robinson);

(5) Question regarding the 2ndary jets to the north and south of the main jet. (J. Sawyer)

Encouraging remarks from Eady:

I think Dr. Phillips has presented a really brilliant paper which deserves detailed study from many different aspects. I am in complete agreement with the point of view he has taken and can find no fault with his arguments, either in the paper or in the presentation. With regard to the statement by Prof. Sheppard and Dr. Sutclife, I think Dr. Phillips's experiment was well designed. <u>Numerical integrations of the kind Dr. Phillips has carried out gives us a unique opportunity to study large scale meteorology as an experimental science.</u> By using a simple model and initial conditions which never occur in the real atmosphere he has bee able to isolate, and study separately.

Atmospheric Science as an Experimental Science!

Nonlinear computational instability
and the Arakawa Jacobian (1966)

$$J(\psi,\zeta)$$

When the Arakawa Jacobian is used for the advection terms in the QG baroclinic model, together with the vertical differencing, the sum of kinetic energy and available potential energy is conserved, as well as potential enstrophy, in the absence of heating and friction.

➔**energy and enstrophy conservation**

➔穩定的大氣，大氣環流之數值模式

Nonlinear energy transfer

Aliasing error

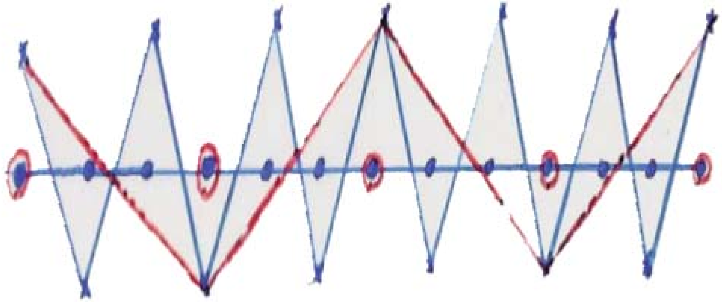

I myself was also extremely inspired by Phillips' work. My interest around the mid-50s was in general circulation of the atmosphere, mainly those aspects as revealed by observational studies on the statistics of eddy transports by Starr and White at MIT and Bjerknes and Mintz at UCLA, and laboratory experiments by Fultz [at University of Chicago] and Hide at MIT. At the same time, I was also interested in numerical weather prediction, through which dynamical meteorologists began to be directly involved in actual forecasts. Phillips' work highlighted the fact, which people began to recognize around that time, that the dynamics of cyclones and that of general circulation are closely related. I was so excited about these findings that I published a monograph through Japan Meteorological Society (Arakawa 1958) . . . to let Japanese meteorologists recognize the important ongoing progress in our understanding of general circulation of the atmosphere.

(A. Arakawa 1997, personal communication)[4]

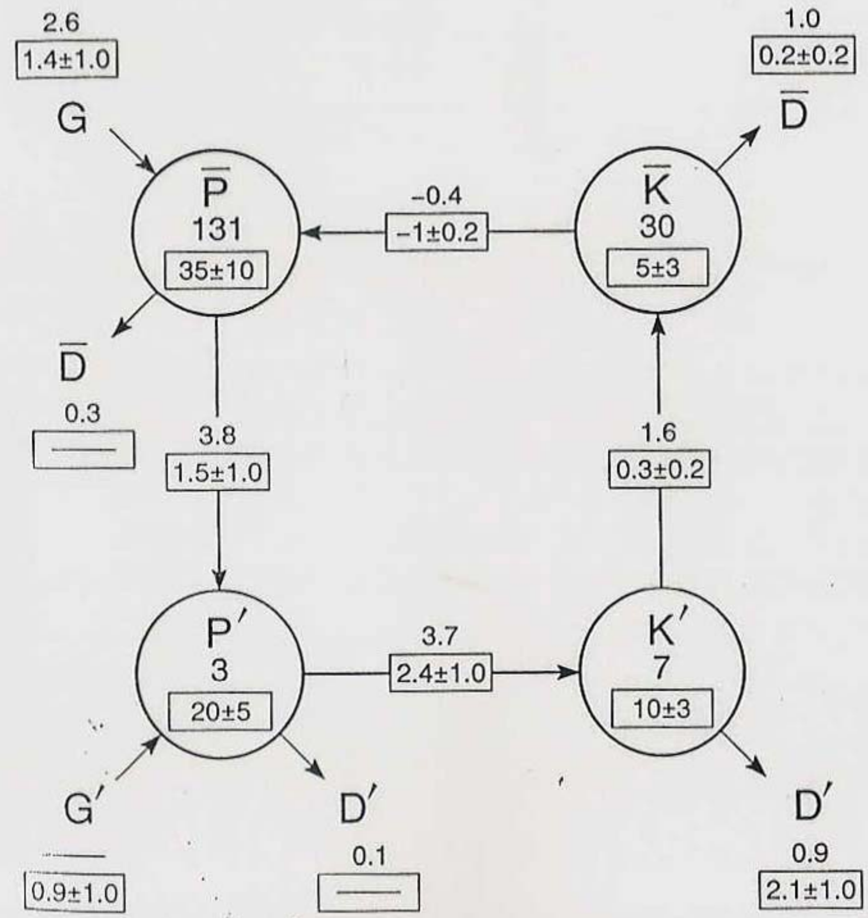

FIG. 9. Energy diagram showing the reservoirs of kinetic (K) and available potential energy (P), where zonal-mean and eddy components are denoted by $\overline{(\ldots)}$ and $\overline{(\ldots)}'$, respectively. The transformation rates between the various components are indicated along the lines connecting the reservoirs; if positive, the energy is transferred in the direction indicated. Energy generation/dissipation is denoted by G/D, respectively. Oort's observationally based statistics are shown in the rectangular boxes, and Phillips's simulated statistics are written above these boxes. The energy units are 1) reservoirs—J m^{-2} 10^5, and 2) transformation rates –W m^{-2}.

Aliasing

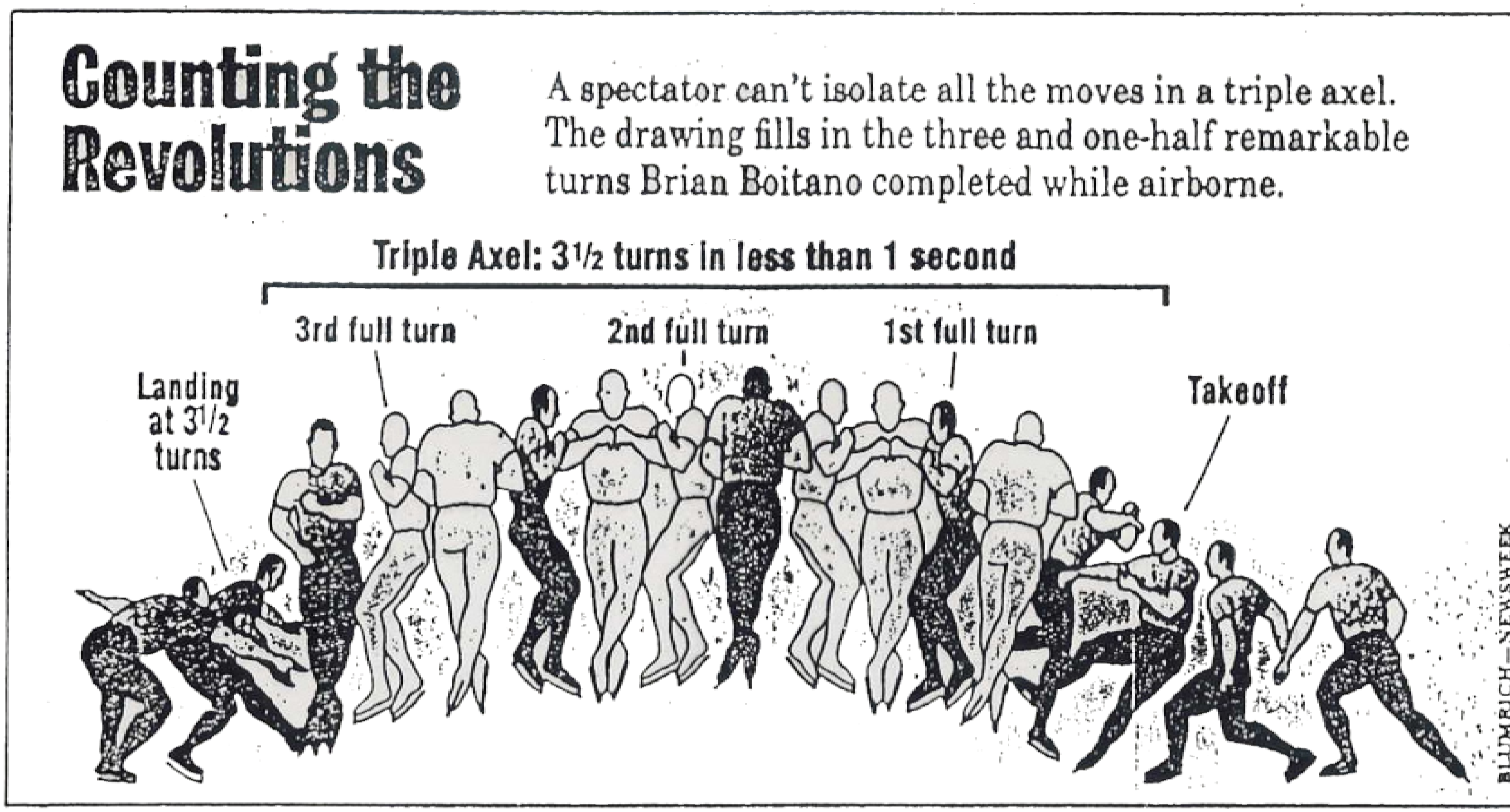

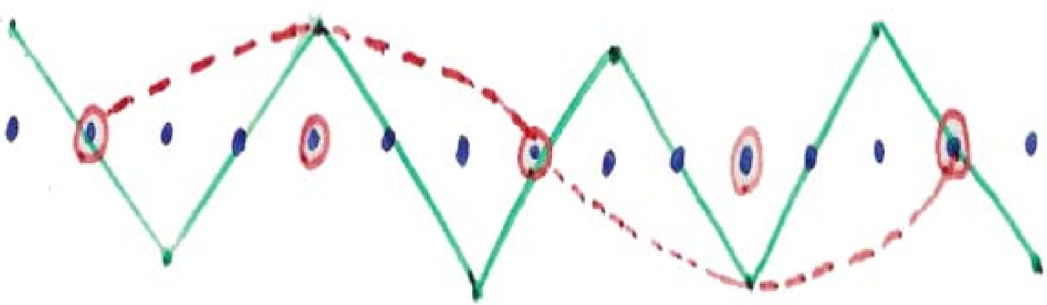

計 算

相位錯置

RAINEX (2005)

Shear/strech deformation outside the radius of maximum wind

ELDORA composite
~120 x 120 km^2

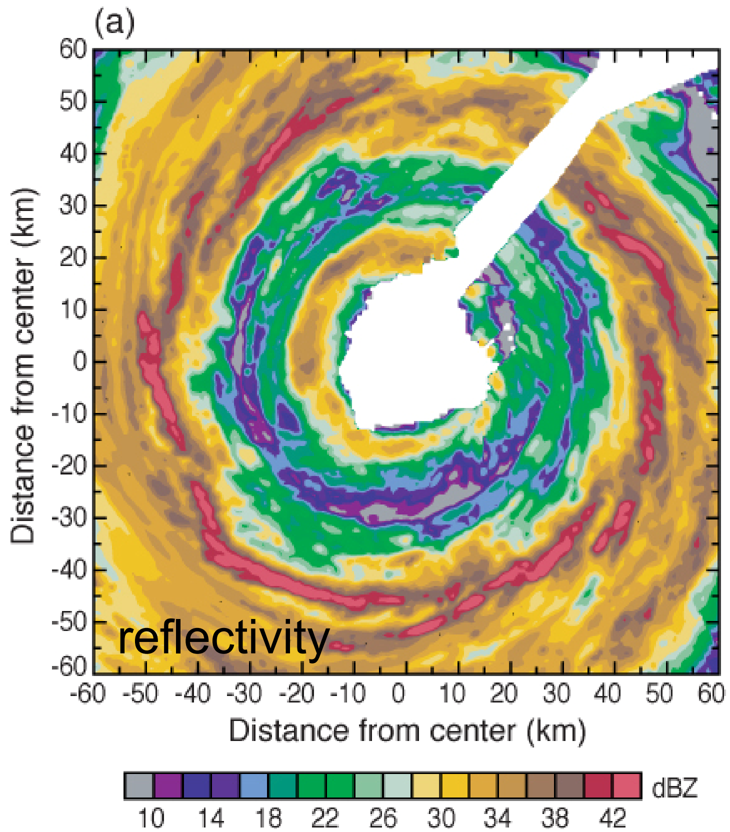

Kossin et al. (2000)
Instability Experiment

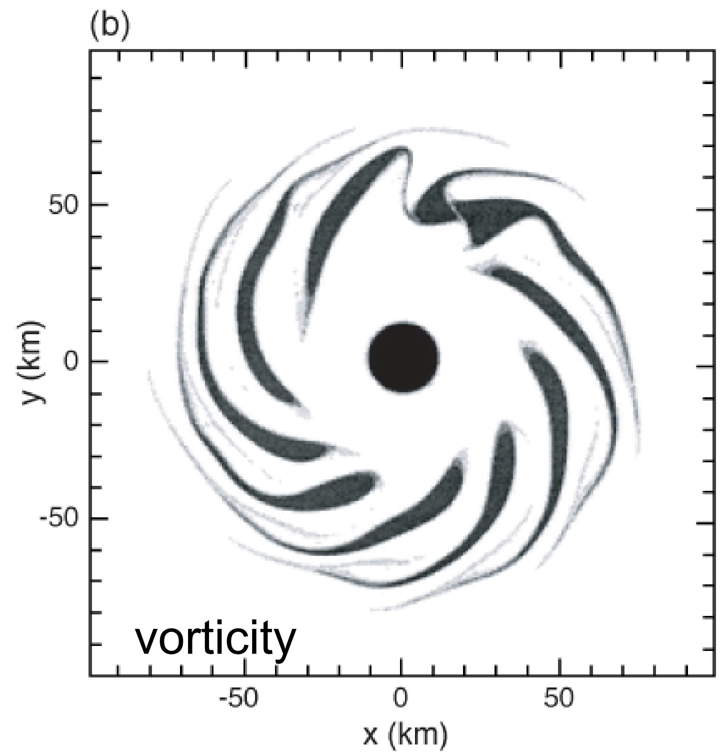

Exponential Convergence

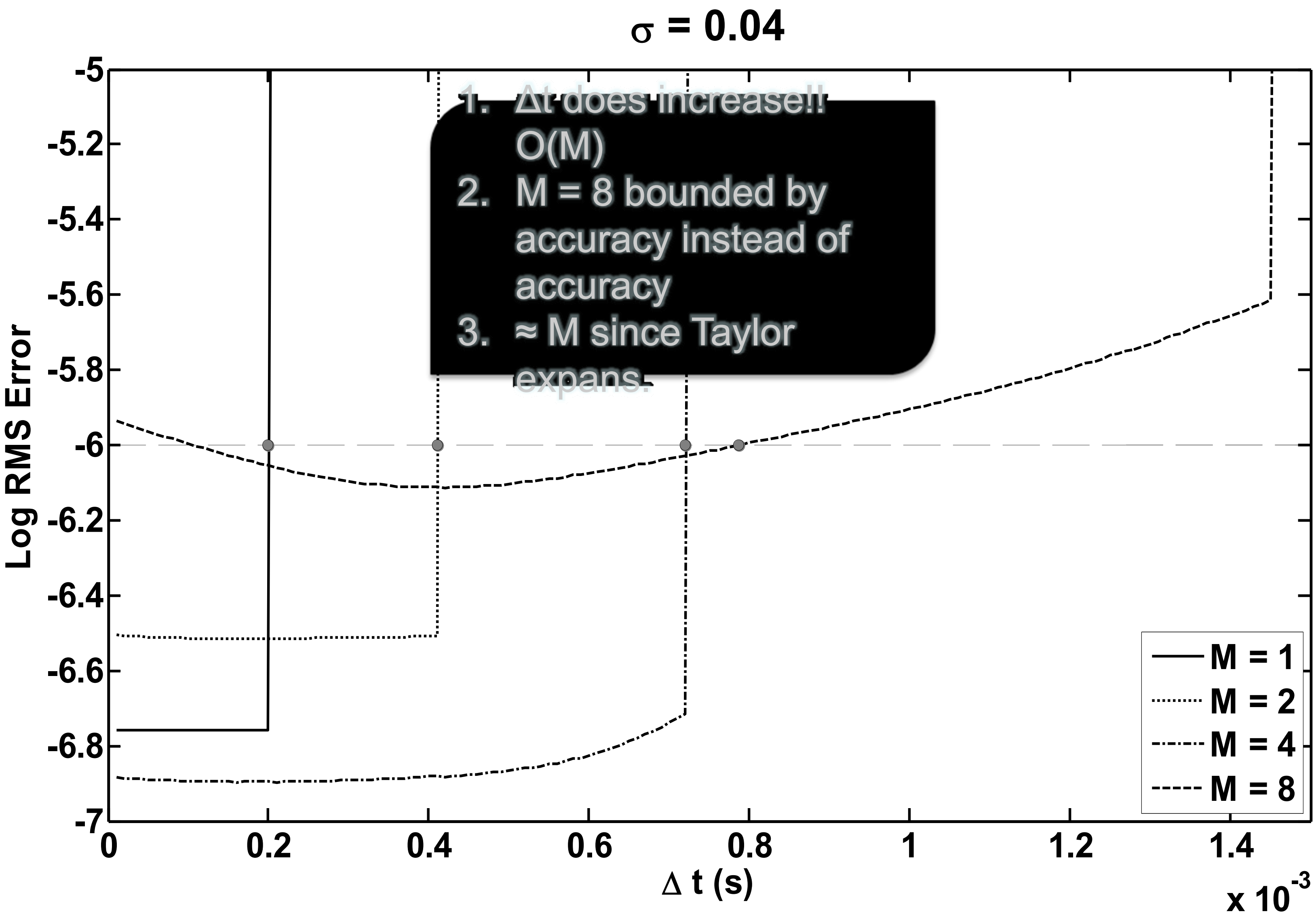

1. Δt does increase!! O(M)
2. M = 8 bounded by accuracy instead of accuracy
3. ≈ M since Taylor expans.

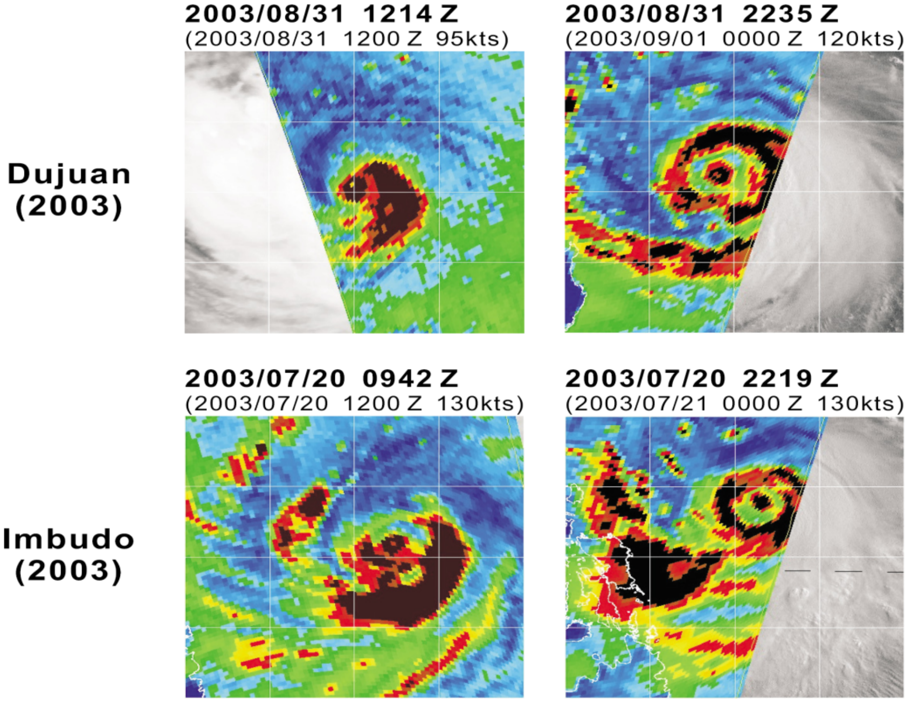

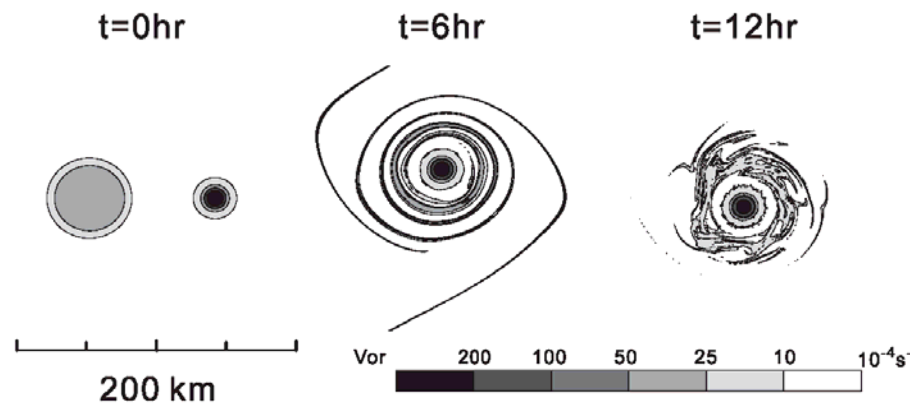

The contraction and the increase of the secondary wind maximum by nonlinear advection dynamics.